

# UC San Diego

## UC San Diego Electronic Theses and Dissertations

### Title

Characterization of Copper-Binding Ligands and Copper Speciation in Open Ocean and Coastal Marine Systems using Electrochemical Methods

### Permalink

<https://escholarship.org/uc/item/8j94r7jp>

### Author

Ruacho, Angel

### Publication Date

2019

Peer reviewed|Thesis/dissertation

UNIVERSITY OF CALIFORNIA SAN DIEGO

Characterization of Copper-Binding Ligands and Copper Speciation in Open Ocean and Coastal  
Marine Systems using Electrochemical Methods

A dissertation submitted in partial satisfaction of the requirements for the degree Doctor of

Philosophy

in

Oceanography

by

Angel Ruacho

Committee in charge:

Professor Katherine Barbeau, Chair  
Professor Lihini Aluwihare  
Professor Todd Martz  
Professor Brian Palenik  
Professor Akif Tezcan

2019

Copyright

Angel Ruacho, 2019

All rights reserved.

The Dissertation of Angel Ruacho is approved, and it is acceptable in quality and form for publication on microfilm and electronically:

---

---

---

---

---

Chair

University of California San Diego

2019

## **DEDICATION**

For my family;

Mom, Dad, Enrique, Mariela, Joanna and Daisy

## EPIGRAPH

Your focus determines your reality

- *Qui-Gon Jinn*

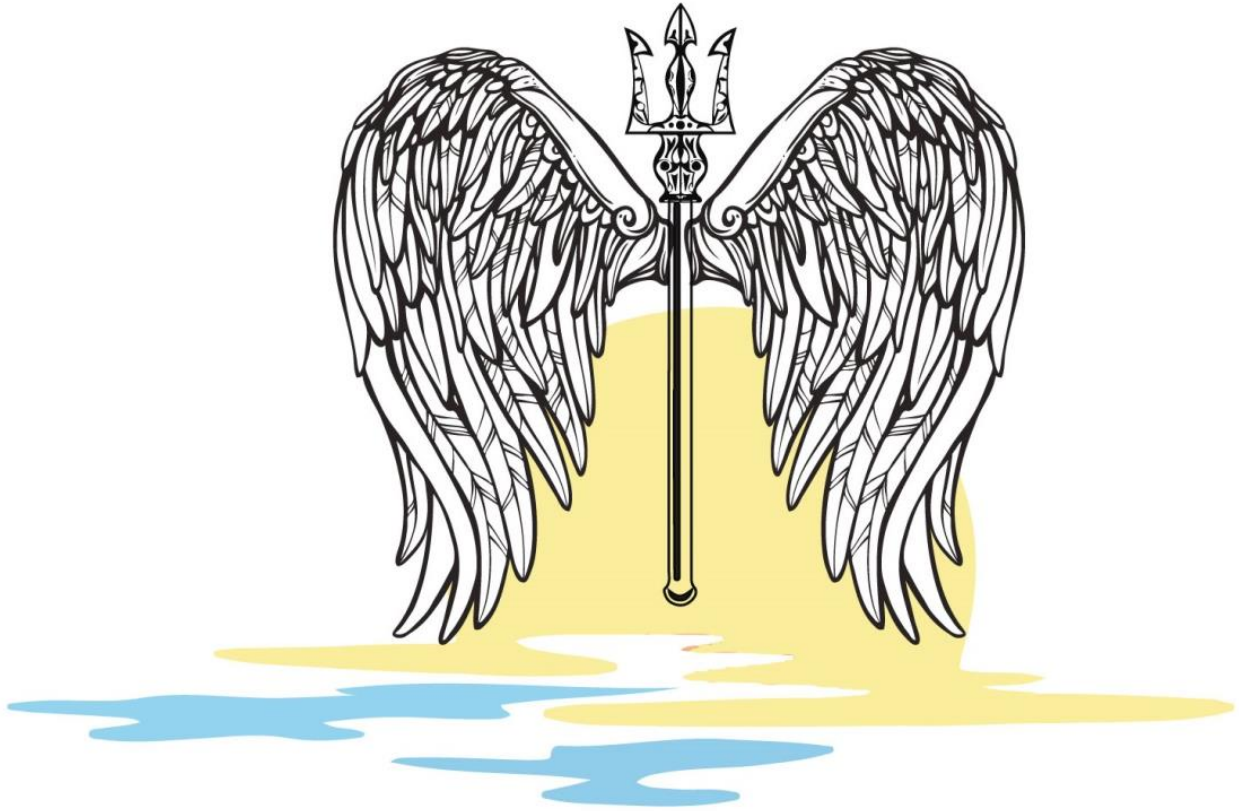


## TABLE OF CONTENTS

Signature page.....	iii
Dedication.....	iv
Epigraph.....	v
Table of Contents.....	vi
List of Figures and Tables.....	x
Acknowledgements.....	xiv
Vita.....	xv
Abstract of the Dissertation.....	xvi
Introduction.....	1
<i>References</i> .....	6
CHAPTER 1: Copper Speciation Across the U.S. GEOTRACES Equatorial Pacific Zonal	
Transect GP16.....	9
1.1 Abstract.....	10
1.2 Introduction.....	10
1.3 Methods.....	14
1.3.1 <i>Sample collection</i> .....	14
1.3.2 <i>Total dissolved copper measurements</i> .....	15
1.3.3 <i>Copper speciation</i> .....	16

1.3.4	<i>Reagents</i> .....	17
1.3.5	<i>EPZT analytical comparison with NAZT</i> .....	17
1.4	Results.....	18
1.4.1	<i>Dissolved copper</i> .....	18
1.4.2	<i>Copper speciation analytical and intercalibration tests</i> .....	18
1.4.3	<i>General trends in organic ligand features</i> .....	21
1.4.4	<i>Ligand features near the shelf</i> .....	21
1.4.5	<i>Ligand features within HNLC and the OMZ</i> .....	21
1.4.5	<i>Ligand features in the oligotrophic and hydrothermal region</i> .....	22
1.4.6	<i>Cu<sup>2+</sup> trends</i> .....	22
1.5	Discussion.....	23
1.5.1	<i>Copper speciation at the shelf</i> .....	23
1.5.2	<i>Copper speciation at the surface HNLC, OMZ, and oligotrophic waters</i> ...	24
1.5.3	<i>Copper speciation at the hydrothermal vent and plume</i> .....	26
1.5.4	<i>Copper speciation in the deep waters</i> .....	28
1.5.5	<i>Pacific vs. Atlantic comparison</i> .....	30
1.5.6	<i>Pacific vs. Atlantic dissolved copper comparison</i> .....	30
1.5.7	<i>Pacific vs. Atlantic copper speciation comparison</i> .....	30
1.6	Conclusion .....	33
1.6	Figures and Tables .....	35
1.7	Acknowledgements.....	50
1.8	References.....	51



## CHAPTER 2: A Novel Method for the Processing of Multiple Analytical Window

Electrochemical Titration Metal Speciation Data.....	57
2.1 Abstract.....	58
2.2 Introduction.....	58
2.3 Methods.....	63
2.3.1 <i>Sample collection</i> .....	63
2.3.2 <i>Total dissolved copper analysis</i> .....	64
2.3.3. <i>Reagents</i> .....	65
2.3.4 <i>Copper speciation analysis</i> .....	65
2.3.5 <i>Simulated unified analysis of multiwindow data</i> .....	66
2.3.6 <i>GP16 MAW processing</i> .....	67
2.4 Results and Discussion .....	68
2.4.1 <i>MAW processing results</i> .....	68
2.4.2 <i>GP16 MAW data</i> .....	72
2.5 Conclusion .....	76
2.6 Figures and Tables .....	78
2.7 Acknowledgements.....	87
2.8 References.....	88
CHAPTER 3: Copper Speciation and Toxicity in San Diego Bay.....	92
3.1 Abstract.....	93
3.2 Introduction.....	93

3.3 Methods.....	97
3.3.1 <i>Sampling and location</i> .....	97
3.3.2 <i>Reagents</i> .....	99
3.3.3 <i>Acid washing</i> .....	99
3.3.4 <i>Dissolved copper analysis</i> .....	99
3.3.5 <i>Dissolved carbon analysis</i> .....	100
3.3.6 <i>Synechococcus and picoeukaryote concentration determination</i> .....	100
3.3.7 <i>Copper speciation</i> .....	100
3.4 Results.....	102
3.4.1 <i>Hydrography</i> .....	102
3.4.2 <i>Dissolved organic carbon</i> .....	102
3.4.3 <i>Synechococcus results</i> .....	102
3.4.4 <i>Dissolved copper</i> .....	103
3.4.5 <i>Copper speciation</i> .....	104
3.5 Discussion .....	104
3.5.1 <i>Previous San Diego Bay work</i> .....	104
3.5.2 <i>Comparison with other harbors</i> .....	105
3.5.3 <i>Copper speciation in San Diego Bay</i> .....	108
3.5 Conclusion .....	112
3.6 Figures and Tables .....	113
3.7 Acknowledgements.....	124
3.8 References.....	125

## LIST OF FIGURES AND TABLES

<b>Table 1.1.</b> Results from intercomparison for GA03 samples. Data with a SA window of 2.5 $\mu\text{M}$ utilized NAZT analytical protocols and data with 5 $\mu\text{M}$ SA window utilized EPZT analytical protocols. ....	35
<b>Figure 1.1.</b> (A) Regional map of the U.S. GEOTRACES EPZT (GP16) cruise track of stations where speciation samples were collected. (B) Depth locations for speciation samples on top of oxygen concentrations along the transect. ....	36
<b>Figure 1.2.</b> Section plot of dissolved [Cu] across the transect as shown in Roshan et al. (2016) and contributed by Claire Till (pers. comm.).....	37
<b>Figure 1.3.</b> Titration curves for SA equilibration tests conducted with a 15 min SA equilibration and an overnight equilibration. ....	38
<b>Figure 1.4.</b> (A) Section plot of organic copper-binding ligands ([L]) across the transect. (B) Zoomed in section of [L] for near shore profiles. ....	39
<b>Figure 1.5.</b> Ligand concentrations for deep samples (> 2500 meters) with the same scale as in Fig. 4A. ....	40
<b>Figure 1.6.</b> Dissolved organic copper-binding ligand stability constants (logK) across the transect. ....	41
<b>Figure 1.7.</b> Free copper ion, $\text{Cu}^{2+}$ , concentrations displayed as $\log[\text{Cu}^{2+}]$ across the transect. ...	42
<b>Figure 1.8.</b> Upper ocean (< 500 m) concentrations of dissolved copper (dissolved Cu) along the transect (A), and (B) dissolved organic copper-binding ligands ([L])......	43

<b>Figure 1.9.</b> Cu concentrations ([Cu]) versus dissolved organic copper-binding ligands ([L]) in each of the water masses identified within the GP16 transect. Water masses identified in plot: Equatorial Subsurface Waters (ESSW), Pacific Deep Water (PDW), Equatorial Pacific Intermediate Water (EQPIW). .....	44
<b>Figure 1.10.</b> Excess ligand concentrations (e[L]) versus carbon-14 (C14_delta), a water mass age proxy, and overlaid with depth (colors). More negative C-14 values correspond to older water masses. ....	45
<b>Figure 1.11.</b> (A) Free Cu concentrations versus carbon-14 (C14_delta), a proxy for water mass age, with color overlays for depth, and (B) ligand binding strength (logK).....	46
<b>Figure 1.12.</b> Relationship plots of total dissolved Cu ligands versus DOC (A) and excess dissolved Cu ligands versus DOC (B) for the GP16 transect. ....	47
<b>Figure 1.13.</b> GP16 vs. GA03. (A) Dissolved Cu concentrations, (B) copper ligand concentrations, (C) excess ligand concentrations, and (D) Cu <sup>2+</sup> concentrations between the Pacific (GP16) and Atlantic (GA03) GEOTRACES zonal transects. ....	48
<b>Figure 1.14.</b> Plot of excess ligand and Cu binding ligands in both the Pacific (red) and Atlantic (blue) basins. ....	49
<b>Table 2.1.</b> Table of preset limits used in KINETEQL for MAW processing methods 1 and 3. Ligand concentrations are in nanomolar concentrations. ....	78
<b>Table 2.2.</b> MAW results for the three processing methods utilizing simulated data, as well as the source of the sensitivity. The error for the KINETEQL method is calculated as a root mean square error of all fitting parameters (Hudson et al., 2003), while the error for the PromCC method is reported as the “average error” (Omanović et al., 2015). ....	79

<b>Table 2.3.</b> Speciation results from analytical window optimization tests and speciation results from the use of all windows and simulated data.....	80
<b>Table 2.4.</b> Cu speciation results for GP16 MAW samples, processed with method (3) described in methods section.....	81
<b>Figure 2.1.</b> Conceptual figure of method (3) for processing MAW data, as described in the methods section. (A) is raw generated titration data which is (B) imported to KINETEQL for processing.....	82
<b>Figure 2.2.</b> (A) Map of GP16 speciation profile locations. (B) Profiles highlighted in red boxes were used for MAW analysis. The GP16 stations highlighted from right to left are station 1, 11, 26, and 36.....	83
<b>Figure 2.3.</b> Profile of GP16 station 26 displaying (A) [Cu], [L <sub>1</sub> ], [L <sub>2</sub> ], and total ligand ([L <sub>t</sub> ]) concentrations and (B) profile of free Cu ion concentrations.....	84
<b>Figure 2.4.</b> Profile of GP16 station 1 displaying (A) [Cu], [L <sub>1</sub> ], [L <sub>2</sub> ], and total ligand ([L <sub>t</sub> ]) concentrations and (B) profile of free Cu ion concentrations.....	85
<b>Figure 2.5.</b> (A) Plot of all L <sub>1</sub> ligand concentrations in the dataset with depth. (B) Plot of excess L <sub>1</sub> ligands with depth. ....	86
<b>Table 3.1.</b> Hydrography data collected with a YSI probe at each station, DO values with n.d. indicate no data available.....	113
<b>Table 3.2.</b> Results for dissolved Cu, Cu speciation, <i>Synechococcus</i> , picoeukaryotes. ....	114
<b>Table 3.3.</b> Dissolved copper, DOC data and DOC:Cu ratios for all samples in San Diego Bay (this study ) and San Francisco Bay (Buck and Bruland, 2005). Values in bold represent measurements from Shelter Island Yacht Basin (Station C). ....	115

**Figure 3.1.** Map of stations sampled within San Diego Bay., with the Shelter Island Yacht Basin highlighted by the red marker. Map generated using Google Earth. .... 116

**Figure 3.2.** Graph of tides during each sampling event ((A) summer (B) spring, (C) fall) with a red box to indicate the time and duration of sampling. Graph and data generated by NOAA. .... 117

**Figure 3.3.** Results of DOC analysis for stations during the three sampling events. No DOC data available for Station B in the summer, Station F in the spring, and Station G in the fall. .... 118

**Figure 3.4.** (A) *Synechococcus* counts for all sampling in San Diego Bay. (B) Picoeukaryote cell counts for each sampling in San Diego Bay. .... 119

**Figure 3.5.** Dissolved copper determined for each station during the three sampling periods.. 120

**Figure 3.6.** Free copper concentrations determined from MAW analysis through ProMCC. The red line represents the toxicity threshold for *Synechococcus*, anything above the red line exceeds the toxicity levels for *Synechococcus*..... 121

**Figure 3.7.** Free Cu concentrations determined from the 5µM SA analytical window results for the summer samples. The red line represents the toxicity threshold for *Synechococcus*, anything above the line represents Cu toxicity. .... 122

## ACKNOWLEDGEMENTS

I would like to acknowledge Professor Katherine Barbeau as chair of my committee. Kathy provided an endless amount of patience and support to me throughout my years here, she helped me refocus on the big picture of my research whenever I got lost in the analytical aspects of my work. I am forever grateful to her for taking a chance on me and helping better myself as a scientist and team player. I would also like to thank my committee members for their time and input: Lihini Aluwihare, Todd Martz, Brian Palenik, and Akif Tezcan.

Chapter 1, in part, is currently being prepared for submission for publication of the material with the following co-authors: Ruacho, Angel; Barbeau, Katherine; Bundy, Randelle; Parker-Till, Claire; Roshan, Saeed; Wu, Jingfeng. The dissertation author was the primary author on this paper.

Chapter 2, in full, is currently being prepared for submission for publication of the material with the following co-authors: Ruacho, Angel; Bundy, Randelle; Barbeau, Katherine; The dissertation author was the primary author of this paper.

Chapter 3, in full, is currently being prepared for submission for publication of the material with the following co-authors: Ruacho, Angel; Barbeau, Katherine; Nagakar, Maitreyi; Palenik, Brian. The dissertation author was the primary author of this paper.

## VITA

- 2011 Bachelor of Sciences, University of California Irvine
- 2014 Master of Sciences, Scripps Institution of Oceanography
- 2019 Doctor of Philosophy, University of California San Diego

## PUBLICATIONS

Boiteau, R.M., Till, C.P., **Ruacho, A.**, Bundy, R.M., Hawco, N.J., McKenna, A.M., Barbeau, K.A., Bruland, K.W., Saito, M.A. and Repeta, D.J., 2016. Structural characterization of natural nickel and copper binding ligands along the US GEOTRACES Eastern Pacific Zonal Transect. *Frontiers in Marine Science*, 3, p.243.

Stukel, M.R., Aluwihare, L.I., Barbeau, K.A., Chekalyuk, A.M., Goericke, R., Miller, A.J., Ohman, M.D., **Ruacho, A.**, Song, H., Stephens, B.M. and Landry, M.R., 2017. Mesoscale ocean fronts enhance carbon export due to gravitational sinking and subduction. *Proceedings of the National Academy of Sciences*, 114(6), pp.1252-1257.



## **ABSTRACT OF THE DISSERTATION**

Characterization of Copper-Binding Ligands and Copper Speciation in Open Ocean and Coastal  
Marine Systems using Electrochemical Methods

by

Angel Ruacho

Doctor of Philosophy in Oceanography

University of California San Diego, 2019

Professor Katherine Barbeau, Chair

This dissertation explores the role that organic ligands play in controlling copper speciation in a range of oceanic and coastal environments, using voltammetric methods. Chapter 1 details the analysis of samples collected on the 2013 U.S. GEOTRACES cruise in the Equatorial Pacific from Peru to Tahiti (GP16). This represents one of the largest copper speciation datasets to date, covering 22 full ocean depth profiles. Results demonstrate that copper ligands follow a similar pattern to dissolved copper of increasing concentrations with increasing depth. Free copper ion concentrations ( $[\text{Cu}^{2+}]$ ) also increase with depth. This dataset provides

insight into the impact of large-scale ocean circulation and water mass aging with respect to copper speciation, with increasing  $\text{Cu}^{2+}$  and decreasing excess ligand concentrations in the oldest waters of the deep Pacific.

In Chapter 2, copper speciation from select samples in the GP16 data set is analyzed via a novel processing protocol that enables competitive ligand exchange titrations at multiple competition strengths to be analyzed as a unified dataset. This method utilizes publicly available processing tools to determine a unified sensitivity for the data set as a whole. In this way the full spectrum of the copper-binding ligand pool can be most accurately characterized at a range of analytical windows, revealing both weak and strong ligands. For GP16 samples, this analysis reveals two classes of copper-binding ligands present throughout the oceanic water column, with the weaker  $L_2$  ligands present at higher concentrations. Strong  $L_1$  ligands are present at or above dissolved copper concentrations, dominating copper speciation especially in surface waters where  $L_1$  concentrations exceed that of dissolved copper.

Copper binding ligands play a vital role in maintaining low concentrations of the  $\text{Cu}^{2+}$  ion in coastal environments, which helps buffer such systems from copper toxicity. In Chapter 3, the processing method developed in Chapter 2 is applied to an assessment of the ligand pool and free copper ion levels in San Diego Bay, an impacted urban environment with high concentrations of recreational watercraft coated with copper-based antifouling paint. Sampling campaigns at 7 locations within the Bay took place in Summer 2015, Spring 2016 and Fall 2016. Samples for total dissolved copper and copper speciation were collected, as well as samples for *Synechococcus* concentrations as a biological indicator of copper toxicity. Results from the three samplings show elevated levels (30 –120 nM) of dissolved copper throughout the Bay and a ligand pool capable of buffering most of the locations within the Bay from reaching toxic levels

of the free copper ion. Shelter Island Yacht Basin, however, was consistently found to contain toxic levels of  $\text{Cu}^{2+}$ , results that show a relationship with the lowest *Synechococcus* concentrations in two out of the three samplings. Findings of this study are relevant for ongoing remediation and regulation efforts in San Diego Bay.

## INTRODUCTION

### **Background:**

Trace metals in the ocean like copper (Cu) play an important role in biological processes. Cu facilitates such biological functions as the acquisition of iron (Fe) (Peers et al, 2005), photosynthesis (Peers and Price, 2006) as well as ammonia oxidation by archaea (Walker et al, 2010). Cu in the ocean is found in low, nanomolar, concentrations and is subjected to biogeochemical cycles that exert various controls on the concentration of Cu. Inputs of Cu, and other trace metals, into the ocean range from shelf sediments (Boyle et al., 1981) to dust deposition (Buck et al., 2013), as well as upwelling of deep waters, remineralization, and input from rivers and estuaries. Removal processes for Cu involve adsorption to particles as well as uptake by micro-organisms. In addition to its biological requirement Cu can become a toxicant at high concentrations of the unbound  $\text{Cu}^{2+}$  ion (Brand et al., 1986). Excess  $\text{Cu}^{2+}$  concentrations are more commonly found in coastal regions where anthropogenic Cu is the primary source of Cu. Anthropogenic Cu is derived from runoff, brake pad dust, and Cu based antifouling paint (Rosselot, 2006; Earley et al., 2014). Various boat harbors have been shown to be under Cu stress (Moffett et al., 1997; Eriksen et al., 2001; Blake et al., 2004) due to the use of antifouling boat paint which slowly leaches Cu to prevent growth of algae and encrusting organisms on the hull.

The bioavailability of Cu is dependent on its chemical speciation, which is controlled by organic Cu binding ligands. The majority of dissolved Cu (> 99%) is bound by organic ligands (van den Berg, 1987), a circumstance which maintains low  $\text{Cu}^{2+}$  concentrations in many marine and aquatic environments. The identities of these Cu binding ligands are not entirely known, as it is difficult to identify specific chelators within the heterogeneous and dilute ligand pool.

However, microorganisms, like the marine cyanobacterium *Synechococcus*, have been shown to produce Cu ligands during Cu stress (Moffett et al. 1990; Moffett and Brand 1996).

Coccolithophores, which are calcifying marine organisms, have been shown to produce thiols capable of binding Cu as a response to increased Cu concentrations (Dupont et al., 2004). Humic acid has been suggested to contribute to Cu binding in marine systems, in particular as part of the weaker ligand pool. Cu binding by humic acid has been shown to occur in estuaries as well as marine environments (Whitby and van den Berg, 2015, Whitby et al., 2018; Abualhaija et al., 2015). Though some possible identities of Cu ligands have been proposed, the various sources and sinks of Cu ligands have not been entirely quantified. The few biologically or terrestrially derived Cu ligands that have been tentatively identified likely don't account for the majority of the ligand pool (Whitby et al, 2018). The GEOTRACES program, an international collaboration to study trace elements in the ocean, has conducted several basin-wide research cruises in an attempt to find out more information about the biogeochemical cycling of metal-binding ligands, as well as associated trace elements. As a result of this program full depth profiles have been collected across many ocean features such as oxygen minimum zones, upwelling regions, hydrothermal vents, oligotrophic waters, as well as coastal waters. The work through GEOTRACES may provide more insights into possible sources and sinks of naturally-occurring metal-binding organic ligands.

### **Electrochemical methods for ligand characterization:**

Analytical methods for characterizing Cu binding ligands are grounded in electrochemical methods introduced and refined decades ago. The current electrochemical approach binds the natural ligands with increasing concentrations of Cu until the natural ligands are saturated. Subsequently a well-known ligand is added to compete with the natural ligands for

Cu (Campos and van den Berg, 1994; Buck and Bruland 2005). The amount of metal bound by the added ligand is measured via cathodic stripping voltammetry, producing a reduction peak. The data generated is processed utilizing various fitting methods (Gerringa et al., 1995; Mantoura and Riley, 1975; Scatchard, 1949). Recent contributions from the speciation community have led to software packages capable of processing raw titration data and generating speciation parameters including ligand concentrations and binding constants (e.g. Omanović et al., 2015). The electrochemical method does not provide information on the chemical structure of the natural ligands detected.

Modifications to the analytical approach for characterizing ligands were proposed to capture more of the ligand pool (Bruland et al., 2000). Traditionally, most electrochemical analyses have utilized a single analytical window, i.e. a single concentration of the added ligand, which limits how much of the ligand pool is detected. By varying the analytical window, or concentration of the added ligand, more aspects of the ligand pool can be captured. A high analytical window will target stronger Cu ligands while a lower analytical window will target weaker ligands, thus the use of multiple analytical windows (MAW) was aimed at elucidating more information from the natural ligand pool. Early utilization of the MAW method (Buck and Bruland 2005; Bundy et al., 2013) detected both strong and weak Cu ligands, though analysis was limited to evaluating each analytical window individually and generating speciation data for each individual window. The inability to process MAW data as a single dataset was a hurdle overcome recently with the advent of advanced processing tools (Hudson et al., 2003; Omanović et al., 2015). The current use and processing of MAW titrations as a single dataset is providing a more natural view of the continuum of ligands in a sample, rather than the targeted ligands detected with the use of a single analytical window.

### **Impacts of copper ligands in coastal regions:**

Cu binding ligands play an important role for controlling the availability and toxicity of Cu both in open ocean and coastal regions. Organic ligands serve as an especially essential buffer against Cu toxicity in coastal regions like boat harbors. Ideal harbors are largely protected from the direct influences of the ocean, thus many harbors and marinas are located along the coast within protected regions with constrained circulation. The combination of protected waters and the high density of watercraft in some harbors can result in impacted sites for Cu toxicity. Organizations like the Port of San Diego utilize total dissolved Cu as an indicator of toxicity, but a more biologically relevant indicator is the unbound  $\text{Cu}^{2+}$  ion whose concentrations is determined by ambient Cu ligands. The use of MAW, for example, has been shown to reveal an excess pool of weak ligands capable of buffering San Francisco Bay from reaching toxic  $\text{Cu}^{2+}$  levels (Buck and Bruland, 2005). The continued use of MAW competitive ligand exchange techniques in coastal regions can help provide accurate determinations of the  $\text{Cu}^{2+}$  ion as well as the buffering ability of the ligand pool against further Cu input.

### **Thesis organization:**

Chapter 1 of the dissertation will focus on Cu speciation samples collected along a transect in the south Pacific from Peru to Tahiti as part of the GEOTRACES program. Samples from this chapter were analyzed with a single analytical window to characterize Cu ligands along the various ocean features crossed during the transect.

Chapter 2 is focused on the integration of available Cu speciation processing software for developing a method to analyze MAW titration data simultaneously. The method developed for MAW processing is applied to select profiles from the GEOTRACES transect analyzed in Chapter 1.

Chapter 3 utilizes the MAW processing method from Chapter 2 for evaluating locations within San Diego Bay for Cu toxicity. The use of a bioindicator, *Synechococcus*, is coupled with  $\text{Cu}^{2+}$  determinations for determining locations likely to be under Cu stress.



## REFERENCES

- Abualhaija, Mahmoud M., Hannah Whitby, and Constant MG van den Berg. "Competition between copper and iron for humic ligands in estuarine waters." *Marine Chemistry* 172 (2015): 46-56.
- Blake, A. C., D. B. Chadwick, A. Zirino, and I. Rivera-Duarte. "Spatial and temporal variations in copper speciation in San Diego Bay." *Estuaries* 27, no. 3 (2004): 437-447.
- Boyle, Edward A., Sarah S. Husted, and Susan P. Jones. "On the distribution of copper, nickel, and cadmium in the surface waters of the North Atlantic and North Pacific Ocean." *Journal of Geophysical Research: Oceans* 86, no. C9 (1981): 8048-8066.
- Brand, L. E.; Sunda, W. G.; Guillard, R. R. L., Reduction of marine-phytoplankton reproduction rates by copper and cadmium. *Journal of Experimental Marine Biology and Ecology* 1986, 96 (3), 225-250.
- Bruland, Kenneth W., Eden L. Rue, John R. Donat, Stephen A. Skrabal, and James W. Moffett. "Intercomparison of voltammetric techniques to determine the chemical speciation of dissolved copper in a coastal seawater sample." *Analytica Chimica Acta* 405, no. 1-2 (2000): 99-113.
- Buck, Clifton S., William M. Landing, and Joseph Resing. "Pacific Ocean aerosols: Deposition and solubility of iron, aluminum, and other trace elements." *Marine Chemistry* 157 (2013): 117-130.
- Buck, K. N., and Bruland, K. W. (2005). Copper speciation in San Francisco Bay: A novel approach using multiple analytical windows. *Mar. Chem.* 96, 185–198. doi:10.1016/j.marchem.2005.01.001.
- Bundy, R. M., Barbeau, K. A., and Buck, K. N. (2013). Sources of strong copper-binding ligands in Antarctic Peninsula surface waters. *Deep. Res. Part II Top. Stud. Oceanogr.* 90, 134–146. doi:10.1016/j.dsr2.2012.07.023.
- Campos, M. L. A. M., and van den Berg, C. M. G. (1994). Determination of copper complexation in sea water by cathodic stripping voltammetry and ligand competition with salicylaldoxime. *Anal. Chim. Acta* 284, 481–496. doi:10.1016/0003-2670(94)85055-0.
- Dupont, Christopher L., Robert K. Nelson, Saj Bashir, James W. Moffett, and Beth A. Ahner. "Novel copper-binding and nitrogen-rich thiols produced and exuded by *Emiliania huxleyi*." *Limnology and oceanography* 49, no. 5 (2004): 1754-1762.
- Earley, Patrick J., Brandon L. Swope, Katherine Barbeau, Randelle Bundy, Janessa A. McDonald, and Ignacio Rivera-Duarte. "Life cycle contributions of copper from vessel painting and maintenance activities." *Biofouling* 30, no. 1 (2014): 51-68.

- Eriksen, Ruth S., Denis J. Mackey, Rick van Dam, and Barbara Nowak. "Copper speciation and toxicity in Macquarie Harbour, Tasmania: an investigation using a copper ion selective electrode." *Marine Chemistry* 74, no. 2-3 (2001): 99-113.
- Hudson, Robert JM, Eden L. Rue, and Kenneth W. Bruland. "Modeling complexometric titrations of natural water samples." *Environmental science & technology* 37, no. 8 (2003): 1553-1562.
- Gerringa, L. J. A., P. M. J. Herman, and T. C. W. Poortvliet. "Comparison of the linear van den Berg/Ružić transformation and a non-linear fit of the Langmuir isotherm applied to Cu speciation data in the estuarine environment." *Marine Chemistry* 48, no. 2 (1995): 131-142.
- Mantoura, R. F. C., and J. P. Riley. "The analytical concentration of humic substances from natural waters." *Analytica chimica acta* 76, no. 1 (1975): 97-106.
- Moffett, J. W., R. G. Zika, and Larry E. Brand. "Distribution and potential sources and sinks of copper chelators in the Sargasso Sea." *Deep Sea Research Part A. Oceanographic Research Papers* 37, no. 1 (1990): 27-36.
- Moffett, J. W., and L. E. BRAND. 1996. The production of strong, extra-cellular Cu chelators by marine cyanobacteria in response to Cu stress. *Limnol. Oceanogr.* 41: 288-293.
- Moffett, James W., Larry E. Brand, Peter L. Croot, and Katherine A. Barbeau. "Cu speciation and cyanobacterial distribution in harbors subject to anthropogenic Cu inputs." *Limnology and Oceanography* 42, no. 5 (1997): 789-799.
- Omanović, Dario, Cédric Garnier, and Ivanka Pižeta. "ProMCC: an all-in-one tool for trace metal complexation studies." *Marine Chemistry* 173 (2015): 25-39.
- Peers, G., Quesnel, S. A., & Price, N. M. (2005). Copper requirements for iron acquisition and growth of coastal and oceanic diatoms. *Limnology and oceanography*, 50(4), 1149-1158.
- Peers, G., & Price, N. M. (2006). Copper-containing plastocyanin used for electron transport by an oceanic diatom. *Nature*, 441(7091), 341-344.
- Rosselot, Kirsten Sinclair. "Copper released from brake lining wear in the San Francisco Bay Area." Prepared for the Brake Pad Partnership by Process Profiles, Calabasas, CA (2006).
- Scatchard, George. "The attractions of proteins for small molecules and ions." *Annals of the New York Academy of Sciences* 51, no. 4 (1949): 660-672.
- van den Berg, C.M.G., 1987. Organic complexation and its control on the dissolved concentrations of copper and zinc in the Scheldt Estuary. *Estuarine Coastal Shelf Sci.* 24 (6), 785-797.

Walker, C.B., de la Torre, J.R., Klotz, M.G., Urakawa, H., Pinel, N., Arp, D.J., Brochier-Armanet, C., Chain, P.S.G., Chan, P.P., Gollagbir, A., Hemp, J., Hügler, M., Karr, E.A., Könneke, M., Shin, M., Lawton, T.J., Lowe, T., Martens-Habbena, W., Sayavedra-Soto, L.A., Lang, D., Sievert, S.M., Rosenzweig, A.C., Manning, G., Stahl, D.A., 2010. Nitrosopumilus maritimus genome reveals unique mechanisms for nitrification and autotrophy in globally distributed marine Crenarchaea. PNAS 107 (19), 8818–8823.

Whitby, Hannah, and Constant MG van den Berg. "Evidence for copper-binding humic substances in seawater." Marine Chemistry 173 (2015): 282-290.

Whitby, Hannah, Anna M. Posacka, Maria T. Maldonado, and Constant MG van den Berg. "Copper-binding ligands in the NE Pacific." Marine Chemistry 204 (2018): 36-48.

**CHAPTER 1: Copper Speciation Across the U.S. GEOTRACES Equatorial Pacific Zonal**

**Transect GP16**

## 1.1 ABSTRACT

Samples for organic copper (Cu)-binding ligand characterization were collected along the 2013 U.S. GEOTRACES Pacific (GP16) cruise transect from Peru to Tahiti. Full depth profiles of Cu speciation were collected across a dynamic range in oceanographic conditions ranging from a highly productive coastal region, an oxygen minimum zone, a high nutrient low chlorophyll (HNLC) region, an oligotrophic region and a hydrothermal vent plume. Speciation results, along with other results from the GP16 cruise, point towards a possible shelf sediment source near the coast of Peru for strong Cu-binding ligands. Surface waters from Peru to Tahiti exhibit elevated dissolved Cu and ligand concentrations near Peru and then decrease in concentration ( $< 1\text{nM}$ ) offshore towards the oligotrophic waters. Throughout most of the transect dissolved Cu and ligand concentrations are lower in the upper waters and increase with depth, with the highest concentrations near the ocean bottom. The hydrothermal vent sampled during the cruise does not seem to be a source for dissolved Cu but there is a slight elevation of Cu ligands at the vent site. When the GP16 dataset is compared with Cu speciation results from the North Atlantic GEOTRACES (GA03) cruise, similar vertical patterns are seen in both datasets. The most notable difference between the two datasets is seen in the deep waters of the Pacific. The older water masses of the Pacific are highlighted by higher concentrations of dissolved Cu, Cu binding ligands, and in the free Cu ion ( $\text{Cu}^{2+}$ ) relative to the deep Atlantic. Observations related to excess Cu ligands in both GP16 and GA03 point to a possible fraction of Cu inert to ligand exchange accumulating in the oldest deep waters sampled during GP16.

## 1.2 INTRODUCTION

Copper (Cu) is one of the essential trace metal micronutrients required for phytoplankton growth in the ocean in addition to other bioactive trace metals such as iron (Fe), zinc (Zn) and

cadmium (Cd). Cu is significant in that it facilitates various chemical and biological processes like Fe acquisition (Peers et al., 2005), photosynthesis (Peers and Price, 2006), ammonia oxidation (Walker et al., 2010), and nitrous oxide reduction (Stiefel, 2007). Cu is also known to act as a toxicant if the bioavailable free Cu ion ( $\text{Cu}^{2+}$ ) is present in a high enough concentration, as has been shown with cyanobacteria which are especially sensitive to Cu toxicity (Brand et al., 1986; Moffett et al., 1997). In natural oceanic waters over 99% of the dissolved Cu is bound by organic ligands (L) which maintain  $\text{Cu}^{2+}$  in generally low concentrations (van den Berg, 1987) thus buffering against Cu toxicity. Though the identity of these ligands is not entirely known it has been shown that micro-organisms like coccolithophores produce thiols capable of binding Cu (Dupont et al., 2004). Other compounds like humic acids have been found to also bind Cu in both freshwater and seawater systems (Kogut and Voelker, 2001; Whitby and van den Berg, 2015). The sources, sinks, and cycling of these ligands are not well defined and until recently virtually no ocean basin wide Cu ligand datasets were readily available. The international GEOTRACES program ([www.geotraces.org](http://www.geotraces.org)) has helped facilitate Cu ligand sample collection in remote oceanographic regions as well as generate basin-wide high resolution datasets (Jacquot and Moffett, 2015; Thompson et al., 2014; Heller and Croot, 2015).

Dissolved Cu, like Fe, is affected by both biological and chemical process as Cu exhibits a “hybrid” type vertical profile with biological drawdown at the surface and particle scavenging within the water column. Dissolved Cu concentrations increase gradually with depth, due to remineralization, but continue to undergo scavenging processes in intermediate waters (Bruland and Lohan 2003). Currently there are a limited but growing number of studies with deep water Cu ligand data to provide insight as to whether the observed increase in total dissolved Cu concentration with depth also leads to an increase in  $\text{Cu}^{2+}$  concentrations with depth. One early

study showed  $\text{Cu}^{2+}$  concentrations to increase with depth (Bruland and Franks, 1983) as ligand concentrations decreased, but more recent studies have shown that organic ligands throughout the water column are capable of buffering  $\text{Cu}^{2+}$  to low concentrations, approximately  $10^{-14}$  M, below levels considered to be toxic ( $10^{-11}$  e.g. Buck et al., 2012; Moffet and Dupont, 2007). These studies highlight the importance of understanding the controls on Cu ligand distributions in the water column and the changes ligands undergo, in particular between surface waters and deep waters (>2000m). To date the primary tool employed for the study of Cu speciation has been an electrochemical competitive ligand exchange analysis utilizing a known ligand to compete with the natural ligands (Campos and van den Berg 1994; Buck and Bruland 2005). The electrochemical technique enables characterization of the natural ligands with regard to both concentration and conditional binding constants for Cu, and with these two measurements (plus the total dissolved Cu concentration) the free Cu ion concentration can be calculated.

This study, conducted on the EPZT transect between Peru and Tahiti, provides insight into the cycling of Cu ligands across a range of ocean conditions. This study, led by the U.S. GEOTRACES program, provided a unique opportunity to generate high resolution data on various trace elements including Cu and organic Cu-binding ligands. Samples from full depth profiles were collected along the transect generating speciation data for samples as deep as 5000 meters while crossing an oxygen minimum zone (OMZ) and an oligotrophic subtropical gyre off the coast of Tahiti with a hydrothermal vent in the deep waters of the western section of the transect. The surface waters of the transect begin near the Peruvian coast, where deep nutrient and trace metal rich waters upwell to the surface fueling one of the most biologically productive coastal regions (Pennington et al., 2006). The open ocean waters over the Eastern half of the transect are characterized by low metal concentrations which can influence microbial

communities (Moore et al., 2013), while the offshore waters west of Peru are found to be a region of high nutrients and low chlorophyll (HNLC), thus are generally considered to be iron-limited.

The OMZ region is of particular importance to understanding the cycling of Cu ligands in low oxygen environments. The OMZ region off the South American coast has been shown to have elevated concentrations of ammonium oxidizing archaea (AOA) (Molina et al., 2010). AOA are known to contain Cu dependent electron transport systems for various genes (Walker et al., 2010) likely leading to an elevated demand for Cu. AOA are currently believed to play a bigger role in global nitrogen cycling than previously thought (Francis et al., 2005; Bayer et al., 2016). Understanding what kind of effects this region has on Cu ligands, as well as  $\text{Cu}^{2+}$  concentrations, can provide insights into the availability of Cu to AOA and if in-situ free Cu concentrations can be limiting, thus better constraining the impact of Cu availability on nitrogen cycling carried out by AOA in this region.

The hydrothermal plume found in the Western portion of the cruise has an extensive non-buoyant plume enriched with Fe and other trace metals (Resing et al., 2015), which may have extended the influence of the hydrothermal vent beyond a localized effect. The hydrothermal plume sampled during the GP 16 cruise originated from the East Pacific Rise which is known to have a fast spreading center (DeMets et al., 1990) possibly leading to large fluxes of metals as other hydrothermal vents have been shown to act as a source of trace metals like Fe (Yucel et al., 2011). During the GP16 cruise the plume was determined to have an elevated concentration of dissolved Fe, manganese and aluminum which was shown to be transported over 4000 km from the vent site (Resing et al., 2015). Evidence for the relative importance of hydrothermal vents as sources of dissolved Cu and Cu ligands is somewhat mixed (Sander et al., 2007; Sander and



Koschinsky, 2011; Jacquot and Moffett 2015), so the hydrothermal vent and extensive plume sampled during the EPZT can potentially provide further information on the role, if any, hydrothermal vents play in the cycling of Cu and Cu binding ligands.

In recent years, in part due to GEOTRACES activities, there has been a significant increase in the availability of Cu speciation data from the Atlantic (Jacquot and Moffett, 2015; Heller and Croot, 2015) and the Pacific (Jaquot et al., 2015; Thompson et al., 2014). In this context, the work presented here contributes to the growing knowledge of Cu speciation in the oceans. The data generated here gives insights into how unique ocean regimes can influence the speciation and distribution of Cu ligands as well as elucidate some of the similarities and differences in Cu speciation across different ocean basins.

## **1.3 METHODS**

### ***1.3.1 Sample collection***

Cu speciation samples were collected aboard the R/V *Thompson* during the U.S. GEOTRACES Eastern Pacific Zonal Transect (GP16) cruise at 22 stations in full depth profiles, (Fig 1.1). Samples were collected with the U.S. GEOTRACES carousel equipped with twenty four 12L Teflon coated GO-Flo bottles (General Oceanics) and a sensor package for pressure, conductivity, temperature, and oxygen (Cutter and Bruland, 2012). The carousel system was lowered over the side of the ship for discrete water sample collection. Upon recovery GO-Flo bottles were transferred to a clean van and pressurized for sub-sampling through clean Teflon tubing and an acid-cleaned 0.2  $\mu\text{m}$  Acropak capsule filter into a 500mL or 1L fluorinated low-density polyethylene (FLPE) bottles. Surface seawater samples were also collected from 3m depth with a trace metal clean tow-fish pump system while steaming between stations (Bruland et al., 2005), and were filtered in the same way as samples from the GO-Flos. Speciation samples

were then stored in a -20 C freezer. Samples for total dissolved Cu determination were collected simultaneously with Cu speciation samples, into low density polyethylene (LDPE) bottles, and acidified at sea with 4mL of 6M quartz-distilled HCl per liter of seawater, resulting in a pH of 1.7-1.8.

All speciation sampling bottles underwent a rigorous cleaning process: (1) soaked in a Citranox detergent bath for one week, (2) soaked in a 3N trace metal grade nitric acid bath for a week, (3) soaked in a 3N hydrochloric acid bath for a week, and (4) left to sit, in a laminar flow hood, for a week partially filled with clean Milli-Q (MQ) water before discarding the MQ and individually double-bagging each bottle. The Milli-Q water was passed through a purification system beginning with distilled water and going through a UV light to reduce organic carbon and then through several filters resulting in an ultra-pure water. In between each step the bottles were thoroughly rinsed with clean MQ a minimum of three times. Bottles for dissolved Cu analysis underwent a similar rigorous washing process with protocols found in Roshan et al., (2016) and Cutter et al., (2017).

### ***1.3.2 Total dissolved copper measurements***

Dissolved Cu for the Eastern section of the transect (stations 1-17) was analyzed using previously described methods (Biller and Bruland, 2012; Parker et al., 2016), with Cu preconcentrated by extraction onto a Nobias PA-1 resin from buffered seawater (pH 6.0) and analyzed on an Element XR inductively coupled plasma mass spectrometer (ICP-MS). Samples were UV-irradiated prior to preconcentration. Dissolved Cu samples from the Western section of the transect (stations 18-36) were analyzed according to an isotope dilution method (Wu and Boyle, 1997; Roshan and Wu, 2018) utilizing a multiple collector high resolution ICP-MS. This

method also utilizes a UV step prior to analysis. SAFe seawater standards were also determined to assess the accuracy of the method (Roshan et al. 2016).

### ***1.3.3 Copper speciation***

A competitive ligand exchange adsorptive cathodic stripping voltammetry (CLE-ACSV) method was utilized for the characterization of organic Cu binding ligands across the EPZT section. The basics of the CLE-ACSV method are detailed in Buck and Bruland (2005). This method employs the competition for Cu between a well-characterized ligand (salicylaldoxime; SA) and the natural seawater ligands to determine the thermodynamic stabilities of the natural ligands (originally published in Campos and van den Berg, 1994). The analytical methods and electrochemical parameters follow those outlined in Bundy et al. (2013) and Buck and Bruland (2005). Frozen samples were thawed in a refrigerator and vigorously shaken prior to analysis. The sample was then aliquoted (10 mL) into pre-conditioned Teflon vials and buffered with 1.5 M boric acid-ammonia (BA) to pH 8.2. The vials were spiked with increasing concentrations of Cu ranging from 0-25 nM, to saturate the natural ligands. The BA and Cu were equilibrated with the natural ligands for two hours, after which the competing ligand, SA, was added at a concentration of 5  $\mu$ M and left to equilibrate for a minimum of 15 minutes prior to analysis. EPZT speciation samples were analyzed in 11-point titrations carried out in duplicate, for approximately 51% of samples, on a controlled growth mercury electrode (Bioanalytical Systems Incorporated). Peaks generated from titrations were extracted using the ECDSOft software package and processed with ProMCC (Omanović et al., 2015) utilizing a single ligand model. An average and standard deviation for ligand concentration, logK, and free Cu concentration were calculated for samples with duplicate titrations. Samples without duplicate titrations utilized

ligand concentrations, logK, and free Cu values and confidence intervals determined within ProMCC,

#### ***1.3.4 Reagents***

The BA buffer was prepared by dissolving boric acid (Alfa Aesar, 99.99%) in 0.4 N aqueous  $\text{NH}_4\text{OH}$  (Optima, Fisher Scientific). A 4 mM stock of salicylaldehyde (SA; > 98%) was prepared in methanol (Optima LC/MS, Fisher Scientific) and replaced every six months or as needed. Cu standards (100 nM to 10  $\mu\text{M}$ ) were diluted from an atomic adsorption standard (1000 ppm, Spex CertiPrep) into pH 2 MQ water (acidified with Optima grade HCl).

#### ***1.3.5 EPZT analytical comparison with NAZT***

The analytical method employed for the EPZT closely followed the method used for the GEOTRACES North Atlantic Zonal Transect (NAZT) (Jacquot and Moffett, 2015) to facilitate cross comparison between the datasets. There are slight differences in analytical methods between the EPZT and NAZT samples along with a difference in the processing of data for ligand characterization. The difference in analytical methods is highlighted in the use of a 5  $\mu\text{M}$  SA concentration addition for electro-chemical analysis for EPZT samples, compared with 2.5  $\mu\text{M}$  SA concentration used for the NAZT. Furthermore, EPZT samples were analyzed with slightly higher Cu additions than NAZT samples, 0-25 nM Cu compared with 0-16 nM Cu, as well as utilizing a constant pH of 8.2 for analysis unlike NAZT samples which underwent pH adjustments to match in-situ pH, 7.6-8.2. An additional difference between EPZT and NAZT samples lies in data processing, with EPZT sample processing utilizing a newly available software package ProMCC (Omanovic et al., 2015). To ensure comparability with NAZT results an intercalibration was carried out by analyzing NAZT samples with analytical protocols employed in EPZT analysis.

## 1.4 RESULTS

### *1.4.1 Dissolved copper*

Dissolved Cu concentrations across the transect exhibited typical distribution patterns associated with dissolved Cu with depletion at the surface and linear increases in concentration with depth (Fig 1.2). Dissolved Cu concentrations ranged from 0.22 nM at the lowest in the offshore region of the transect to over 5 nM near the ocean bottom, with average concentrations around 2 nM. Near surface dissolved Cu concentrations were elevated, approximately 1-2 nM, just off the coast of South America and within Equatorial Subsurface Waters (ESSW) with a decline in surface concentrations (~0.80 nM) beginning around 100° W where ESSW mixes with Eastern South Pacific Intermediate Water (ESPIW) (Peters et al., 2018). In surface waters on the Western half of the transect, between the mixing region of ESSW and ESPIW to just offshore of Tahiti, concentrations decreased to levels between 0.40 and 0.60 nM. The oligotrophic region of the western section of the transect has the lowest Cu concentrations in surface waters, with a linear increase in Cu concentrations after 360 meters. Dissolved Cu concentrations around the hydrothermal vent, located at the middle of the transect, do not exhibit elevated concentrations. Dissolved Cu concentration data was provided by Saeed Roshan (Roshan and Wu, 2018) for the Western half of the transect while data from the Eastern half were provided by Claire Till. Dissolved Cu data for the GP16 cruise can be found online in the BCO-DMO database (<https://www.bco-dmo.org/project/499723>).

### *1.4.2 Copper speciation analytical and intercalibration tests*

A primary analytical difference between various labs involved in Cu speciation, (e.g. Croot et al. (2015); Whitby and van den Berg et al. (2015); Thompson et al. (2014); Buck and Bruland (2005); Jacquot and Moffett (2015); and Bundy et al. (2013)), is the equilibration time

with SA prior to electrochemical analysis. Currently, labs tend to use one of two methods to equilibrate the SA: (1) an SA equilibration time that is a 6 hr minimum, but typically lasting overnight (12-15 hrs); or (2) an SA equilibration time of 15 - 30 mins. In this work, equilibration tests of the added ligand were conducted, as there has been speculation that a 15-30 min equilibration is not enough to accurately determine ligand concentrations (Heller and Croot, 2015). A sample from GP16 (ID 2356) was used to test how varying the SA equilibration time prior to electrochemical analysis may affect ligand results. Two titrations were carried out, one with an SA equilibration of 15 min and one for 2 hours. Ligand concentration results from both titrations were very similar. From the 15 min equilibration a ligand concentration of  $2.83 \pm 0.35$  nM was detected with a  $\log K$  of  $13.77 \pm 0.01$  and the 2 hr equilibration result yielded a ligand concentration of  $2.68 \pm 0.23$  nM with a  $\log K$  of  $14.19 \pm 0.14$ . The 15 min equilibration titration was run in duplicate, but due to volume constraints the 2 hr equilibration titration only had one replicate. To test how an extended SA equilibration time may affect results, another GP16 sample (ID 2348) was used to perform titrations, in duplicate, with SA equilibrating for 15 min or overnight (Fig. 1.3). Duplicates from the 15 min equilibration produced an average ligand concentration of  $2.48 \pm 0.40$  nM and a  $\log K$  of  $13.81 \pm 0.25$  while titrations from the overnight equilibration produced an average ligand concentration of  $2.50 \pm 0.10$  nM and a  $\log K$  of  $14.02 \pm 0.08$ . A *t*-test was performed for results from the 15 min and overnight equilibration to show that there is no statistical difference between the two equilibration times. Results show that a minimum equilibration time of at least 15 min was sufficiently long in order to get comparable results to studies using a longer equilibration time. Due to the time intensity of processing a single sample as well as the volume of samples to process, the ability to use a shorter equilibration time can help process samples more efficiently. Samples from GA03 were

also analyzed using shorter equilibrations for SA, further allowing for a direct comparison between the two datasets by using the shorter equilibration time for the GP16 dataset.

As a check on external consistency, and given that reference materials for seawater Cu speciation are lacking, we undertook an intercomparison exercise with Jim Moffett using archived frozen samples from the 2010-2013 US GEOTRACES North Atlantic Zonal Transect (GA03; sample IDs 6806, 6808, 6952, 6868, 6870). We analyzed a number of samples from GA03 station 10, spanning the upper water column (samples 6806 and 6808, from 345 and 420 meters depth respectively), and deeper depths (samples 6952, 6868, and 6870 from 2101 meters, 4350 meters and 4440 meters depth respectively). We analyzed each sample twice, once replicating Moffett's GA03 analytical protocol (analytical window 2.5  $\mu\text{M}$  SA addition, pH buffered to 8.05 (6806 and 6808) or 7.95 (all deep samples) with EPPS, 10-point titration out to 16 nM Cu addition) and once using our own GP16 protocol (analytical window 5.0  $\mu\text{M}$  SA addition, pH buffered to 8.2 with boric acid, 11-point titration out to 25 nM Cu addition). Equilibration times for added Cu and SA as well as deposition times were the same between the two protocols. We used ProMCC (Omanovic et al. 2015) to process data from both protocols and calculate ligand concentration and logK. Results are shown in Table 1.1, along with comparison to ligand concentration and logK data previously reported by Moffett from near-depth samples analyzed from the same profile (samples 6804, 6932, 6946, 6864 and 6874). The consistency of results throughout the profile is encouraging, especially given that in addition to slightly different analytical protocols a different data processing technique (non-linear regression fitting, Jacquot and Moffett 2015 and ProMCC this study) was used. These results are consistent with previous intercalibration exercises for Cu organic speciation (Bruland et al. 2000; Buck et al. 2012), which included the methods used here and obtained excellent results, especially for free Cu ion

determinations, with predictable differences in ligand concentration and logK across different analytical windows

#### ***1.4.3 General trends in organic ligand features***

Cu binding ligand concentrations along the GP16 transect exceeded dissolved Cu concentrations with ligand concentrations increasing with depth in a similar fashion as dissolved Cu (Fig 1.4A). Ligand concentrations ranged from 0.75 to almost 9 nM with an average ligand concentration just above 3 nM. The lowest ligand concentrations were found in the offshore oligotrophic region of the transect, coinciding with the lowest dissolved Cu concentrations. The highest ligand concentrations were found in the near ocean bottom as well as in surface waters just off the coast of South America (Fig 1.4B) indicating the ocean bottom and shelf regions may be a source of Cu ligands. Similar to the dissolved Cu concentrations, the hydrothermal vent does not appear to be a strong and extensive source of Cu ligands. There may have been a very localized effect on Cu ligands due to hydrothermal input (Fig 1.5), as a slight elevation in the Cu ligand concentration can be observed close to the ridge crest. Ligand concentrations in the upper waters (300-1000 m) of the transect near Tahiti begin to increase above levels of the oligotrophic section of the transect.

#### ***1.4.4 Ligand features near the shelf***

Ligand concentrations on the shelf off Peru exhibited higher concentrations at the surface than at depth (Fig 1.4B) possibly due to elevated primary production near the coast or a terrestrial source. The near shore stations on the shelf off Peru were detected to have some of the strongest ligands, based on conditional stability constants, with an average logK of ~14 and a maximum logK of 14.53 (Fig 1.6).

#### ***1.4.5 Ligand features within HNLC and the OMZ***



Ligand concentrations away from the shelf stations and within the low oxygen waters (upper 500 m), between 80° and 110° west, continue to exhibit elevated concentrations. These concentrations were often twice the ligand concentrations detected in the offshore shallow waters of the transect. Ligands within this region are also found to have relatively strong logKs (13.5-14). Strong ligands, logKs >14, were detected below the OMZ in particular near the shelf between 500 and 2500 meters and near the ocean bottom possibly indicating a shelf or sediment source for strong ligands.

#### ***1.4.5 Ligand features in the oligotrophic and hydrothermal region***

The lowest ligand concentrations of the transect, similar to the dissolved Cu concentrations, were detected in the open ocean oligotrophic region of the transect. Concentrations at the surface were below 1 nM, and stayed relatively consistent in the upper 1000 m before increasing to ~6 nM in the deepest samples. There is a slight elevation in ligand concentrations just above the ridge crest of the hydrothermal vent, though the elevated ligand concentrations do not extend beyond the immediate vicinity above the hydrothermal vent. The region around the hydrothermal vent was found to have relatively “weak” ligands with logKs between 12 and 13. The rest of the western section of the transect has stronger ligands with logKs of 13 to 14.

#### ***1.4.6 Cu<sup>2+</sup> trends***

Cu<sup>2+</sup> concentrations were determined for the transect and are reported as a log value of the Cu<sup>2+</sup> concentration (Fig. 1.7). The lowest Cu<sup>2+</sup> concentrations were found in surface waters and primarily in waters near the South American coast with values ranging from log[Cu<sup>2+</sup>] of -14 to -15. The lowest Cu<sup>2+</sup> concentrations just off the coast coincided with some of the strongest and highest ligand concentrations. The highest Cu<sup>2+</sup> concentrations are found in the deep waters

and in near bottom waters with the majority of values ranging from  $\log[\text{Cu}^{2+}]$  -11 to -12. Over the whole transect the average  $\log[\text{Cu}^{2+}]$  is -13, with higher concentrations found in the deep waters especially around the hydrothermal vent where the weaker ligands of the transect were detected.

Within the OMZ,  $\text{Cu}^{2+}$  concentrations are slightly elevated from concentrations immediately off the coast, but is bound both above 100 m and below 250 m by regions with higher levels of the free Cu ion. The region of slightly lower  $\text{Cu}^{2+}$  concentrations levels within the OMZ may be due to biological processes within the OMZ utilizing free Cu. Low  $\text{Cu}^{2+}$  concentrations were also found in the upper waters in the offshore oligotrophic region between Tahiti and the hydrothermal vent where the lowest dissolved Cu concentrations were also found. At depth,  $\text{Cu}^{2+}$  concentrations are elevated within the proximity of the hydrothermal vent reaching  $\log[\text{Cu}^{2+}]$  levels of -12.3.

## 1.5 DISCUSSION

### 1.5.1 Copper speciation at the shelf

Work on the GP16 cruise by the Charette group documented a plume of  $^{228}\text{Radium}$  in intermediate waters (1000-2500 m) coming from the continental shelf off the coast of Peru (Sanial et al., 2018). This observation coincides with some of the strongest Cu ligands detected over the transect, suggesting that shelf sediments may be the ultimate source of the strong ligands ( $\log K > 14$ ; Fig. 1.6). High levels of  $^{228}\text{Radium}$  are also observed near the ocean bottom just off Peru, and this region is also highlighted by ligands of similar strength as those detected in the intermediate waters with elevated  $^{228}\text{Radium}$ . The high levels of  $^{228}\text{Radium}$  and strong ligands detected in near bottom waters further implicate the sediments as a possible source of strong ligands. Past studies have determined sediments to be a source of Cu ligands, but these

studies were done in estuaries and lagoons with the majority of the ligands detected having logKs of 7-11, much weaker than those reported for this study (Shank et al., 2004; Skrabal et al., 2000). A study by Chapman et al. (2009) in Venice Lagoon also observed the sediments as a possible source of Cu ligands with logKs of 12.5-14, more in line with our study. In addition, Chapman et al. (2009) also detected benthic fluxes of thiols, known to bind Cu, which they postulated as making up part of the L<sub>2</sub> ligand pool. Further evidence for shelf derived ligands comes from a shelf region in the Antarctic Peninsula which attributed shelf sediments as a source of Cu ligands (Bundy et al. 2013), although in that work the shelf was found to be a source of weaker ligands relative to Antarctic Circumpolar Current waters. It is possible that the shelf sediments off Peru may be a source of strong Cu ligands. Notably this region is also where Buck et al. (2018) primarily detected the highest concentrations of L<sub>1</sub> Fe binding ligands for GP16.

### ***1.5.2 Copper speciation at the surface HNLC, OMZ, and oligotrophic waters***

Surface waters across the transect experienced the most dynamic changes in terms of dissolved Cu and ligand concentrations. Concentrations for both parameters were highest near the coast within the highly productive upwelled waters and in the HNLC region, and were lowest in the oligotrophic region near Tahiti. The trend of high dissolved Cu and ligand concentrations near the coast to decreasing concentrations with distance from shore was first reported in Boiteau et al. (2016). Boiteau et al. (2016) also showed that Cu ligands, detected via a solid phase extraction technique followed by analysis using liquid chromatography, were a diverse and complex assemblage of organic polar compounds highlighting the heterogeneity of the ligand pool, particularly near the shore. Boiteau et al. (2016) highlighted that offshore surface waters on this transect had lower concentrations of both Cu and Cu binding ligands, with a portion of these ligands being comprised of structurally well-defined ligands. This was in contrast with the

undefined polar compounds that were detected in the productive coastal waters that were not able to be chromatographically resolved. The region just off Peru was also shown to have some of the lowest  $\text{Cu}^{2+}$  concentrations,  $\sim 10^{-14}$  M, possibly due to biological utilization of the free Cu ion or production of strong Cu ligands to either alleviate Cu stress from the influx of Cu from deeper waters and shelf sources or to facilitate the uptake of Cu needed for cellular metabolic processes. AOA have been shown to reach Cu limitation at  $\text{Cu}^{2+}$  concentrations of approximately  $10^{-13}$  M (Amin et al., 2013). This threshold is higher than the  $\text{Cu}^{2+}$  concentrations observed for this region, likely causing AOA near the coast to be experiencing Cu limiting conditions. High abundances of AOA coinciding with very low concentrations of  $\text{Cu}^{2+}$  have previously been reported in this same region by Jacquot et al. (2013). Amin et al. (2013) presented evidence that AOA do not necessarily produce Cu binding ligands when Cu-limited, thus potentially other organisms or shelf sediments may be the source of the strong ligands detected. The OMZ waters of GP16 overlapped with the HNLC waters and were highlighted by elevated concentrations of Cu ligands with relatively high binding strengths ( $\log K$  13-14) and low free Cu concentrations. Findings within the OMZ are in line with findings by Jacquot et al. (2013) in the OMZ off Peru. Similar to the Jacquot et al. (2013) study, some of the lowest dissolved Cu and free Cu concentrations within the OMZ are found in the region around the nitrite maxima, with Cu concentrations increasing below the nitrite maxima in our study. AOA in this region may be Cu-limited, which may affect the oxidation of ammonia. However, it has been shown through incubation experiments (Ward et al., 2008) that denitrifying microbes in the OMZ are not influenced by additional Cu. This interplay between Cu availability and the organisms either oxidizing ammonia or performing denitrification may have an impact on nitrogen cycling in this region.

Near surface waters in the outer edge of the HNLC region just off the coast (~80° W) displayed elevated Cu and ligand concentrations. From this point of elevated Cu and ligand concentrations in the upper surface waters, concentrations of both parameters exhibited a sharp decrease extending west toward Tahiti. Buck et al. (2018) demonstrated that the HNLC waters of GP16 have low Fe concentrations as well as a negative Si\*, a proxy for Fe limitation, indicating the likelihood that there is Fe limitation occurring in these waters. Low dissolved Cu concentrations of ~0.82 to 1.5 nM were also observed in these waters. Diatoms require Cu for uptake of Fe and low concentrations of Cu have been shown to induce Fe limitation (Peers et al., 2005). It is possible that the interplay between Cu and Fe and their low concentrations in HNLC waters are leading to Fe limitation in diatoms of this region.

The open ocean waters in this oligotrophic region are not in close contact with upwelled nutrient rich waters or near sediment inputs, likely leading to the lower concentrations detected. It is possible that both the lack of ligand sources in this region and the degradation of coastal ligands result in lower ligand concentrations offshore. Dissolved Cu concentrations observed in the open ocean offshore region are in line with previously reported values for the open ocean in the North Pacific (Bruland, 1980; Boyle et al. 1981). As noted earlier, the offshore region was shown via liquid chromatography combined with mass spectrometry techniques to have well defined ligands that bind both dissolved Cu and nickel (Boiteau et al., 2016). The sources of these ligands are undetermined, but could be related to biological sources due to metal limitation. Cu plays an important role for Fe acquisition in low Fe regions (Peers et al., 2005; Maldonado et al., 2006; Semeniuk et al. 2016) similar to the oligotrophic waters sampled, possibly leading to the strong ligands detected offshore deriving from a biological source.

### ***1.5.3 Copper speciation at the hydrothermal vent and plume***

Throughout the Western half of the transect a hydrothermal plume was observed (Jenkins et al., 2018) with enrichment of  $^3\text{He}$  ~2500 meters. Roshan and Wu (2018) detected elevated Cu concentrations below 3000 meters, indicating that the hydrothermal vent is unlikely to be a strong source of dissolved Cu in contrast with other trace metals like Fe, manganese, and aluminum which have been shown to have elevated concentrations at the vent site and extend out away from the vent within the plume (Buck et al., 2018; Resing et al., 2015). Although model results, from another study, predict 14% of deep ocean Cu to come from hydrothermal fluids (Sander and Koschinsky, 2011), from available data it seems this vent in the southern East Pacific Rise (EPR) is not a significant source for deep ocean dissolved Cu. Roshan and Wu (2018) posit that with efficient transport of hydrothermal particles there could be reversible exchange of Cu into the dissolved phase, indicating the hydrothermal vent has a slight effect on dissolved Cu. Lee et al. (2018), however, demonstrated that particulate Cu around the southern EPR vent is found in sub-nanomolar concentrations, in stark contrast with particulate Fe, indicating that there may not be enough particles for Cu to account for the solubilization of Cu into the dissolved phase. When dissolved Cu data from the Mid-Atlantic Ridge vent sampled in GA03 is compared to the GP16 vent there is a relative lack of a Cu signal from the southern EPR vent, yet hydrothermal vents in both basins do demonstrably have elevated dissolved Fe concentrations in surrounding deep waters (Buck et al., 2015, 2018; Resing et al., 2015).

Cu binding ligands do show a small increase just above the GP16 hydrothermal vent, but the extent is limited and is not shown in other surrounding data points like it is for Fe binding ligands (Buck et al. 2018). A similar result of elevated Cu ligands near the vent was seen during the GA03 cruise, though the ligands found in GA03 had higher binding strengths than those detected during this study. Elevated concentrations of both dissolved Cu and Cu binding ligands

have been found previously in vent fluids (Sander et al., 2007), with Cu ligands reaching concentrations of 4000 nM and logKs of 12.5 – 13.5. Samples for the Sander et al. (2007) study were taken at the Brothers volcano in the Pacific with one sample coming directly from a black smoker. The Sander study also found thiols that can serve as Cu binding ligands, suggesting hydrothermal fluid may provide an influx of dissolved Cu and Cu binding ligands when vent fluids mix with ambient seawater. It is not clearly evident that the southern EPR hydrothermal vent sampled for GP16 is a source of Cu and Cu ligands. It is possible that much of the Cu is associated with Fe-oxides in sediments around the vent, as was found in Chakraborty et al. (2014). Dissolved Cu has been observed to undergo rapid adsorption onto hydrothermal particulate phases with preferential removal from the neutrally buoyant plume, likely with sulphides in the Mid-Atlantic Ridge (German et al., 1991). Effects of hydrothermal vents on Cu and Cu-binding ligands may be highly localized to the vicinity of the vent. At the Mid-Atlantic Ridge an excess of Cu and Cu binding ligands (>700 nM) (Cotte et al., 2018) were observed from samples collected 1-2 m from a vent orifice, while the closest sample above the GP16 vent orifice is about 20 m above the vent at station 18.

#### ***1.5.4 Copper speciation in the deep waters***

Based on the water mass analysis done by Peters et al. (2018), the deep waters in the GP16 transect are made up primarily of Pacific Deep Water (PDW), one of the oldest water masses in the world ocean. The dissolved Cu and Cu ligand concentrations associated with the old deep PDW waters are found to have an almost one to one relationship, in contrast with shallower water masses like ESSW and Equatorial Pacific Intermediate Water (EQPIW) which are found to have a surplus of Cu ligands relative to dissolved Cu (Fig. 1.9). The influence of the PDW water mass can also be seen in the low excess ligands (eL) found in the deep waters along

the GP16 transect. Excess ligands are defined as,  $eL = \text{Total Ligands} - \text{dissolved Cu}$ , and thus represent the Cu-free ligands present in a given sample. The low concentrations of eL found in PDW is in contrast with surface waters which have a higher excess ligand concentration (Fig 1.10). The low excess ligand concentrations of the deep waters are also paired with higher concentrations of the free Cu ion (Fig 1.11A). The accumulation of Cu in the deep waters may be reducing the Cu binding ligand capacity, leading to the low eL concentration and higher free Cu ion concentrations found. This low eL found in the deep waters may also be indicative of an inert fraction of Cu. When plotting total ligands and excess ligands versus dissolved organic carbon (DOC) (Fig 1.12) the high ligand concentration at low DOC concentrations as well as the low eL concentrations at low DOC concentrations point to a possible fraction of exchange inert dissolved Cu. If there is a presence of inert Cu, this could lead to an overestimation of the Cu ligand detected with our electrochemical technique (Gledhill and Buck, 2012).

Along with the low excess ligand concentrations found in deep waters, some of the weakest ligands were also detected (Fig 1.11B). Together the presence of both weaker ligands as well as low excess ligand concentration cause the free Cu to be higher in deep waters. Overall, however, the logKs of Cu-binding ligands in the oldest waters are not much weaker than in other water masses. Thus it may be that eL has more of an effect on free Cu rather than the ligand binding strength. The ligands in deep waters are almost completely titrated with dissolved Cu and this corresponds to the region with the highest fraction of colloidal (0.02-0.2  $\mu\text{m}$ ) Cu. Below 3000 m in the Western section of the transect approximately 39% of dissolved Cu is in the colloidal as opposed to the truly soluble (< 0.02  $\mu\text{m}$ ) fraction (Roshan and Wu, 2018). The high concentrations of dissolved Cu, Cu binding ligands and  $\text{Cu}^{2+}$  in the deep waters of the Pacific



have also been observed in the North Pacific, with concentrations within range of those reported for GP16 (Moffett and Dupont, 2007; Tanita et al., 2015).

### ***1.5.5 Pacific vs. Atlantic comparison***

Along the GP16 cruise section approximately 326 samples for Cu speciation were analyzed with 51% of the samples analyzed in duplicate titrations. The GP16 cruise crossed a strong upwelling region coupled with an OMZ and reaching an oligotrophic offshore region with a hydrothermal vent located in the middle of the transect. The GA03 cruise in the North Atlantic shared similar oceanographic features as the GP16 cruise with 275 samples analyzed for Cu speciation. An intercomparison was done to ensure the feasibility of comparison between GP16 and GA03 Cu speciation results due to slight differences in analytical procedures, as outlined in the methods and results section.

### ***1.5.6 Pacific vs. Atlantic dissolved copper comparison***

Both, GP16 and GA03, exhibited similar patterns in dissolved Cu concentrations with low concentrations at the surface and linearly increasing concentrations with depth. The GA03 average dissolved Cu concentration was found to be ~1 nM while the GP16 average dissolved Cu was higher at 2 nM. A major difference between the two ocean basins is found in the overall maximum Cu concentration in the Pacific basin being higher at 5.80 nM compared to 3.07 nM in the Atlantic basin (Jacquot and Moffett, 2015). This is likely a result of the high percentage of the older Pacific water found throughout the GP16 transect (Peters et al., 2018) highlighting the accumulation of Cu in old water masses.

### ***1.5.7 Pacific vs. Atlantic copper speciation comparison***

Samples from both the Pacific and Atlantic transects were processed with a single ligand model and thus only one ligand is reported for each sample. Ligand concentrations in both basins

largely followed Cu distributions and increased with depth, with the highest ligand concentration found in deep waters particularly near the ocean bottom. The Pacific basin had overall higher concentrations of Cu ligands with ligand concentrations maxing out just under 9 nM, while ligand concentrations in the Atlantic max out at 5.26 nM (Fig. 1.13B). The higher ligand concentrations in the Pacific may be due to degradation of stronger ligands along the ocean conveyor, leading to increased concentrations of slightly weaker ligands in the older waters of the Pacific, however the differences in binding strength between surface and deep waters was not significant. The older waters may also have an effect on the excess ligand concentration detected in both basins. When plotted against ligand concentrations in both basins it is clear that excess ligands in the Pacific are lower relative to total ligand concentrations in the Atlantic (Fig 1.14). In the Pacific the highest ligand concentrations, typically in deep waters, are found with the lowest excess ligand concentrations. We speculate that the low excess ligands in the Pacific, despite the high concentrations of total ligands, may be due to an inert fraction of dissolved Cu. It may be possible that as water masses age, an inert fraction of dissolved Cu begins accumulating to account for the low eL in the deep Pacific, while the deep Atlantic with younger water masses generally has eL at a 1:1 ratio with total ligands. Data is not available for GA03 but Roshan and Wu (2018) show the highest concentrations of colloidal Cu, at least in the western half of the transect, are found in the deep waters below 2500 meters with concentrations between 1.5 and 2 nM while the upper waters generally had colloidal Cu in concentrations of ~0.5 nM. Kogut and Voelker (2003) demonstrated that colloids could physically sequester Cu rendering it kinetically inert to ligand exchange. The aged waters of the deep Pacific may hold a fraction of Cu in an inert state, which would have consequences for accurate measurements of ligand parameters through electrochemical methods. It should be noted that this trend of older water

masses having lower relative excess Cu ligand concentrations is perceptible both within the EPZT dataset itself (e.g. comparing shallow vs deep water masses), and when comparing the deep water EPZT and NAZT datasets to each other. This robust and oceanographically consistent observation increases confidence in the intercomparability of the EPZT and NAZT Cu speciation datasets.

The binding stability constants determined in the Pacific are similar to those that were found in the Atlantic, as both basins had logKs spanning a range between 12 and 15. Strong ligands in the Pacific were detected near the surface of coastal waters of Peru as well as at depth just off the shelf and near the ocean bottom. Strong ligands ( $\log K > 13.5$ ) were also found in the Atlantic near the surface and off the shelf, likely with a fraction of these ligands in both basins deriving from biological sources near the surface and possibly from shelf sediments. A contrast between the two basins is seen in the binding strengths of deep Pacific ligands, particularly around the hydrothermal vent. Ligands in this region had a range in logKs of 12.5-13, while ligands in the deep Atlantic basin were found with logKs generally above 13. It appears ligands in the older Pacific waters around the hydrothermal vent may have lost some of their binding capabilities over time, or that the hydrothermal vent is a source of weaker ligands. The binding strengths of the detected ligands are not significantly weaker than those of Cu ligands detected throughout PDW dominated waters, however, so other factors may be responsible for the binding capacity loss. Overall, free Cu ion concentrations in the Pacific were found to be higher than in the Atlantic (Fig 1.12C) and free Cu in the upper 1000 meters of the transect are in line with previously reported values in the North Pacific (Coale and Bruland 1988; Moffett and Dupont 2007; Jacquot et al., 2013). This suggests that ligands are less able to buffer the free Cu ion activity as deep water masses age. A loss in binding capacity was also seen in organic Fe-binding

ligands, as only 46% of samples with PDW had detectable L<sub>1</sub> ligands (Buck et al. 2018), with the majority of Fe ligands in the older PDW waters being made up primarily of weaker L<sub>2</sub> and L<sub>3</sub> ligands. Buck et al. (2018) reported a secondary peak appearing in most of the scans during electrochemical analysis for deep samples of the Pacific for Fe binding ligands. They attributed the secondary peak to humic-like substances (HS) binding to Fe. Although this was not observed in deep samples for Cu ligands, HS may be a possible ligand binding Cu in the deep waters of the Pacific as it has been shown that HS can bind both Fe and Cu (Abualhaija et al., 2015). HS Cu ligands have been shown to have conditional stability constants lower than the strongest Cu ligands (logK < 14) in line with a L<sub>2</sub> ligand class (Whitby and van den Berg, 2015) and similar to the binding strengths observed in this study.

## **1.6 CONCLUSION**

The GP16 dataset is highlighted by high dissolved Cu concentration in the surface near the shelf and in deep waters, particularly near the sediments. Dissolved Cu concentrations throughout the transect generally increased with depth along with Cu ligand concentrations. The regions of high dissolved Cu near the shelf and in the deep waters coincide with the Cu ligands having the highest logKs detected, as well as elevated levels of <sup>228</sup>Radium indicating the sediments as a possible source of the strong ligands. Surface waters in the oligotrophic region have the lowest dissolved Cu and ligand concentrations detected over the transect, in line with previous reported dissolved Cu in the open ocean North Pacific. The hydrothermal vent sampled during the cruise does not act as a source of dissolved Cu in contrast with other trace metals like Fe, manganese, and aluminum, but there is limited evidence that the vent may have been a localized source for weaker Cu binding ligands. The identity of Cu ligands detected is still not entirely known, but the potential for deep ocean HS likely being detected by Buck et al. 2018

indicates that part of the deep Cu ligand pool may be bound to HS. This study provided the second large scale Cu speciation data set for the U.S. GEOTRACES program which highlights the effects water mass age has on Cu speciation.

The GP16 and GA03 GEOTRACES transects both share similar oceanographic features which provides for comparison between observations. Cu speciation observations in the GP16 transect shared similarities with results observed in the GA03 transect. In both ocean basins the hydrothermal vents don't act as sources of dissolved Cu despite a notable increase in dissolved iron. The hydrothermal vents seem to be a source of Cu ligands, although observed elevated ligand concentrations in the Pacific are not as extensive as in the Atlantic. Both ocean basins show evidence for strong ligands originating from sediments and in the Pacific observations of strong ligands tended to coincide with a strong sediment signal based on  $^{228}\text{Ra}$ . A major disparity between the two ocean basins is that Cu ligand concentrations, dissolved Cu concentrations, and free Cu concentrations are higher at depth in the Pacific (Fig. 1.13). This is likely due to the older waters of the Pacific accumulating Cu and titrating ligands in the deep waters leading to low eL and an increase in free Cu ions in the deep Pacific relative to the deep Atlantic. The difference in eL between the two basins is also notable (Fig. 1.14). The deep old waters in GP16 are found to have high concentrations of Cu ligands, but relatively low concentrations of eL, while the deep waters in GA03 are found to have Cu ligands and eL in similar concentrations. This difference may be driven by the water mass age effect, leading to an inert fraction of Cu in the old Pacific Deep Waters in GP16. More work is needed to assess the possible existence of this inert Cu fraction and whether it is due to colloids, a mixed organic fraction, water mass age, or another factor.

## 1.6 FIGURES AND TABLES

**Table 1.1.** Results from intercomparison for GA03 samples. Data with a SA window of 2.5  $\mu\text{M}$  utilized NAZT analytical protocols and data with 5  $\mu\text{M}$  SA window utilized EPZT analytical protocols.

Sample ID	SA Window	Depth (m)	[L] nM	logK	Lab
6804	2.5 $\mu\text{M}$	285	$1.49 \pm 0.15$	13.5-13.7	Moffett
6806	2.5 $\mu\text{M}$	345	$2.02 \pm 0.46$	13.68 +/- 0.34	Barbeau
6806	5 $\mu\text{M}$	345	$1.87 \pm 0.53$	13.76 +/- 0.28	Barbeau
6808	2.5 $\mu\text{M}$	420	$2.92 \pm 0.22$	13.52 +/- 0.06	Barbeau
6808	5 $\mu\text{M}$	420	$2.77 \pm 0.73$	13.14 +/- 0.28	Barbeau
6932	2.5 $\mu\text{M}$	800	$2.77 \pm 0.27$	13.0-13.2	Moffett
6946	2.5 $\mu\text{M}$	1650	$5.20 \pm 0.82$	12.5-12.7	Moffett
6952	2.5 $\mu\text{M}$	2101	$3.30 \pm 0.11$	13.80 +/- 0.04	Barbeau
6952	5 $\mu\text{M}$	2101	$3.40 \pm 0.34$	13.56 +/- 0.18	Barbeau
6864	2.5 $\mu\text{M}$	3900	$4.26 \pm 0.30$	12.9-13.0	Moffett
6868	2.5 $\mu\text{M}$	4350	$4.88 \pm 1.40$	13.09 +/- 0.30	Barbeau
6868	5 $\mu\text{M}$	4350	$4.66 \pm 0.84$	12.71 +/- 0.16	Barbeau
6870	2.5 $\mu\text{M}$	4440	$5.20 \pm 1.23$	12.70 +/- 0.25	Barbeau
6870	5 $\mu\text{M}$	4440	$5.50 \pm 1.07$	12.71 +/- 0.16	Barbeau
6874	2.5 $\mu\text{M}$	4531	$2.29 \pm 0.13$	13.5-13.7	Moffett

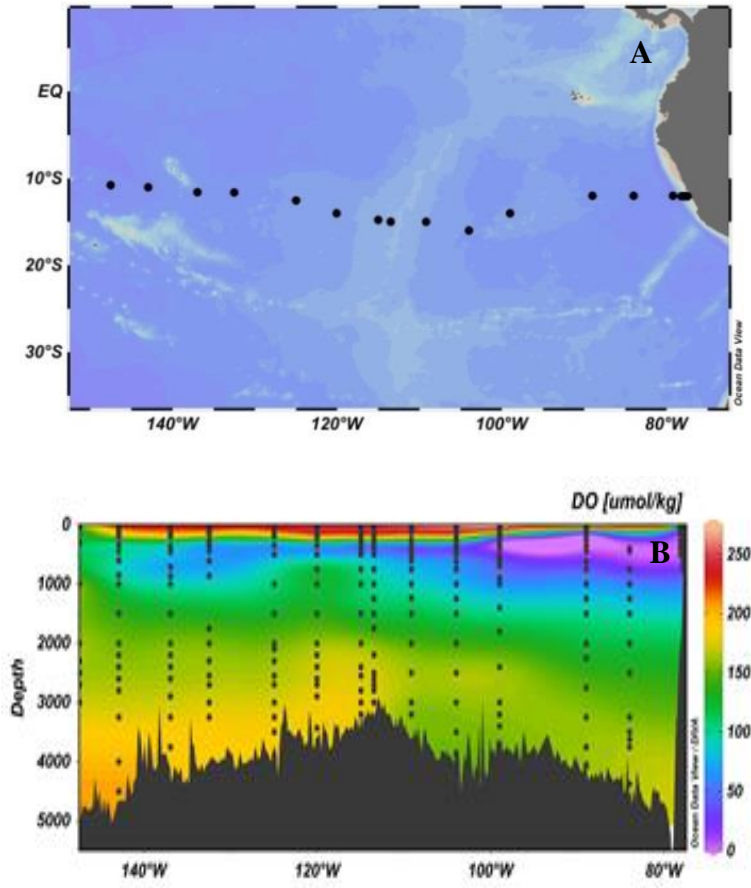


**Figure 1.1.** (A) Regional map of the U.S. GEOTRACES EPZT (GP16) cruise track of stations where speciation samples were collected. (B) Depth locations for speciation samples on top of oxygen concentrations along the transect.

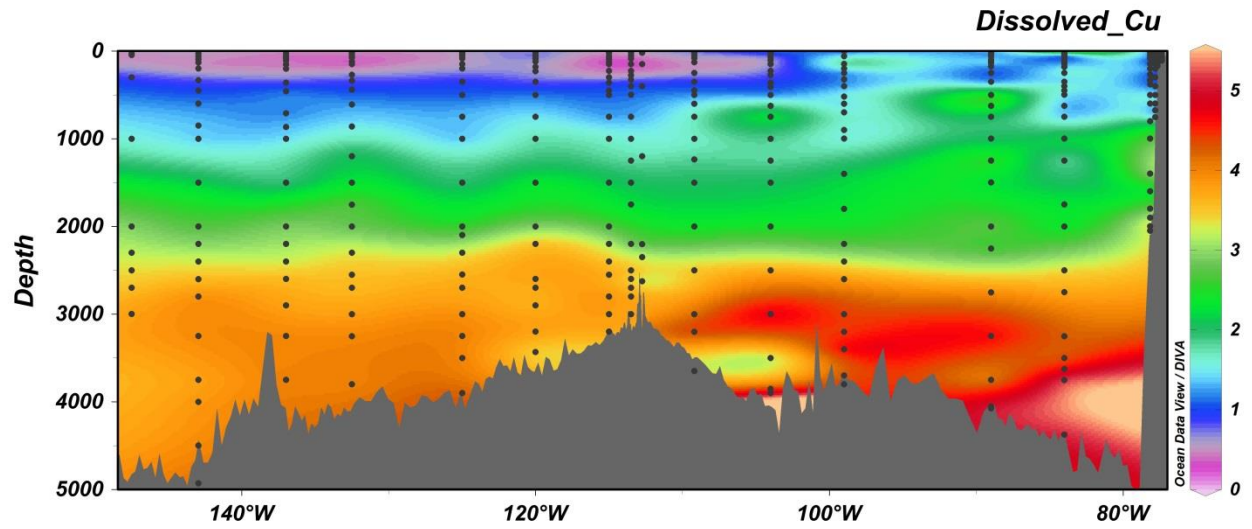


**Figure 1.2.** Section plot of dissolved [Cu] across the transect as shown in Roshan et al. (2016) and contributed by Claire Till (pers. comm.).



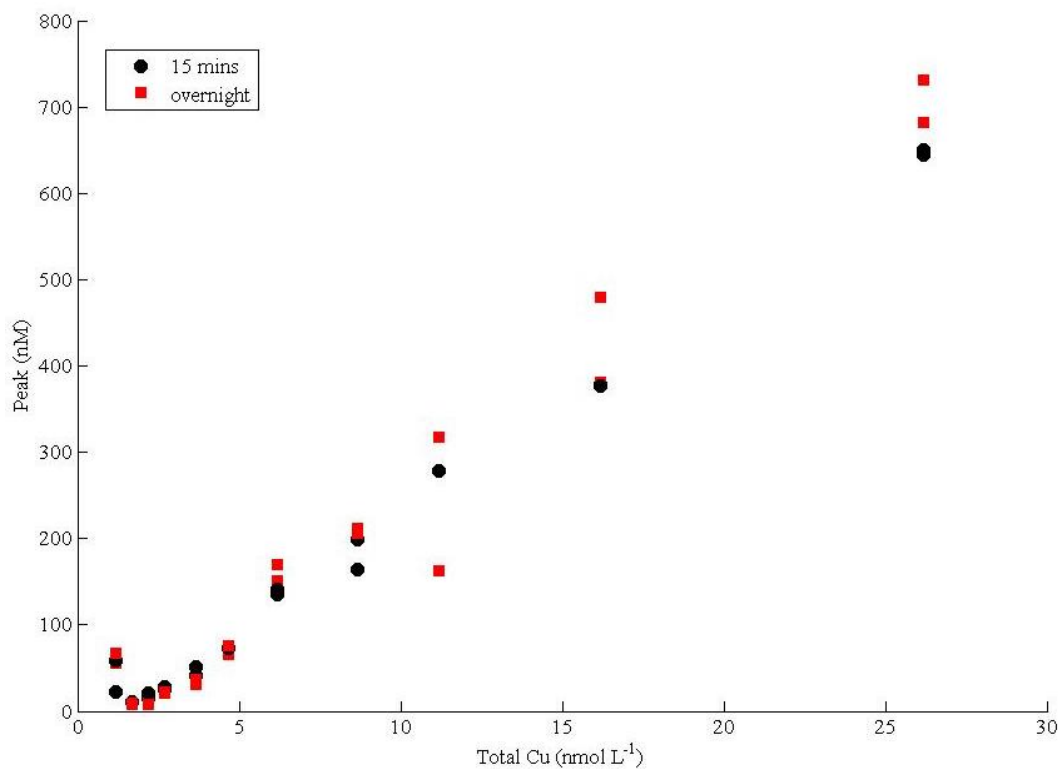


**Figure 1.3.** Titration curves for SA equilibration tests conducted with a 15 min SA equilibration and an overnight equilibration.

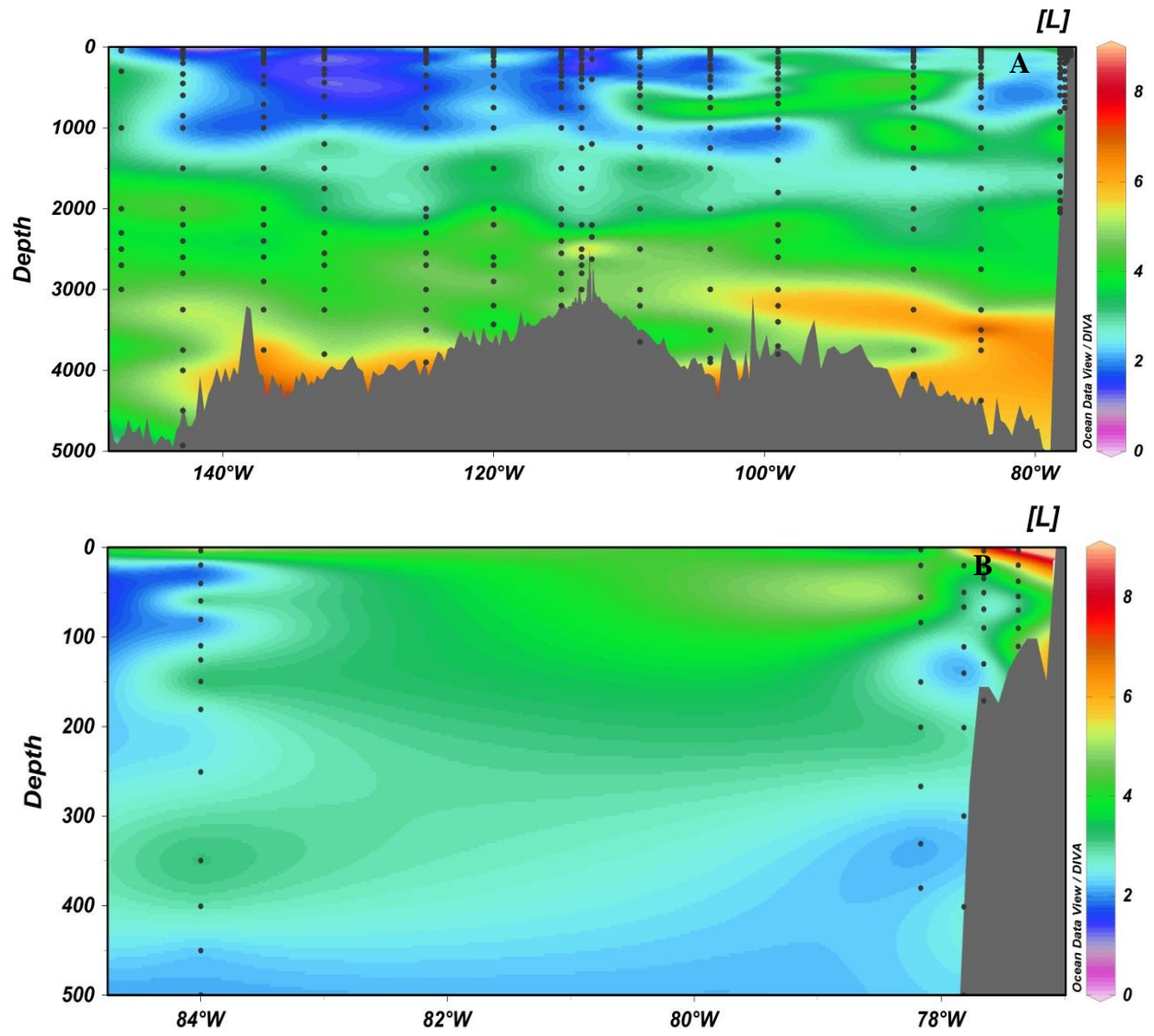


**Figure 1.4.** (A) Section plot of organic copper-binding ligands ([L]) across the transect. (B) Zoomed in section of [L] for near shore profiles.

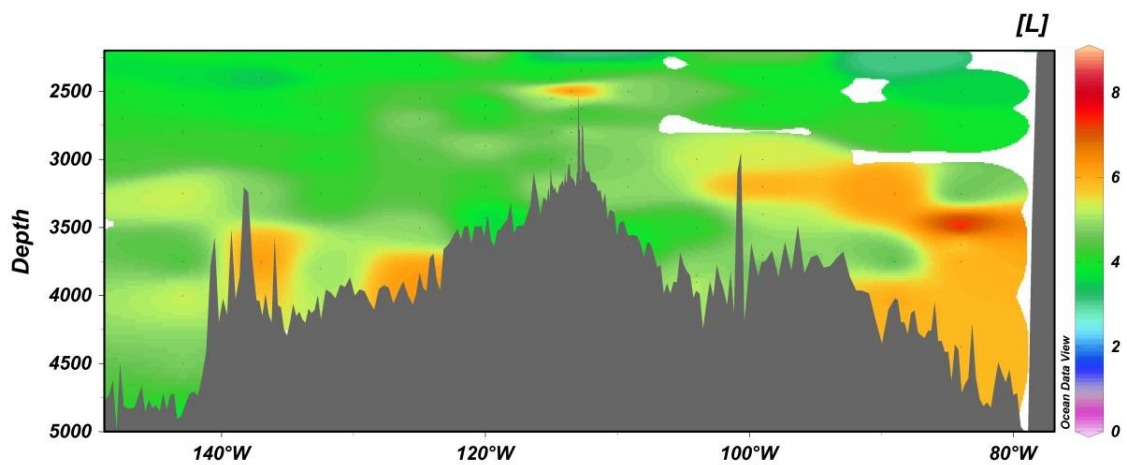


**Figure 1.5.** Ligand concentrations for deep samples (> 2500 meters) with the same scale as in Fig. 4A.

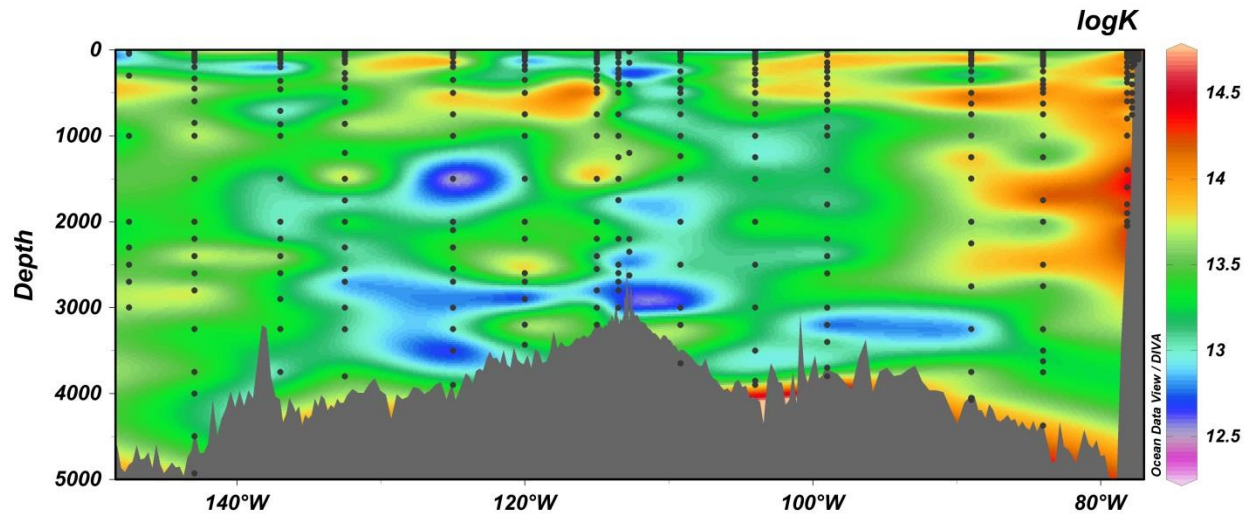


**Figure 1.6.** Dissolved organic copper-binding ligand stability constants ( $\log K$ ) across the transect.

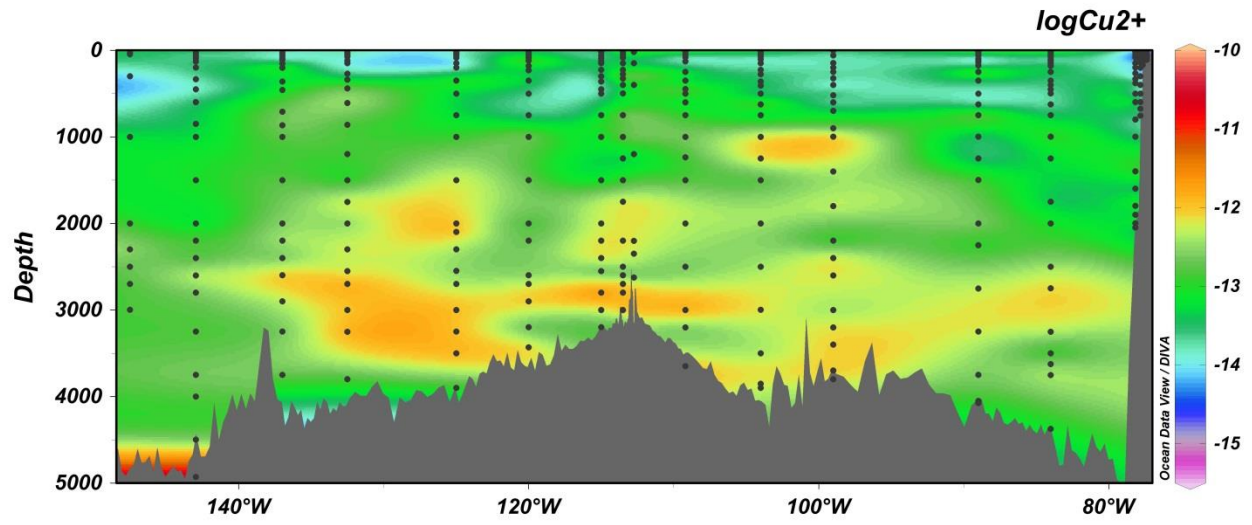


**Figure 1.7.** Free copper ion,  $Cu^{2+}$ , concentrations displayed as  $\log[Cu^{2+}]$  across the transect.

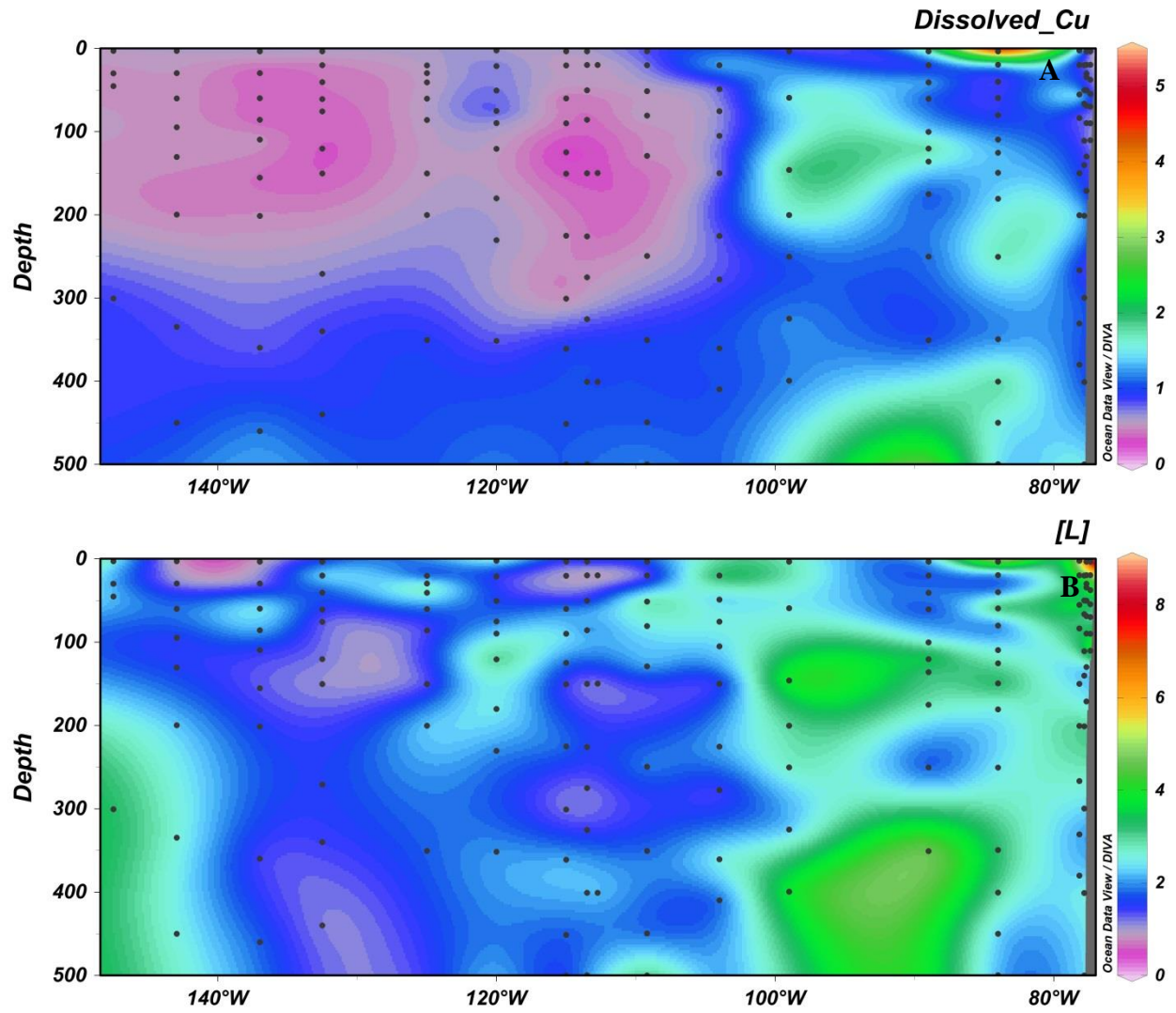


**Figure 1.8.** Upper ocean (< 500 m) concentrations of dissolved copper (dissolved Cu) along the transect (A), and (B) dissolved organic copper-binding ligands ([L]).

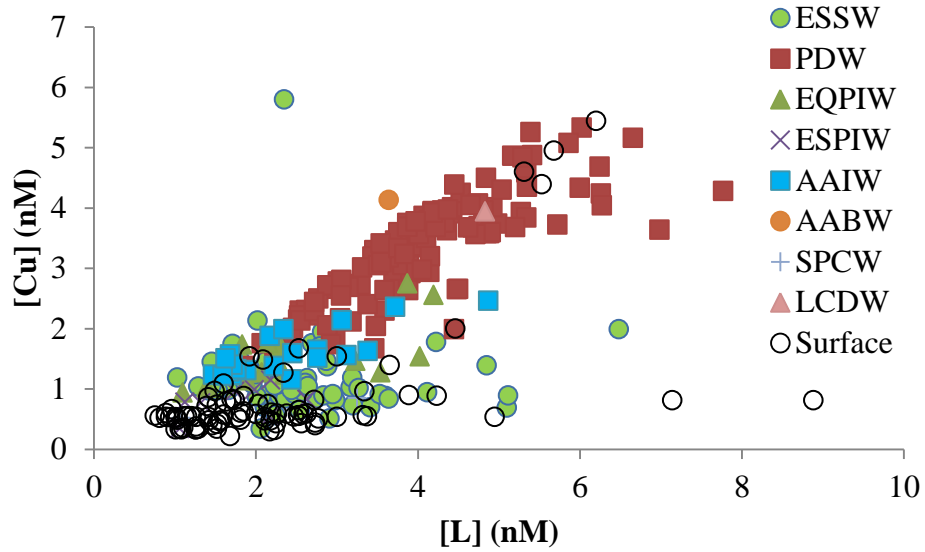


**Figure 1.9.** Cu concentrations ([Cu]) versus dissolved organic copper-binding ligands ([L]) in each of the water masses identified within the GP16 transect. Water masses identified in plot: Equatorial Subsurface Waters (ESSW), Pacific Deep Water (PDW), Equatorial Pacific Intermediate Water (EQPIW), Eastern South Pacific Intermediate Water (ESPIW), Antarctic Intermediate Water (AAIW), Antarctic Bottom Water (AABW), South Pacific Central Water (SPCW), Lower Circumpolar Deep Water (LCDW).

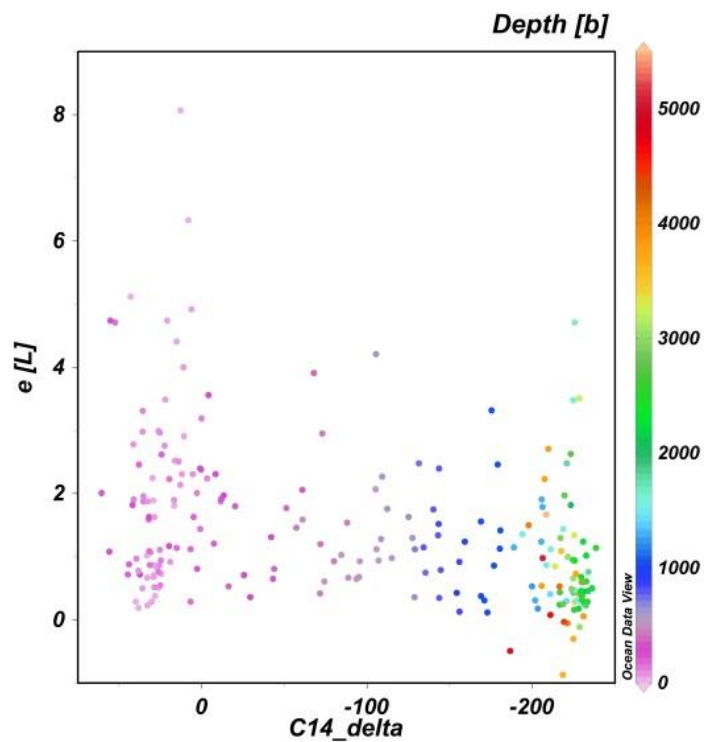


**Figure 1.10.** Excess ligand concentrations ( $e[L]$ ) versus carbon-14 ( $C14\_delta$ ), a water mass age proxy, and overlaid with depth (colors). More negative C-14 values correspond to older water masses.



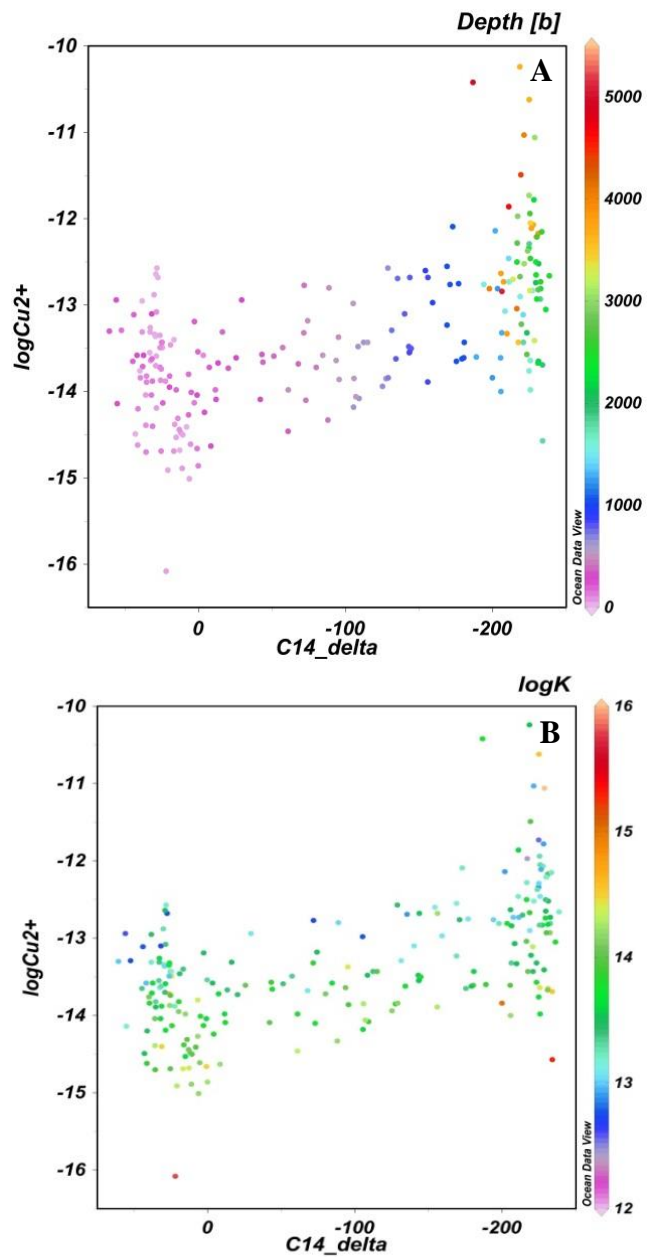


**Figure 1.11.** (A) Free Cu concentrations versus carbon-14 ( $\text{C14\_delta}$ ), a proxy for water mass age, with color overlays for depth, and (B) ligand binding strength ( $\log K$ ).

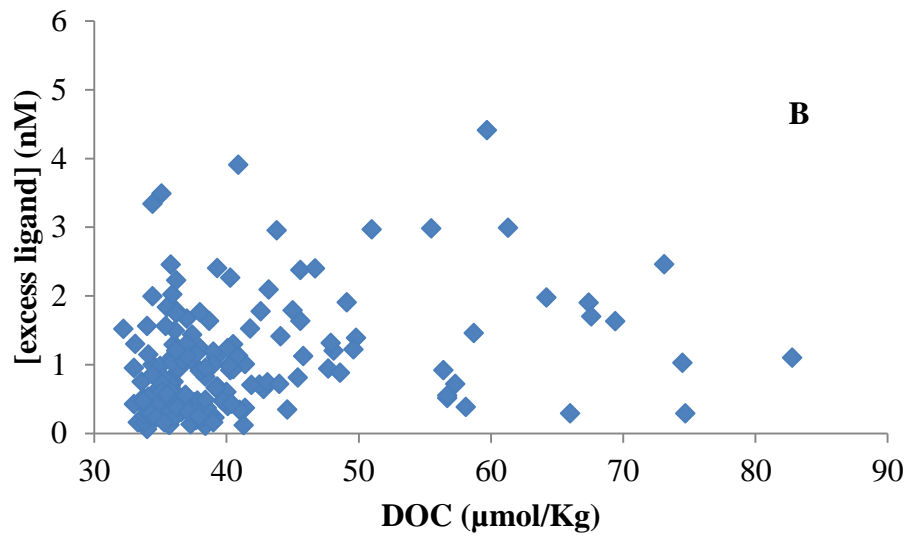
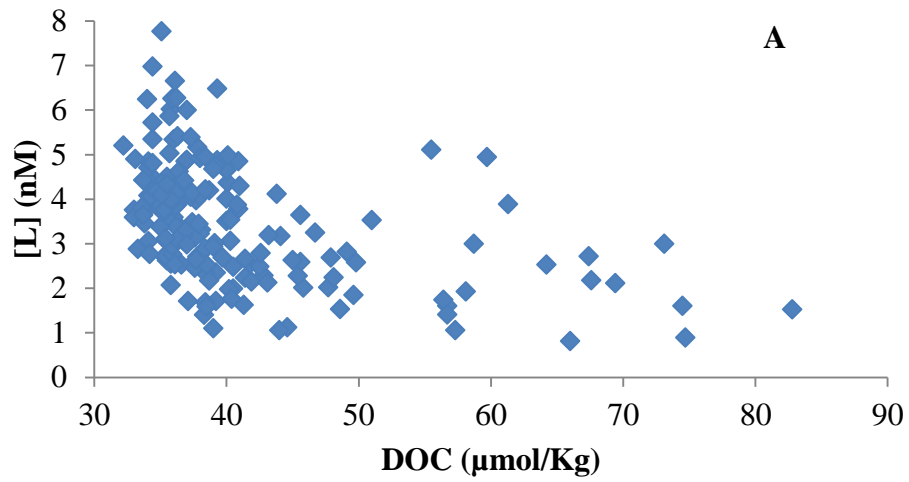


**Figure 1.12.** Relationship plots of total dissolved Cu ligands versus DOC (A) and excess dissolved Cu ligands versus DOC (B) for the GP16 transect.

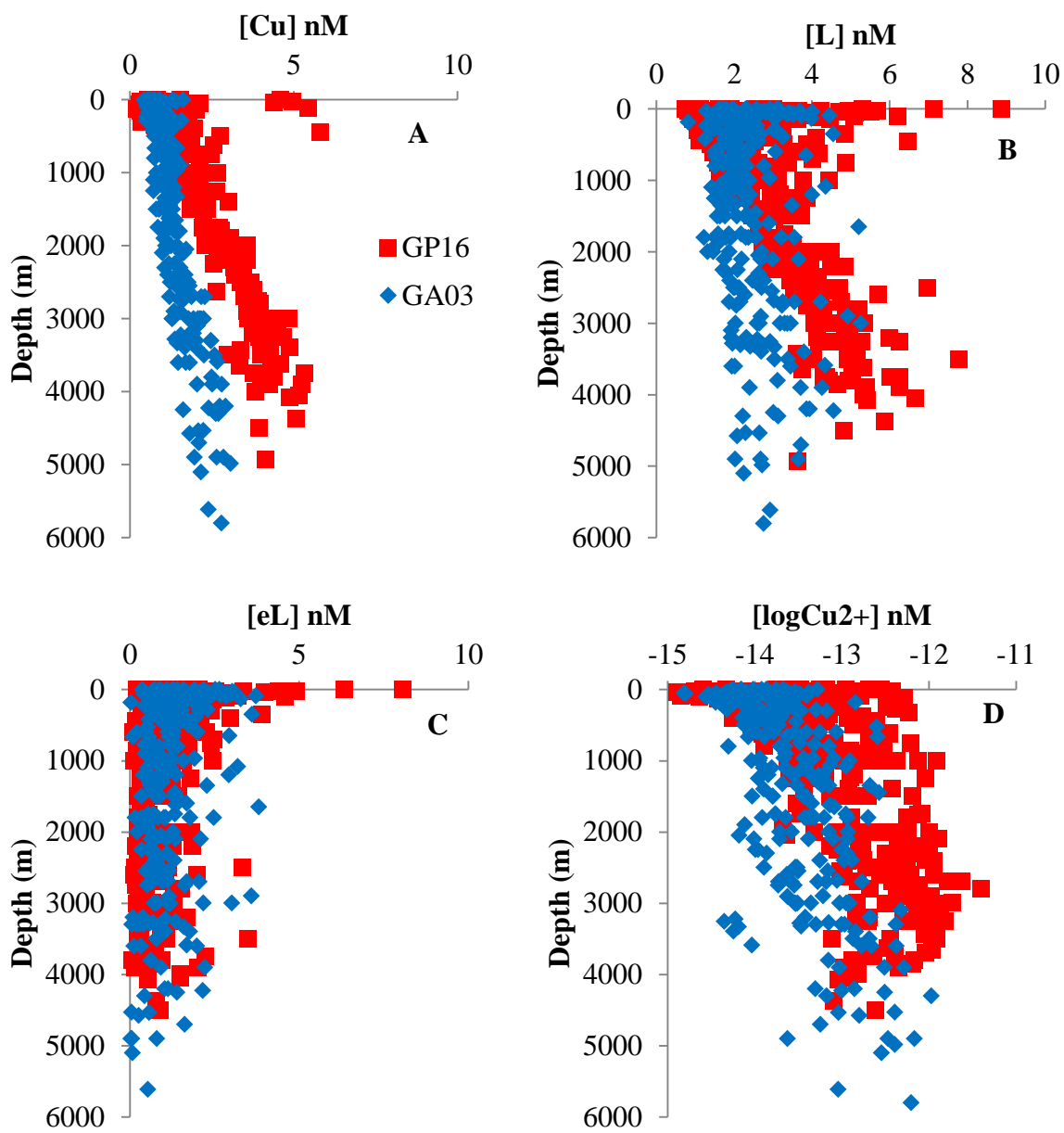


**Figure 1.13.** GP16 vs. GA03. (A) Dissolved Cu concentrations, (B) copper ligand concentrations, (C) excess ligand concentrations, and (D) Cu<sup>2+</sup> concentrations between the Pacific (GP16) and Atlantic (GA03) GEOTRACES zonal transects.

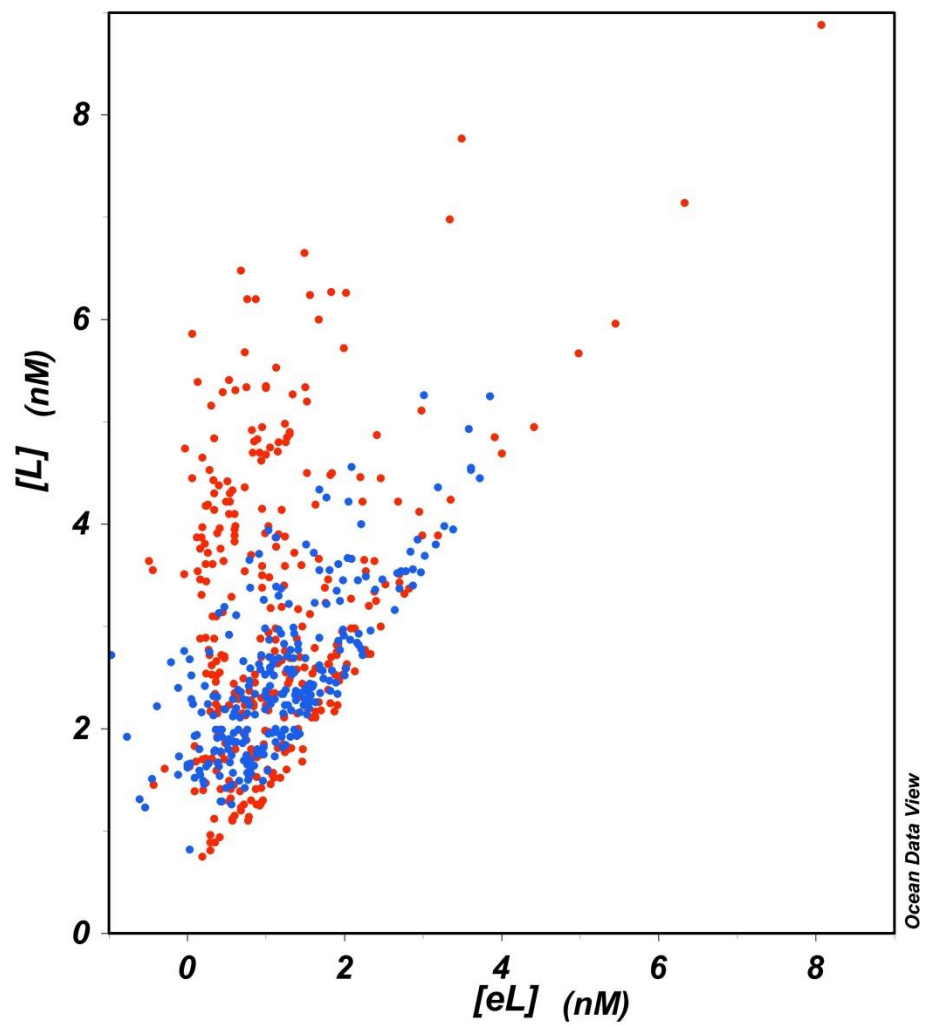


**Figure 1.14.** Plot of excess ligand and Cu binding ligands in both the Pacific (red) and Atlantic (blue) basins.

## **1.7 ACKNOWLEDGEMENTS**

Funding for this project was provided through a National Science Foundation grant. We thank the captain and crew of the R/V Thompson as well as Claire Parker-Till and Cheryl Zurbrick for collecting the copper speciation samples during the two month GEOTRACES cruise.

Chapter 1, in part, is currently being prepared for submission for publication of the material with the following co-authors: Ruacho, Angel; Barbeau, Katherine; Bundy, Randelle; Parker-Till, Claire; Roshan, Saeed; Wu, Jingfeng. The dissertation author was the primary author on this paper.

## 1.8 REFERENCES

- Abualhaija, Mahmoud M., Hannah Whitby, and Constant MG van den Berg. "Competition between copper and iron for humic ligands in estuarine waters." *Marine Chemistry* 172 (2015): 46-56.
- Amin, Shady A., James W. Moffett, Willm Martens-Habbena, Jeremy E. Jacquot, Yang Han, Allan Devol, Anitra E. Ingalls, David A. Stahl, and E. Virginia Armbrust. "Copper requirements of the ammonia-oxidizing archaeon *Nitrosopumilus maritimus* SCM1 and implications for nitrification in the marine environment." *Limnology and Oceanography* 58, no. 6 (2013): 2037-2045.
- Bayer, Barbara, Jana Vojvoda, Pierre Offre, Ricardo JE Alves, Nathalie H. Elisabeth, Juan AL Garcia, Jean-Marie Volland, Abhishek Srivastava, Christa Schleper, and Gerhard J. Herndl. "Physiological and genomic characterization of two novel marine thaumarchaeal strains indicates niche differentiation." *The ISME journal* 10, no. 5 (2016): 1051.
- Biller, D. V., and Bruland, K. W. (2012). Analysis of Mn, Fe, Co, Ni, Cu, Zn, Cd, and Pb in seawater using the Nobias-chelate PA1 resin and magnetic sector inductively coupled plasma mass spectrometry (ICP-MS). *Mar. Chem.* 130-131, 12–20. doi:10.1016/j.marchem.2011.12.001.
- Boiteau, Rene M., Claire P. Till, Angel Ruacho, Randelle M. Bundy, Nicholas J. Hawco, Amy M. McKenna, Katherine A. Barbeau, Kenneth W. Bruland, Mak A. Saito, and Daniel J. Repeta. "Structural characterization of natural nickel and copper binding ligands along the US GEOTRACES Eastern Pacific Zonal Transect." *Frontiers in Marine Science* 3 (2016): 243.
- Boyle, Edward A., Sarah S. Husted, and Susan P. Jones. "On the distribution of copper, nickel, and cadmium in the surface waters of the North Atlantic and North Pacific Ocean." *Journal of Geophysical Research: Oceans* 86, no. C9 (1981): 8048-8066.
- Brand, L. E.; Sunda, W. G.; Guillard, R. R. L., Reduction of marine-phytoplankton reproduction rates by copper and cadmium. *Journal of Experimental Marine Biology and Ecology* 1986, 96 (3), 225-250.
- Bruland, K. W., Oceanographic distributions of cadmium, zinc, nickel, and copper in the north Pacific, *Earth Planet. SciL Lett.*, 47, 176-198, 1980.
- Bruland, K. W., & Franks, R. P. (1983). Mn, Ni, Cu, Zn and Cd in the western North Atlantic. In *Trace metals in sea water* (pp. 395-414). Springer US.
- Bruland, K. W., & Lohan, M. C. (2003). Controls of trace metals in seawater. In: Elderfield, H. (Ed.), *The oceans and geochemistry*. Elsevier-Pergamon, Oxford, pp. 23-47.

- Bruland, K. W., Rue, E.L., Donat, J.R., Skrabal, S.A. and Moffett, J.W. 2000. Intercomparison of voltammetric techniques to determine the chemical speciation of dissolved copper in a coastal seawater sample. *Analytical Chimica Acta* 405: 99-113.
- Bruland, K. W., Rue, E. L., Smith, G. J., and DiTullio, G. R. (2005). Iron, macronutrients and diatom blooms in the Peru upwelling regime: brown and blue waters of Peru. *Mar. Chem.* 93, 81–103. doi:10.1016/j.marchem.2004.06.011.
- Buck, K. N., and Bruland, K. W. (2005). Copper speciation in San Francisco Bay: A novel approach using multiple analytical windows. *Mar. Chem.* 96, 185–198. doi:10.1016/j.marchem.2005.01.001.
- Buck, K. N., Moffett, J., Barbeau, K. A., Bundy, R. M., Kondo, Y., & Wu, J. (2012). The organic complexation of iron and copper: an intercomparison of competitive ligand exchange-adsorptive cathodic stripping voltammetry (CLE-ACSV) techniques. *Limnology and Oceanography: Methods*, 10(7), 496-515.
- Buck, K. N., Sedwick, P. N., Sohst, B., & Carlson, C. A. (2018). Organic complexation of iron in the eastern tropical South Pacific: results from US GEOTRACES Eastern Pacific Zonal Transect (GEOTRACES cruise GP16). *Marine Chemistry*, 201, 229-241.
- Bundy, R. M., Barbeau, K. A., and Buck, K. N. (2013). Sources of strong copper-binding ligands in Antarctic Peninsula surface waters. *Deep. Res. Part II Top. Stud. Oceanogr.* 90, 134–146. doi:10.1016/j.dsr2.2012.07.023.
- Campos, M. L. A. M., and van den Berg, C. M. G. (1994). Determination of copper complexation in sea water by cathodic stripping voltammetry and ligand competition with salicylaldoxime. *Anal. Chim. Acta* 284, 481–496. doi:10.1016/0003-2670(94)85055-0.
- Chakraborty, Parthasarathi, Sylvia G. Sander, Saranya Jayachandran, B. Nagender Nath, G. Nagaraju, Kartheek Chennuri, Krushna Vudamala, N. Lathika, and Maria Brenda L. Mascarenhas-Pereira. "Fate of copper complexes in hydrothermally altered deep-sea sediments from the Central Indian Ocean Basin." *Environmental pollution* 194 (2014): 138-144.
- Chapman, Conrad S., Gabriele Capodaglio, Clara Turetta, and Constant MG Van den Berg. "Benthic fluxes of copper, complexing ligands and thiol compounds in shallow lagoon waters." *Marine environmental research* 67, no. 1 (2009): 17-24.
- Coale, Kenneth H., and Kenneth W. Bruland. "Copper complexation in the Northeast Pacific." *Limnology and Oceanography* 33, no. 5 (1988): 1084-1101.
- Cotte, Laura, Dario Omanović, Matthieu Waeles, Agathe Laës, Cécile Cathalot, Pierre-Marie Sarradin, and Ricardo D. Riso. "On the nature of dissolved copper ligands in the early

- buoyant plume of hydrothermal vents." *Environmental Chemistry* 15, no. 2 (2018): 58-73.
- Cutter, Gregory A., and Kenneth W. Bruland. "Rapid and noncontaminating sampling system for trace elements in global ocean surveys." *Limnology and Oceanography: Methods* 10, no. 6 (2012): 425-436.
- Cutter, Gregory, Karen Casciotti, Peter Croot, Walter Geibert, Lars-Eric Heimbürger, Maeve Lohan, H  l  ne Planquette, and Tina van de Flierdt. "Sampling and Sample-handling Protocols for GEOTRACES Cruises. Version 3, August 2017." (2017).
- Demets, C., Gordon, R. G., Argus, D. F., and Stein, S., 1990, Current Plate Motions, *Geophys. J. Int.* 101, 425–478.
- Dupont, Christopher L., Robert K. Nelson, Saj Bashir, James W. Moffett, and Beth A. Ahner. "Novel copper-binding and nitrogen-rich thiols produced and exuded by *Emiliana huxleyi*." *Limnology and oceanography* 49, no. 5 (2004): 1754-1762.
- Francis, C. A., Roberts, K. J., Beman, J. M., Santoro, A. E., & Oakley, B. B. (2005). Ubiquity and diversity of ammonia-oxidizing archaea in water columns and sediments of the ocean. *Proceedings of the National Academy of Sciences*, 102(41), 14683-14688.
- German, C. R., A. C. Campbell, and J. M. Edmond. "Hydrothermal scavenging at the Mid-Atlantic Ridge: modification of trace element dissolved fluxes." *Earth and Planetary Science Letters* 107, no. 1 (1991): 101-114.
- Gledhill, Martha, and Kristen N. Buck. "The organic complexation of iron in the marine environment: a review." *Frontiers in microbiology* 3 (2012): 69.
- Heller, M. I., & Croot, P. L. (2015). Copper speciation and distribution in the Atlantic sector of the Southern Ocean. *Marine Chemistry*, 173, 253-268.
- Jacquot, Jeremy E., Yoshiko Kondo, Angela N. Knapp, and James W. Moffett. "The speciation of copper across active gradients in nitrogen-cycle processes in the eastern tropical South Pacific." *Limnology and Oceanography* 58, no. 4 (2013): 1387-1394.
- Jacquot, Jeremy E., and James W. Moffett. "Copper distribution and speciation across the International GEOTRACES Section GA03." *Deep Sea Research Part II: Topical Studies in Oceanography* 116 (2015): 187-207.
- Jenkins, William J., Dempsey E. Lott III, Christopher R. German, Kevin L. Cahill, Joanne Goudreau, and Brett Longworth. "The deep distributions of helium isotopes, radiocarbon, and noble gases along the US GEOTRACES East Pacific Zonal Transect (GP16)." *Marine Chemistry* 201 (2018): 167-182.



- Kogut, B.M. Voelker. Strong copper-binding behavior of terrestrial humic substances in seawater. *Environ. Sci. Technol.*, 35 (6) (2001), pp. 1149-1156
- Kogut, M.B. and Voelker, B.M., 2003. Kinetically inert Cu in coastal waters. *Environmental Science & Technology*, 37(3): 509-518.
- Lee, Jong-Mi, Maija I. Heller, and Phoebe J. Lam. "Size distribution of particulate trace elements in the US GEOTRACES Eastern Pacific Zonal Transect (GP16)." *Marine Chemistry* 201 (2018): 108-123.
- Maldonado, Maria T., Andrew E. Allen, Joanne S. Chong, Kevin Lin, Dan Leus, Nataliya Karpenko, and Shannon L. Harris. "Copper-dependent iron transport in coastal and oceanic diatoms." *Limnology and oceanography* 51, no. 4 (2006): 1729-1743.
- Moffett, J. W., Brand, L. E., Croot, P. L., & Barbeau, K. A. (1997). Cu speciation and cyanobacterial distribution in harbors subject to anthropogenic Cu inputs. *Limnology and Oceanography*, 42(5), 789-799.
- Moffett, James W., and Christopher Dupont. "Cu complexation by organic ligands in the sub-arctic NW Pacific and Bering Sea." *Deep Sea Research Part I: Oceanographic Research Papers* 54, no. 4 (2007): 586-595.
- Molina, V., Belmar, L., & Ulloa, O. (2010). High diversity of ammonia-oxidizing archaea in permanent and seasonal oxygen-deficient waters of the eastern South Pacific. *Environmental microbiology*, 12(9), 2450-2465.
- Moore, C. M., Mills, M. M., Arrigo, K. R., Berman-Frank, I., Bopp, L., Boyd, P. W., et al. (2013). Processes and patterns of oceanic nutrient limitation. *Nat. Geosci.* 6, 701–710. doi: 10.1038/ngeo1765
- Omanović, Dario, Cédric Garnier, and Ivanka Pižeta. "ProMCC: an all-in-one tool for trace metal complexation studies." *Marine Chemistry* 173 (2015): 25-39.
- Parker, C. E., Brown, M. T., and Bruland, K. W. (2016). Scandium in the open ocean: A comparison with other group 3 trivalent metals. *Geophys. Res. Lett.*, n/a–n/a.
- Peers, G., Quesnel, S. A., & Price, N. M. (2005). Copper requirements for iron acquisition and growth of coastal and oceanic diatoms. *Limnology and oceanography*, 50(4), 1149-1158.
- Peers, G., & Price, N. M. (2006). Copper-containing plastocyanin used for electron transport by an oceanic diatom. *Nature*, 441(7091), 341-344.
- Pennington, J. T., Mahoney, K. L., Kuwahara, V. S., Kolber, D. D., Calienes, R., and Chavez, F. P. (2006). Primary production in the eastern tropical Pacific: a review. *Prog. Oceanogr.* 69, 285–317. doi: 10.1016/j.pcean.2006.03.012

- Peters, Brian D., William J. Jenkins, James H. Swift, Christopher R. German, James W. Moffett, Gregory A. Cutter, Mark A. Brzezinski, and Karen L. Casciotti. "Water mass analysis of the 2013 US GEOTRACES eastern Pacific zonal transect (GP16)." *Marine Chemistry* 201 (2018): 6-19.
- Resing, J. A., Sedwick, P. N., German, C. R., Jenkins, W. J., Moffett, J. W., Sohst, B. M., & Tagliabue, A. (2015). Basin-scale transport of hydrothermal dissolved metals across the South Pacific Ocean. *Nature*, 523(7559), 200.
- Roshan, S., Wu, J., & Jenkins, W. J. (2016). Long-range transport of hydrothermal dissolved Zn in the tropical South Pacific. *Marine Chemistry*, 183, 25-32.
- Roshan, Saeed, and Jingfeng Wu. "Dissolved and colloidal copper in the tropical South Pacific." *Geochimica et Cosmochimica Acta* 233 (2018): 81-94.
- Sander, S. G., Koschinsky, A., Massoth, G. J., Stott, M. & Hunter, K. A. Organic complexation of copper in deep-sea hydrothermal vent systems. *Environ. Chem.* 4, 81–89 (2007).
- Sander, Sylvia G., and Andrea Koschinsky. "Metal flux from hydrothermal vents increased by organic complexation." *Nature Geoscience* 4, no. 3 (2011): 145.
- Sanial, V., L. E. Kipp, P. B. Henderson, P. Van Beek, J-L. Reyss, D. E. Hammond, N. J. Hawco et al. "Radium-228 as a tracer of dissolved trace element inputs from the Peruvian continental margin." *Marine Chemistry* 201 (2018): 20-34.
- Semeniuk, David M., Rebecca L. Taylor, Randelle M. Bundy, W. Keith Johnson, Jay T. Cullen, Marie Robert, Katherine A. Barbeau, and Maria T. Maldonado. "Iron–copper interactions in iron-limited phytoplankton in the northeast subarctic Pacific Ocean." *Limnology and Oceanography* 61, no. 1 (2016): 279-297.
- Shank, G. Christopher, Stephen A. Skrabal, Robert F. Whitehead, and Robert J. Kieber. "Fluxes of strong Cu-complexing ligands from sediments of an organic-rich estuary." *Estuarine, Coastal and Shelf Science* 60, no. 2 (2004): 349-358.
- Skrabal, Stephen A., John R. Donat, and David J. Burdige. "Pore water distributions of dissolved copper and copper-complexing ligands in estuarine and coastal marine sediments." *Geochimica et Cosmochimica Acta* 64, no. 11 (2000): 1843-1857.
- Stiefel, E. I. 2007. Bioinorganic chemistry and the biogeochemical cycles, p. 7–30. In I. Bertini, H. Gray, E. Stiefel, and J. Valentine [eds.], *Biological inorganic chemistry*. University Science Books. p. 7–30.
- Tanita, Iwao, Shigenobu Takeda, Mitsuhide Sato, and Ken Furuya. "Surface and middle layer enrichment of dissolved copper in the western subarctic North Pacific." *La mer* 53 (2015): 1-18.

- Thompson, C. M., Ellwood, M. J., & Sander, S. G. (2014). Dissolved copper speciation in the Tasman Sea, SW Pacific Ocean. *Marine Chemistry*, 164, 84-94.
- van den Berg, C.M.G., 1987. Organic complexation and its control on the dissolved concentrations of copper and zinc in the Scheldt Estuary. *Estuarine Coastal Shelf Sci.* 24 (6), 785–797.
- Walker, C.B., de la Torre, J.R., Klotz, M.G., Urakawa, H., Pinel, N., Arp, D.J., Brochier-Armanet, C., Chain, P.S.G., Chan, P.P., Gollagbir, A., Hemp, J., Hügler, M., Karr, E.A., Könneke, M., Shin, M., Lawton, T.J., Lowe, T., Martens-Habbena, W., Sayavedra-Soto, L.A., Lang, D., Sievert, S.M., Rosenzweig, A.C., Manning, G., Stahl, D.A., 2010. *Nitrosopumilus maritimus* genome reveals unique mechanisms for nitrification and autotrophy in globally distributed marine Crenarchaea. *PNAS* 107 (19), 8818–8823.
- Ward, Bess B., Caroline B. Tuit, Amal Jayakumar, Jeremy J. Rich, James Moffett, and S. Wajih A. Naqvi. "Organic carbon, and not copper, controls denitrification in oxygen minimum zones of the ocean." *Deep Sea Research Part I: Oceanographic Research Papers* 55, no. 12 (2008): 1672-1683.
- Whitby, Hannah, and Constant MG van den Berg. "Evidence for copper-binding humic substances in seawater." *Marine Chemistry* 173 (2015): 282-290.
- Wu, J., Boyle, E.A., 1997. Low blank preconcentration technique for the determination of lead, copper, and cadmium in small-volume seawater samples by isotope dilution ICPMS. *Anal. Chem.* 69, 2464–2470. <http://dx.doi.org/10.1021/ac961204u>.
- Yücel, M., Gartman, A., Chan, C. S., & Luther III, G. W. (2011). Hydrothermal vents as a kinetically stable source of iron-sulphide-bearing nanoparticles to the ocean. *Nature Geoscience*, 4(6), 367.

**CHAPTER 2: A Novel Method for the Processing of Multiple Analytical Window**

**Electrochemical Titration Metal Speciation Data**

## 2.1 ABSTRACT

Copper speciation was determined at select stations of the U.S. GEOTRACES GP16 transect via a competitive ligand exchange electrochemical technique using multiple analytical windows (MAW), employing a novel method for simultaneous processing of MAW voltammetric titration data. The proposed method uses a combination of publicly available metal speciation processing tools, KINETEQL and ProMCC, as well as a unified sensitivity for the processing of MAW data as a single data set, eliminating the need to derive sensitivities from individual titrations. The processing method developed here was also used to optimize the analytical windows used for MAW analysis, thereby decreasing the number of analytical windows required and reducing the workload. The removal of outlier points proved to be an important step for reducing errors associated with ligand parameters. The application of this method to GP16 samples reveals two copper ligands detected throughout the oceanic water column, with the weaker  $L_2$  ligand in higher concentration. Free copper concentrations throughout the data set remain well below toxicity even at depth, where the strong  $L_1$  ligand has low to no excess ligand concentration. This is one of the first open ocean copper speciation data sets derived from simultaneous processing of MAW electrochemical titrations, providing a more accurate depiction of the natural ligand pool relative to multi-ligand data derived from the analysis of a single analytical window.

## 2.2 INTRODUCTION

Copper (Cu) is scarce in the open ocean and is found in nanomolar concentrations. This is in stark contrast with coastal systems, where Cu is found in concentrations that can exceed oceanic levels by a factor of 10, especially in human-impacted sites such as boat basins (Bruland, 1980; Chadwick et al., 2004). Despite its low concentrations in the surface ocean, Cu has been

shown to play a vital role in facilitating various biological functions such as the acquisition of iron (Fe) (Peers et al, 2005), photosynthesis (Peers and Price, 2006) as well as ammonia oxidation by archaea, which use multiple multi-copper oxidases (Walker et al, 2010). Although Cu is a vital micro-nutrient, Cu has also proven to be toxic, especially for cyanobacteria. When the concentration of the free cupric ion ( $\text{Cu}^{2+}$ ) is high enough cyanobacteria have been shown to reduce their reproductive rates (Brand et al., 1986; Moffett et al., 1997). However, Cu in marine systems is over 99% complexed by organic ligands (van den Berg, 1987), and stabilization by organic ligands helps prevent  $\text{Cu}^{2+}$  concentrations from reaching toxic levels. Thus far the majority of these ligands have gone unidentified and the sources of the ligands are not fully understood. Some of these ligands are thought to be humic-like and are likely terrestrially derived (Whitby et al., 2018; Whitby and van den Berg, 2015; Abualhaija et al., 2015; Kogut and Voelker, 2001). Other ligands capable of binding Cu, like thiols and polysaccharides have also been suggested to be important in natural waters, with polysaccharides being produced by phytoplankton under elevated Cu concentrations (Swarr et al., 2016; Pistocchi et al., 2000).

Competitive ligand exchange voltammetry was first applied several decades ago to characterize Cu-binding ligands in natural waters (Campos and van den Berg, 1994). This electrochemical method employs a well-known ligand added at a specific concentration to compete with the natural ligands for added Cu. This method reveals Cu ligand concentrations and binding strengths ( $\log K$ ). A limitation with this technique is that the detection of the natural ligands is determined by the analytical window used to compete with the natural ligands. The ligand pool is heterogeneous and made up of organic species spanning a spectrum from weak to strong binding agents. Higher analytical windows (i.e. higher concentrations of the added ligand) are most sensitive for the detection of stronger ligands and low analytical windows (i.e. lower

concentrations of the added ligand) target weaker ligands. An intercalibration study by Bruland et al., (2000) demonstrated the effect that analytical window has on Cu speciation results by comparing Cu speciation results between different labs and distinct voltammetric methods. These competitive ligand exchange techniques used three different added ligands, benzoylacetone, salicylaldoxime, and 8-hydroxyquinoline, with each having different Cu-binding strengths and thus distinct analytical windows (Bruland et al., 2000). The intercalibration study revealed that different results for Cu speciation were obtained not only with different added ligands, but even when the same added ligand was used at different concentrations. Generally, when a low analytical window was used, a “weak” Cu ligand was detected at high concentrations, and when a high analytical window was used a “strong” Cu ligand was detected at lower concentrations than the weaker ligands. Despite the different ligand parameters, each method was able to calculate the same  $\text{Cu}^{2+}$  concentrations (Bruland et al., 2000). The interpretation from this study was that there is likely a “continuum” of organic Cu-binding ligands in seawater, and thus the analytical window is important for which pool of Cu-ligands you can identify. The recommendation from this study when characterizing metal binding ligands, was to complete titrations at a range of concentrations of the added ligand in order to span several different analytical windows and broadly characterize this continuum of Cu ligands in seawater. This conclusion was reinforced by the contemporaneous work of Voelker and Kogut (2001) on Cu binding in humic acid solutions analyzed via competitive ligand exchange titrations at multiple analytical windows (Kogut and Voelker 2001; Voelker and Kogut 2001).

An early study that implemented a multiple analytical window (MAW) approach for the analysis of organic Cu speciation in natural seawater was by Buck and Bruland (2005) in the San Francisco Bay estuary. This study analyzed each window separately before combining the results

of the MAW analysis for each sample onto a single plot revealing the buffering ability of the detected ligands to maintain free Cu concentrations at sub-toxic levels, despite elevated dissolved Cu concentrations from anthropogenic sources. This study demonstrated the utility of the MAW approach, but also highlighted the challenges of early MAW datasets. One challenge was that each titration was processed individually using either a Scatchard or Langmuir linearization technique and not as a unified data set (Buck and Bruland, 2005). Following in the steps of the Buck and Bruland (2005) study, Bundy et al. (2013) utilized a similar MAW approach for studying possible sources of Cu ligands to Antarctic surface waters. The Bundy et al. (2013) study also used known linearization methods like the van den Berg/Ruzic and Scatchard to process speciation data from each analytical window separately. Although these studies noted the utility of using MAWs, analyzing samples using MAWs is also extremely time intensive. These analyses involve completing at least five titrations (with an analysis time of approximately 2 hours per titration) compared to only a single titration in traditional methods. In addition several issues have been noted regarding analyzing titration data from each window separately instead of as a unified dataset. Firstly, there can be some overlap between analytical windows that cannot be accounted for by analyzing each titration separately. When viewed separately each analytical window produces its own speciation results which one can interpret as different ligands being detected. Pizeta et al. (2015), however pointed out that the statistical significance of the difference between the ligand parameters from each window has not been explored, and it is more appropriate to analyze multi-window titrations as a single dataset rather than individual curves. Once analyzed as a single dataset the issue of how to determine a sensitivity arises. The sensitivity of a titration is an important variable for calculating speciation parameters. There are several methods available for determining the sensitivity and the



sensitivity for each window can be different, which further complicates how the sensitivity should be determined.

Recently, several studies have tested the approach of processing MAW data simultaneously as a single data set. Select analyses from the Buck and Bruland (2005) publication were reprocessed as a single MAW data set (Wells et al., 2013) employing a numerical method that was developed to handle MAW speciation data via direct modeling (Sander et al., 2011). Wells et al. (2013) found that analyzing MAW data simultaneously helps to fully characterize the strong and weak ligands in a sample and made determination of the free Cu ion more accurate than a single analytical window alone. Another recent study (Pizeta et al., 2015) evaluated speciation results from 15 labs for simulated titration data. This effort revealed that using a unified analysis for MAW data improved results when two or more ligands are in a sample, and in fact gave a better estimation of the true ligand parameters than analysis at a single analytical window. The use of both KINETEQL and ProMCC individually was evaluated in the Pizeta et al. (2015) intercalibration study, though the impact of the sensitivity determination method on MAW analyses was not evaluated.

Sophisticated processing tools have recently become widely and publicly available, making it more routine to process MAW metal speciation data as a single data set. Currently there are two publicly available processing tools for MAW Cu speciation data that can treat multi-window data simultaneously. One, KINETEQL, utilizes a nonlinear regression to fit up to three ligands with an Excel workbook used as an input for the data (Hudson et al., 2003; Hudson, 2014). The KINETEQL software also utilizes a Tableau system that is similar to the other MAW software, ProMCC, a complete complexation model. The complete complexation model is made up of mass balance equations to process MAW speciation data as a combined dataset (Omanović

et al., 2015). The ProMCC tool has a graphic user interface which allows for quick adjustment of speciation data after a fitting. The main difference between ProMCC and KINETEQL is that ProMCC requires sensitivity correction of speciation data before the data can be imported to ProMCC, while KINETEQL solves for the sensitivity as one of the fitting parameters. This is a major distinction between the two methods because the inaccurate determination of the sensitivity introduces the most error into ligand parameter determinations (Pizeta et al., 2015). The KINETEQL solver is able to determine a sensitivity for the dataset as a whole, which can be useful for processing MAW data (Hudson et al., 2003).

In this study, we used KINETEQL and ProMCC concurrently to process Cu MAW data. In brief, the method described here uses KINETEQL to determine a unified sensitivity for the MAW data set and uses it to correct the raw MAW data before final processing with ProMCC. We further optimized the number and range of analytical windows needed for MAW Cu speciation analysis of oceanographic samples, significantly decreasing the time needed for MAW analyses. The use of KINETEQL for determining sensitivity is shown to be advantageous as it provides a sensitivity fitted for the whole data set as opposed to doing an internal calibration for each analytical window. The method is applied to samples collected at “super stations” during the 2013 U.S. GEOTRACES Eastern Pacific Zonal Transect (GP16).

## **2.3 METHODS**

### ***2.3.1 Sample collection***

Samples for the application of the MAW processing method were collected from the 2013 U.S. GEOTRACES Equatorial Pacific Zonal Transect (GP16) in which full depth water column samples were collected (Fig. 2.1). Select samples were chosen from “super stations” to be analyzed using MAW for the determination of Cu ligand concentrations (L) and conditional

binding strengths (logK). All speciation sampling bottles, for GP16 MAW speciation samples underwent a rigorous cleaning process outlined in the GEOTRACES “cookbook” (Cutter et al., 2017). The cleaning process began with a soap bath followed by a bath in nitric acid and ending in a bath of hydrochloric acid. All bottles were individually double bagged for clean storage and filled with Milli-Q (MQ;  $18 \text{ M}\Omega \text{ cm}^{-1}$ ) until use. Water column speciation samples were collected according to GEOTRACES protocols described in Jacquot and Moffett (2015) and outlined by GEOTRACES protocols (Cutter et al., 2017). Surface seawater samples were also collected from 3m depth with a trace metal clean tow-fish pump system while steaming between stations (Bruland et al., 2005), and underwent the same treatment as water column samples. Speciation samples were filtered using a  $0.2 \mu\text{m}$  Acropak 200 capsule filter and were placed in fluorinated polyethylene (FLPE) bottles were then stored in a  $-20 \text{ C}$  freezer for analysis in the lab. Samples for total dissolved Cu determination were collected simultaneously with Cu speciation samples, into low density polyethylene (LDPE) bottles, and acidified at sea with 4mL of 6M quartz-distilled HCl (Optima, Fisher Scientific) per liter of seawater, resulting in a pH of 1.7-1.8 (NBS scale).

### ***2.3.2 Total dissolved copper analysis***

Dissolved Cu for the Eastern section of the transect (stations 1 and 11) was analyzed using previously described methods (Biller and Bruland, 2012; Parker et al., 2016) Cu was preconcentrated by extraction from buffered seawater (pH 6.0) and analyzed on an Element XR Inductively Coupled Plasma Mass Spectrometer (ICP-MS). Samples were UV irradiated prior to preconcentration. Dissolved Cu samples from the Western section of the transect (stations 26 and 36) were analyzed according to an isotope dilution method (Wu and Boyle, 1997; Roshan and Wu, 2018) utilizing a multiple collector high resolution ICP-MS. This method also utilizes a UV

step prior to analysis. SAFe seawater standards were also determined to assess the accuracy of the method.

### ***2.3.3. Reagents***

The boric acid buffer was prepared by dissolving boric acid (Alfa Aesar, 99.99%) in 0.4 N aqueous  $\text{NH}_4\text{OH}$  (Optima, Fisher Scientific). A 4 mM stock of salicylaldehyde (SA; > 98%) was prepared in methanol (Optima LC/MS, Fisher Scientific) and replaced every six months or as needed. Cu standards (100 nM to 10  $\mu\text{M}$ ) were diluted from an atomic adsorption standard (1000 ppm, Spex CertiPrep) into pH 2 MQ water (acidified with Optima grade HCl).

### ***2.3.4 Copper speciation analysis***

A competitive ligand exchange adsorptive cathodic stripping voltammetry (CLE-ACSV) method was utilized for the characterization of organic Cu binding ligands for GP16 samples. The basics of the CLE-ACSV method are detailed in Buck and Bruland (2005). This method employs the competition for Cu between a well-characterized added ligand (SA) and the natural seawater ligands to determine the thermodynamic stabilities of the natural ligands (originally published in Campos and van den Berg, 1994). The analytical methods and electrochemical parameters follow those outlined in Bundy et al. (2013) and Buck and Bruland (2005). Frozen samples were thawed in a refrigerator and vigorously shaken prior to analysis. The samples were then aliquoted (10 mL) into pre-conditioned Teflon vials and buffered with 1.5 M boric acid-ammonia (BA) to pH 8.2. The vials were spiked with increasing concentrations of Cu ranging from 0-75 nM, depending on the analytical window, to saturate the natural ligands. The boric acid buffer and Cu were equilibrated with the natural ligands for two hours, after which the competing ligand, SA, was added. Five titrations were carried out in this manner with a concentration of SA of 1, 2.5, 5, 10, or 25  $\mu\text{M}$ . Titrations with SA concentration between 5 and

25  $\mu\text{M}$  were equilibrated with SA for at least 15 minutes, while titrations with SA concentrations of 1 and 2.5  $\mu\text{M}$  were equilibrated with SA for at least 30 minutes. Speciation samples were analyzed in 11-point titrations carried out on a controlled growth mercury electrode (Bioanalytical Systems Incorporated). Peaks generated from titrations were extracted using the ECDSOFT software package (Omanović et al., 2015).

### ***2.3.5 Simulated unified analysis of multiwindow data***

In order to determine the most effective method for simultaneous processing of multi-window Cu speciation data, the ProMCC simulation feature was used to generate simulated titration data for the five analytical windows used in our MAW analysis. Parameters for the simulated data such as initial Cu concentration and Cu additions used for titrations were based on the analytical processing of GP16 sample 10327, an open ocean sample collected at 45 meters in the oligotrophic region of the cruise. We simulated data that had two ligand classes with  $L_1$  concentration of 1.63 nM and a  $\log K_1$  of 14.16, and  $L_2$  concentration of 7.43 nM and a  $\log K_2$  of 12.75 with a sensitivity of 69.86. Noise was added to the simulated data (up to 30% variability) similar to what was done by Omanović et al. (2015). The simulated data was then processed as a unified dataset with three different processing methods (Table 2.2): (1) utilizing the KINETEQL multi-window tool with preset limits for ligand concentrations, sensitivity, and  $\log K$ ; (2) using the ProMCC software with the internal sensitivity generated during the titration of each analytical window to correct peak heights and fitting with the complete complexation fitting model option; and (3) using a combination of both KINETEQL and ProMCC. In method (2) the internal sensitivity was determined based on the final three points of a titration curve, where the titration is linear and the added Cu is primarily bound by the added ligand. In method (3) (schematic shown in Fig. 2.1), the MAW data was processed by first following method (1), and

then the determined sensitivity was used to correct the peak heights from each analytical window. Once the peak heights were corrected, the corrected unified MAW data was imported to ProMCC and processed. The speciation results and corresponding errors from the three processing methods were compared with each other in order to determine the best method for analyzing the field samples. Method (3) was then also used for further tests in determining the optimal analytical windows to use for MAW analysis while trying to minimize fitting errors. Different combinations of three of the five analytical windows were tested using method (3) to determine whether particular combinations of three windows gave lower or similar average error as using all five windows (Table 2.3).

During the processing steps we found that removing data points helped in reducing errors for calculated speciation parameters. One point removal step occurs after the processing with KINETEQL (Fig. 2.1C). KINETEQL produces a sensitivity line on which all the data is plotted and points that are “off” the line are singled out for removal. This point removal was used for processing data according to method (1) and for the KINETEQL portion of method (3). Point removal was also carried out during data processing in ProMCC. The removal is based on points that are visibly clear outliers primarily on the generated plots for the Scatchard and Langmuir fittings, see Fig. 2.1E. The point removal in ProMCC was used in method (2) as well as method (3) during the ProMCC fitting in method (3).

### ***2.3.6 GP16 MAW processing***

The MAW processing of GP16 samples was done according to method (3) using the “optimized” windows of 2.5, 5, and 10  $\mu\text{M}$  SA. Titration data from the optimized windows was imported into KINETEQL and the solver was run. After the fitting, points off of the sensitivity line were subject to removal. The sensitivity determined in KINETEQL was used to correct raw

peak heights prior to importing to ProMCC. Within ProMCC outlier points were removed based primarily on the Scatchard and Langmuir plots, as described earlier. After this point removal, the solver was run in ProMCC for final processing of the data, generating the ligand data reported in Table 2.4.

## **2.4 RESULTS and DISCUSSION**

### ***2.4.1 MAW processing results***

We first used the simulated data to determine the best way to process our field data analyzed via MAW. Results from the three MAW processing methods outlined in the methods section are displayed in Table 2.2. We simulated the data to have two ligand classes, so all methods were run with two ligands enabled in both the KINETEQL parameters and in ProMCC. All three processing methods determined two ligands with similar binding constants, with the strong ligand ( $L_1$ ) having a  $\log K$  just above 14 and the weaker ( $L_2$ ) ligand having a binding constant of less than 13. Concentrations of  $L_1$  were similar between all three methods, ranging from  $1.68 \pm 0.82$  nM for method (2), 1.41 for method (1) with a root mean square (RMS) error of 0.09 and  $1.35 \pm 0.35$  nM for method (3). Concentrations of the  $L_2$  ligand were more variable between the three methods with method (1) calculating the lowest concentration (5.43 nM) and method (2) the highest ( $14.19 \pm 12.19$  nM). Methods (1) and (2) both offer unique features for processing MAW data simultaneously. In method (1) a unified sensitivity is calculated for the data, while method (2) allows for data visualization and fitting with a graphic user interface that allows for quick adjustments of the data. Method (3) takes advantage of the unique features of both processing tools. A significant difference between methods (1) and (2) is how the sensitivity is determined and utilized. KINETEQL determines a sensitivity for the dataset as a whole (e.g. all analytical windows) while ProMCC requires a correction to raw peak data with the sensitivity

determined first by the user. There are several methods for determining the sensitivity of a titration but there is currently no consensus on which method is the best to use. Recently a MAW Cu speciation study by Wong et al. (2018) utilized ProMCC for the simultaneous analysis of MAW Cu speciation data in an estuary and explored two methods of implementing the sensitivity for the analysis of MAW data as a unified data set in ProMCC. One approach was to use an internal calibration which consists of using the last 3-5 linear points of a titration curve, while the second was to use the last few points of a standard addition of Cu from a UV-irradiated sample. Wong et al. (2018) stated that due to sample size they were unable to establish the “best” sensitivity for the analyses and thus used both sensitivities, with the internal sensitivity serving as a lower limit and the sensitivity from the UV-irradiated sample serving as the upper limit. Through the use of their sensitivity correction and the ProMCC software, Wong et al. (2018) identified two ligand classes in their samples. In a later study Wong et al (2019) compared the use of UV-irradiated sensitivity to sensitivity generated via “overload titration” (Kogut and Voelker, 2001). An overload titration (OT) is similar to an internal calibration, as both are measured directly in the sample, but the OT utilizes a concentration of the added ligand which outcompetes all natural ligands in the sample (Kogut and Voelker, 2001). Wong et al. (2019) found that UV-irradiated sensitivities gave more reproducible results for MAW analyses vs. the OT method. A challenge that comes with using the internal slope of UV irradiated samples, however, is that MAW analysis takes up considerable time and volume which may make it impractical to UV treat each sample. This issue presents a greater difficulty when a high number of samples are collected, particularly for programs like GEOTRACES. The utilization of KINETEQL allows for the determination of the sensitivity for the dataset as a whole, without the added work of UV treating each sample. Additionally, it allows for the correction of raw data



with a unified sensitivity for each analytical window for use in ProMCC. We chose the combination of KINETEQL and ProMCC (method (3) described above) for simultaneous processing of our MAW Cu speciation data as it utilizes the best features of both KINETEQL and ProMCC while providing a uniform method for determining the sensitivity, arguably the most important parameter in speciation analyses (Pizeta et al., 2015).

#### *Optimization of MAW windows*

After deciding on a method for the simultaneous analysis of our MAW Cu speciation data, method (3), the simulated data was then used to assess whether the number of analytical windows used in the analysis can be reduced, since MAW methods are extremely time and volume intensive. We used the simulated data as well as the average error parameter reported from ProMCC to determine which of our analytical windows can be removed from the analysis by seeing which reduced the average error. We determined that an acceptable average error as reported by ProMCC was error that was within the range ( $\pm 20\%$ ) of the error that was determined for that method using the simulated data (Table 2.3). For the optimization tests combinations of three analytical windows were used. All of the combinations using the highest analytical window, 25  $\mu\text{M}$  SA, have the largest average errors. This is likely due to the fact that the highest concentration of SA is slightly outside the detection window for the weaker ligand parameters ( $L_2$ ) used in the simulated data. An analytical window ( $\alpha_L$ ) is defined by,

$$\alpha_L = [L] \times K \quad (1)$$

such that  $\alpha_L$  is a function of ligand concentration and strength. An optimal analytical window used for the analysis of ligand parameters is one where the  $\alpha_{SA}$  is within an order of magnitude of the  $\alpha_L$  of the natural ligands. In the case of the highest analytical window (25  $\mu\text{M}$  SA), the

$\alpha_{SA}$  is equal to  $6.6 \times 10^5$  and the  $\alpha_{LT}$  of the simulated natural ligands is  $2.4 \times 10^5$  when both the stronger and weaker ligands are considered. If only the weaker ligands are considered, the  $\alpha_{L_2}$  of the simulated weaker ligands is  $4.2 \times 10^4$ , which is an order of magnitude lower than the  $\alpha_{SA}$  for the highest window. This may suggest that the 25  $\mu\text{M}$  SA window is high to accurately detect the  $L_2$  ligands, and thus the error associated with the  $L_2$  determinations are high (Table 2.3). When the highest analytical window is not used, the average error drops, as well as the specific error values for ligand concentrations. The lowest average error is obtained when using the mid-range analytical windows, 2.5, 5 and 10  $\mu\text{M}$  SA. When comparing the average error of the three mid-range analytical windows with the use of all five analytical windows, a clear difference in the error is observed (Table 2.3). Although the average error when using all five windows is bigger relative to the “optimized” windows, the speciation results are similar to each other (Table 2.3). When the 25  $\mu\text{M}$  SA window is not used the average error drops below 20. When working with the remaining analytical windows, the removal of the 1  $\mu\text{M}$  SA window lowers the average error further to the lowest seen between the various combinations (11.51; Table 2.3). Thus, removing the lowest and highest analytical windows had the greatest impact for reducing the average error in ProMCC for this particular sample. These results are in contrast to Sander et al. (2011) who proposed that the use of their lowest (0.5  $\mu\text{M}$  SA) and highest (70  $\mu\text{M}$  SA) analytical windows was enough for Cu speciation parameter determination with their numerical method. With our processing method, the use of our highest or lowest windows tended to introduce more error, which led to excluding those windows when selecting the optimized windows for use on field samples. This can likely be explained by the difference in the samples used between the two analyses, and the slight modifications of the processing methods used. Our method has been optimized for open ocean samples, where Cu ligand concentrations and binding strengths fall

within a relatively consistent range across most studies (Bundy et al. 2013; Thompson et al., 2014; Jacquot and Moffett 2015; Whitby et al., 2018). Sander et al. (2011) optimized their method across a huge range in ligand concentrations and strengths in an estuarine setting, with ligand concentrations ranging from 0.5-2500 nM and logK ranging from 7.5-17.5 (Fig. 2 in Sander et al. 2011). Their lowest and highest analytical windows thus would not be either too weak or too strong for their range of ligand parameters, and thus likely would not subject their results to large errors. We choose to focus on optimizing MAW methods for the vast majority of Cu speciation that exists, which is within a much narrower range of ligand parameters in an open ocean setting. Our method is thus applicable to a wide range of open ocean samples, while users conducting MAW analyses on unique sample types should perhaps take special care to choose the appropriate windows based on the expected ligand parameters.

#### **2.4.2 GP16 MAW data**

The MAW processing method (3) described above with the optimized analytical windows (2.5, 5, 10  $\mu$ M SA) was used for the analysis of select open ocean Cu speciation samples from the 2013 GP16 cruise. Results for Cu speciation for GP16 are presented in Table 2.4. Errors for the majority of parameters are low, although errors for the  $L_2$  concentration were more variable. Pizeta et al. (2015) noted the higher overall error associated with determining the concentrations of the  $L_2$  ligand class, and suggested that longer titrations (at least 15 points) should be used in order to determine two ligand classes. Despite having multiple windows, it is likely that experimental variability in the titrations may disproportionately impact the determination of the  $L_2$  parameters, especially in this work when each titration has only 11 points compared to the new recommendations of 15 (Pizeta et al., 2015).

These are some of the first MAW measurements done for Cu speciation samples within a GEOTRACES transect. A profile of samples analyzed with this processing method from GP16 Station 26 in the far west of the transect is shown in Fig. 2.2, displaying Cu concentrations and ligand concentrations for both the  $L_1$  and  $L_2$  ligands that were detected. The concentration of  $L_1$  ligands exceeds the dissolved Cu concentration in the upper 300 m and increases with depth. However, the dissolved Cu concentrations also increase with depth and thus the Cu concentration exceeds the  $L_1$  concentration for the samples below 1500 meters.  $L_2$  ligands are found in higher concentrations than the  $L_1$  ligands and dissolved Cu throughout the water column, except in the deepest sample where  $L_2$  concentrations are similar to dissolved Cu. The free Cu concentration at GP16 Station 26 was very low in the upper 300 m, reaching a concentration of almost  $10^{-15}$  M. The free Cu ion concentration increases with depth, but remains below the toxicity threshold for cyanobacteria,  $10^{-11}$  M (Brand et al., 1986).

The profile for Station 1 at the eastern end of the transect is similar to the profile for Station 26,  $L_1$  ligands exceed dissolved Cu concentrations near the surface (Fig. 2.3). Station 1 is also highlighted by strong ligands with the highest binding constant ( $\log K_1$ ) in the MAW data set, this is similar to stations near the shelf in Chapter 1 which also have the strongest ligands detected demonstrating that a shelf influence may extend to Station 1. Station 1 is highlighted by an oxygen minimum zone (OMZ) feature between 200 and 500 m. Two samples of the Station 1 profile (180 and 211 m) fall within this feature with oxygen concentrations of 1 and 1.10  $\mu\text{mol/kg}$ , respectively, compared to the upper 70 m which have oxygen concentrations over 200  $\mu\text{mol/kg}$ . The 211 m sample found in the OMZ section is found to have low free Cu concentrations comparable to concentrations of the near surface samples. The highest  $L_2$  concentration is also found within the OMZ feature. In the deep waters of the profile (>1500 m)

the  $L_1$  concentration is found in similar concentrations as dissolved Cu while the deepest sample in the profile, and one of the deepest in the dataset (5446 m), is found to have a  $L_1$  concentration less than the dissolved Cu concentration. All free Cu concentrations at Station 1 are calculated to be well below the toxicity threshold including the deepest sample that has  $L_1$  and  $L_2$  concentrations below dissolved Cu concentrations.

Overall for the MAW dataset, when compared to the single analytical window (SAW) analysis of the GP16 transect (Chapter 1), it is likely that the ligands detected using a single window are a combination of the two ligands detected through MAW as the  $\log K$  of the SAW ligands tend to be in between the  $\log K$ s of the  $L_1$  and  $L_2$  ligands detected through MAW. However, despite the differences in the determined ligand parameters the  $\text{Cu}^{2+}$  concentrations were quite similar. The ligand parameters observed in GP16 are in line with previous work in this region (Jacquot et al., 2013) which utilized a single analytical window at 2.5  $\mu\text{M}$  SA. The binding strengths for the majority of ligands detected by Jacquot et al., (2013) are in line with the  $L_2$  ligands detected on GP16 through MAW. This MAW data set also demonstrates the potential for an inert fraction of ligand-bound Cu in deep Pacific waters, as shown in Chapter 1. Buck et al. (2018) attributed the Fe  $L_2$  ligands to the refractory component of deep ocean DOC, further supporting the idea that there is a deep water fraction of metal-binding organic matter inert to ligand exchange. When excess  $L_1$  ( $eL_1$ ) is plotted against depth we see there is a depletion of excess  $L_1$  at depth (Figure 2.5). This inert fraction could have implications for the accurate measurement of ligand parameters, particularly for SAW electrochemical titration, which typically best characterize ligands that are present in excess of the dissolved metal concentration (Buck et al., 2018).

Although MAW analysis provides an improved characterization of the ligand pool relative to SAW analysis, particularly for the L<sub>1</sub> ligands dominating Cu speciation, what remains unknown is the identity of the majority of these Cu binding ligands. Findings by Buck et al. (2018) in the deep waters indicate humic substances as likely being part of the L<sub>2</sub> Fe ligand pool. As humics are known to also bind Cu, it is likely that deep water L<sub>2</sub> Cu ligands are partially made up of humic substances. Recent work by Whitby et al. (2018) in the North Pacific suggests possible candidates like humic substances and various thiol types for the identity of Cu ligands. Whitby et al. (2018) were able to correlate thiourea-like thiols with their L<sub>1</sub> ligand, which shares a binding strength (logK) with some of the strongest ligands we detected. Whitby et al. (2018) suggest that the electrochemical thiourea peak could be part of high affinity Cu chelators like methanobactin or porphyrin. This finding points toward a biological source for the strong L<sub>1</sub> ligand, as the strong ligand detected in our study is similar to that from the Northeast Pacific study. The higher excess ligand concentrations for L<sub>1</sub> that we observe near the surface could be the result of biological production. Deeper waters show virtually no excess L<sub>1</sub>, indicating the saturation of the ligand as dissolved Cu accumulates in older water masses. The L<sub>2</sub> ligand pool in Whitby et al. (2018) seems to be a mix of thiols and humic substances with logKs ranging from 11.6-13.6 which are similar to the binding strengths of our L<sub>2</sub> ligands. We did not evaluate our samples for concentrations of thiols or humic substances, but it is likely that these make up a portion of the Cu ligand pool. There still remains a large fraction of the Cu ligand pool unidentified, as Whitby et al. (2018) were only able to account for about 32% of the total ligands they detected as being thiols (thiourea, glutathione) or humic substances. A difference between our MAW electrochemical method and the voltammetric titrations carried out by Whitby et al. (2018) is that our ligand parameters are derived from a range of analytical windows, while

Whitby et al. (2018) utilized an extended titration at the 10  $\mu\text{M}$  SA window to fit two ligands in ProMCC. The extended titration at 10  $\mu\text{M}$  SA will be biased by targeting and averaging ligands detectable at a relatively high analytical window. With our use of multiple windows, including low analytical windows, we can more broadly characterize the natural ligand pool and derive more accurate measurements of ligand parameters. Our  $L_1$  ligands are, for the most part, somewhat weaker than the  $L_1$  ligands detected by Whitby et al. (2018), spanning a larger range in binding strength, and with a distinct excess in concentration in surface waters. The  $L_1$  ligands detected by Whitby et al. (2018), in contrast, displayed uniformly high log  $K$ 's and occurred in a near 1:1 ratio with dissolved Cu throughout the two stations they sampled. Our findings have implications for both the source and identity of Cu-binding  $L_1$  ligands.

## **2.5 CONCLUSION**

Recent releases of publicly available Cu speciation processing tools have allowed for the simultaneous processing of MAW speciation data. Prior to the advent of these tools MAW data was analyzed on a window by window basis. Bruland et al. (2000) demonstrated that the analytical window used can bias analysis of the natural ligand pool as low analytical windows will find higher ligand concentrations with lower binding constants relative to the higher analytical windows. Early MAW studies highlighted some of the problems associated with analyzing high and low analytical windows individually, as well as with the time intensive nature of analyses. The MAW method described here is able to streamline the analysis of open ocean MAW data, as well as improve the efficiency of MAW data generation. The determination of a unified sensitivity for the entire MAW speciation dataset prior to final processing in ProMCC is an improvement on MAW data processing. The use of a unified sensitivity determined from KINETEQL will help improve speciation results when users would otherwise need to use

various more labor-intensive methods to determine individual window sensitivity before using ProMCC.

For our method, we recommend the use of the 2.5, 5, and 10  $\mu\text{M}$  SA windows for analysts processing open ocean data. These windows produce results with the lowest average error during final data processing, and make MAW data less time intensive to generate. The use of “optimized” windows that provide coverage between both the weak and strong ligand pool should be applied with caution however, as the optimal window may vary depending on the type of sample being analyzed (e.g. open ocean versus estuarine or hydrothermal). We found that incorporating a point removal step was important for reducing errors associated with these processing methods, in particular errors for the  $L_1$  ligand parameters. The new method was applied to samples from the U.S. GEOTRACES GP16 cruise, providing some of the first open ocean Cu speciation samples to be analyzed by simultaneous MAW data processing. Pairing the optimized windows with available processing tools can provide faster analysis of MAW data while still accurately probing the ligand pool.



## 2.6 FIGURES and TABLES

**Table 2.1.** Table of preset limits used in KINETEQL for MAW processing methods 1 and 3. Ligand concentrations are in nanomolar concentrations.

<b>Parameter</b>	<b>Min</b>	<b>Max</b>
log $K_1$	13	17
log $K_2$	10	13
log $K_3$	7	10
$[L_{1T}]$	0.1	100
$[L_{2T}]$	0.32	100
$[L_{3T}]$	0.32	1000
log S	-0.3	3

**Table 2.2.** MAW results for the three processing methods utilizing simulated data, as well as the source of the sensitivity. The error for the KINETEQL method is calculated as a root mean square error of all fitting parameters (Hudson et al., 2003), while the error for the ProMCC method is reported as the “average error” (Omanović et al., 2015).

Software	$L_1$ (nM)	$\pm$	$\log K_1$	$\pm$	$L_2$ (nM)	$\pm$	$\log K_2$	$\pm$	Error	Sensitivity
KINETEQL	1.41		14.14		5.43		12.8		0.089	KINETEQL
ProMCC	1.68	0.82	14.54	0.62	14.19	13.83	12.19	1.16	45.01	Internal
KINETEQL and ProMCC	1.35	0.35	14.20	0.32	9.15	1.74	12.74	0.15	21.21	KINETEQL

**Table 2.3.** Speciation results from analytical window optimization tests and speciation results from the use of all windows and simulated data.

<b>Windows Utilized (<math>\mu\text{M SA}</math>)</b>	<b><math>L_1</math> (nM)</b>	<b><math>\pm</math></b>	<b><math>\log K_1</math></b>	<b><math>\pm</math></b>	<b><math>L_2</math> (nM)</b>	<b><math>\pm</math></b>	<b><math>\log K_2</math></b>	<b><math>\pm</math></b>	<b>AVG error</b>
1, 2.5, 5	1.61	0.29	14.12	0.21	9.01	1.35	12.70	0.11	14.32
1, 2.5, 10	1.34	0.37	14.18	0.32	9.24	1.76	12.73	0.16	17.73
1, 5, 10	2.35	0.33	13.95	0.17	10.04	2.01	12.51	0.15	14.55
2.5, 5, 10	1.62	0.28	14.13	0.21	8.14	1.93	12.67	0.19	11.51
1, 2.5, 25	2.43	2.37	12.91	13.55	7.65	6.12	12.90	1.10	93.57
1, 5, 25	1.27	1.15	14.23	14.80	9.67	6.53	12.72	0.64	78.87
5, 10,25	2.94	1.91	13.72	0.79	8.84	8.62	12.48	12.73	48.56
All windows	1.62	1.58	13.92	14.40	8.95	7.16	12.71	0.64	69.17

**Table 2.4.** Cu speciation results for GP16 MAW samples, processed with method (3) described in methods section.

Station	ID	Depth (m)	[Cu] (nM)	[L <sub>1</sub> ] (nM)	±	logK <sub>1</sub>	±	[L <sub>2</sub> ] (nM)	±	logK <sub>2</sub>	±	Log[Cu <sup>2+</sup> ]	[eL <sub>1</sub> ] (nM)
1	2126	20	1.04	1.93	0.63	15.41	1.08	10.03	3.03	13.22	0.23	-15.01	0.89
1	2124	30	1.71	2.64	0.83	15.96	0.96	10.39	4.16	13.53	0.41	-15.74	0.93
1	2114	180	4.22	3.45	0.44	15.73	16.51	11.48	8.04	12.10	0.42	-13.23	0.00
1	2112	211	1.22	1.91	0.64	15.03	0.79	4.57	4.23	12.84	1.03	-14.83	0.69
1	2224	1614	2.46	2.52	0.88	14.86	1.41	5.26	4.27	12.55	0.69	-13.17	0.06
1	2216	3200	4.22	4.63	0.51	13.95	0.24	5.55	5.41	11.77	12.00	-12.77	0.41
1	2002	5446	5.89	3.79	0.26	14.52	0.40	5.23	0.58	13.20	0.10	-13.22	0.00
11	3635	320	1.45	2.24	0.76	14.58	0.51	6.59	5.11	12.99	0.49	-14.48	0.79
11	3631	400	2.51	2.85	0.60	14.97	0.71	7.11	6.14	12.27	0.71	-14.21	0.34
11	3617	1250	2.84	5.54	0.93	13.83	0.45	4.02	3.92	12.55	1.32	-13.88	2.70
11	3615	1500	2.45	2.66	0.13	14.20	0.14	2.46	2.18	11.70	0.91	-12.91	0.21
11	3518	1750	2.4	2.16	0.45	14.79	0.96	4.65	2.68	12.503	0.44	-13.57	0.00
11	3508	3000	4.25	3.81	0.36	13.88	0.21	5.21	5.49	11.68	0.35	-12.79	0.00
26	9379	80	0.51	1.86	0.27	14.53	0.22	5.37	2.08	12.86	0.26	-14.69	1.35
26	9369	300	0.84	1.70	0.27	14.60	0.26	4.77	1.85	13.00	0.29	-14.70	0.86
26	9433	1750	2.42	1.85	0.27	14.63	1.28	6.39	4.88	11.90	0.39	-12.89	0.00
26	9318	2750	3.9	3.48	0.45	14.98	0.52	5.66	5.52	12.43	12.57	-12.59	0.00
26	9308	3500	3.99	3.60	0.72	14.56	1.17	7.90	7.60	11.65	0.96	-12.86	0.00
26	9306	3750	3.88	2.07	0.35	14.27	1.68	3.98	1.02	12.89	0.23	-12.82	0.00
36	10339	2.4	0.64	3.57	1.46	14.11	0.56	6.87	5.41	12.83	0.87	-14.83	2.93
36	10327	45	0.47	1.21	0.61	14.33	0.57	10.00	3.88	12.88	0.29	-14.50	0.74
36	10319	200	0.50	1.12	0.18	14.76	0.18	8.97	6.39	12.33	0.4	-14.42	0.62
36	10311	600	1.08	1.92	0.93	14.49	0.87	11.47	6.74	12.61	0.41	-14.51	0.84
36	10273	2700	4.36	3.75	0.56	14.22	0.66	5.62	5.48	11.37	11.77	-12.10	0.00
36	10269	2900	3.73	3.73	0.89	14.79	0.41	11.4	5.7	13.35	0.33	-13.55	0.00
36	10263	3500	4.12	4.17	0.73	13.91	0.52	13.59	13.25	11.24	1.12	-12.88	0.05

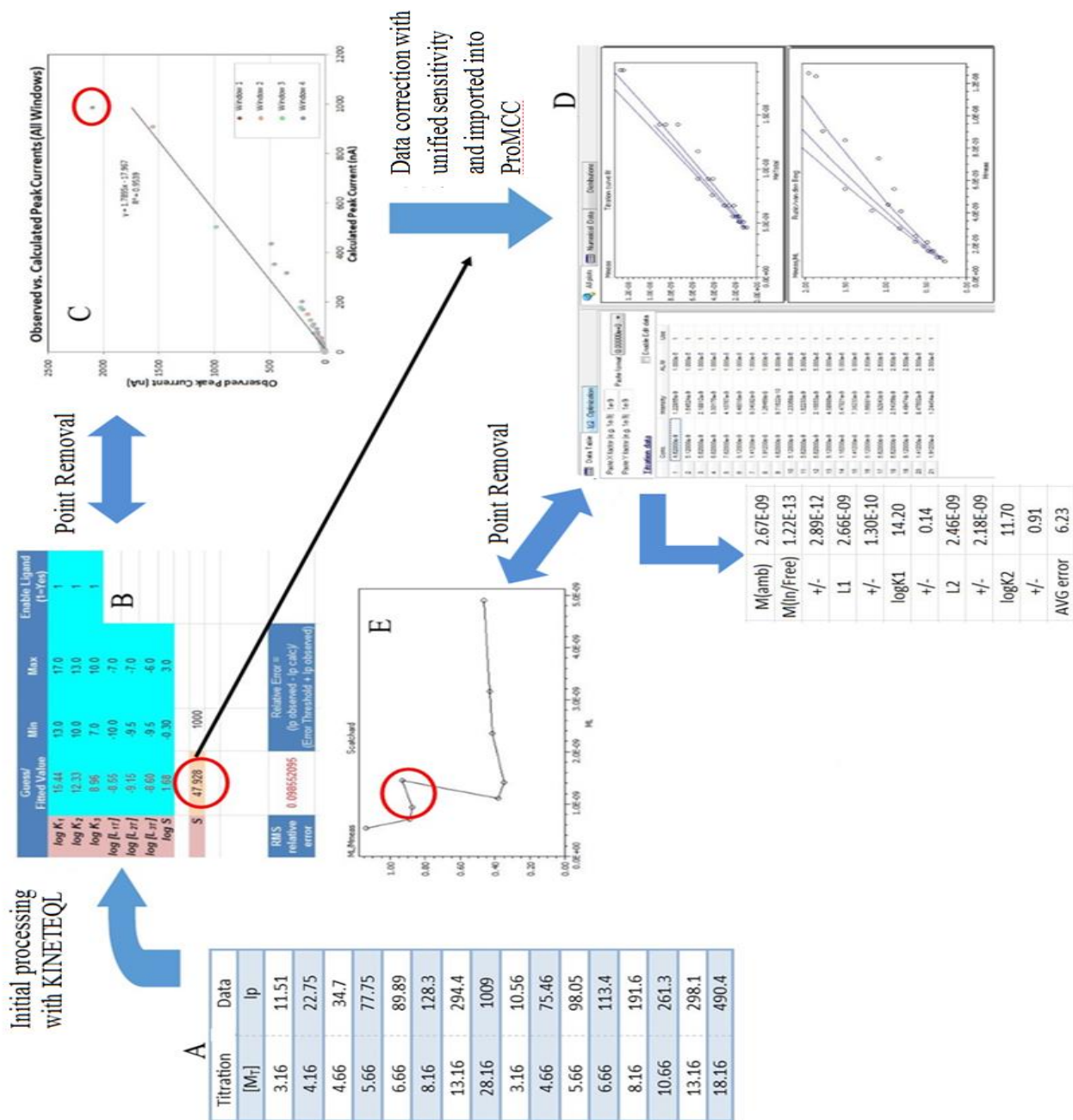


**Figure 2.1.** Conceptual figure of method (3) for processing MAW data, as described in the methods section. (A) is raw generated titration data which is (B) imported to KINETEQL for processing. After processing points away from the sensitivity line are removed (C) after which the determine sensitivity from KINETEQL is used to correct titration peak heights (D) then imported to ProMCC. Prior ro processing with ProMCC another point removal step (E) is carried out based on outliers for the fitting plots (i.e. Scatchard, Langmuir, Ruzic). (F) results are obtained from ProMCC.

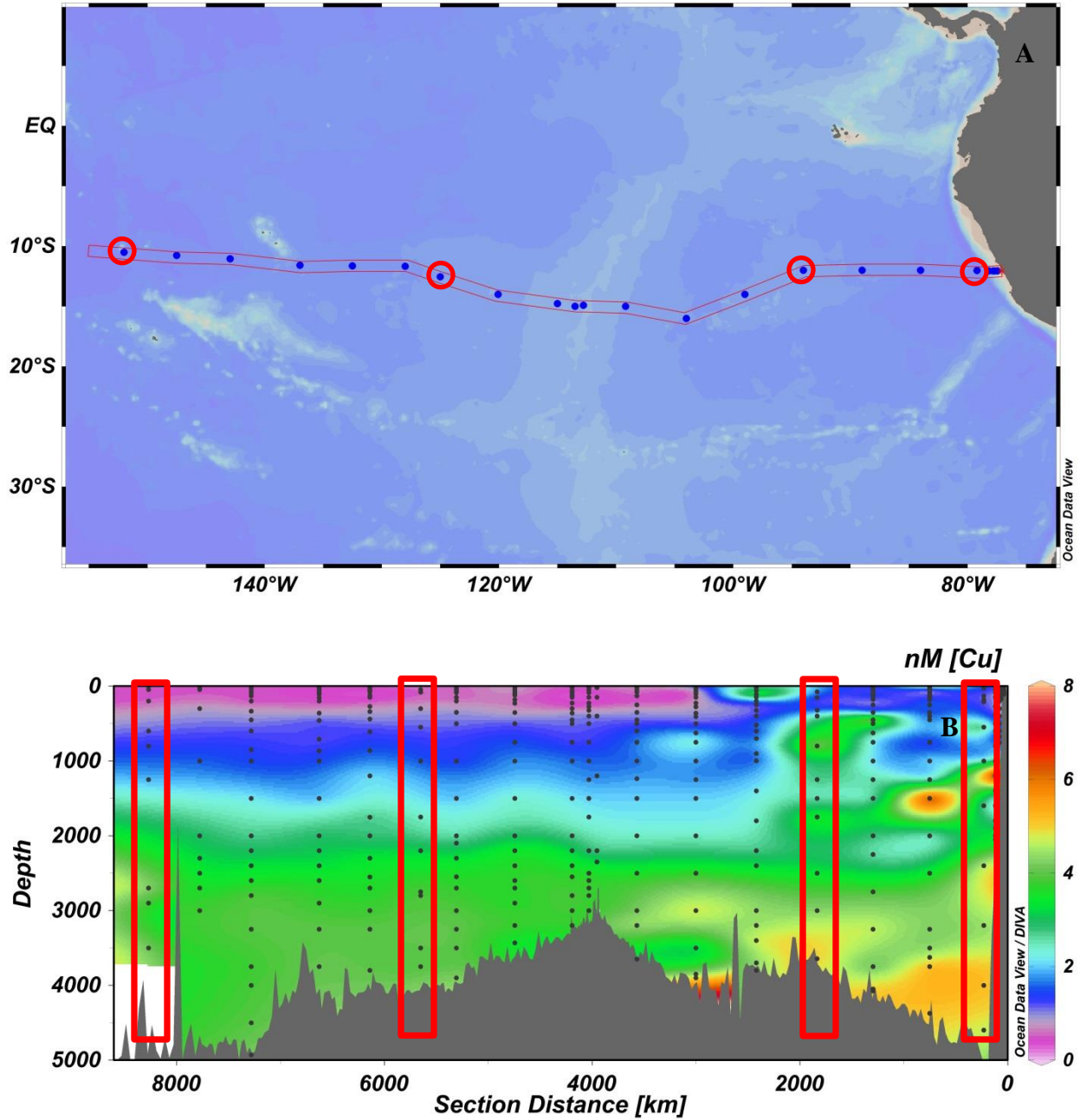


**Figure 2.2.** (A) Map of GP16 speciation profile locations. (B) Profiles highlighted in red boxes were used for MAW analysis. The GP16 stations highlighted from right to left are station 1, 11, 26, and 36.

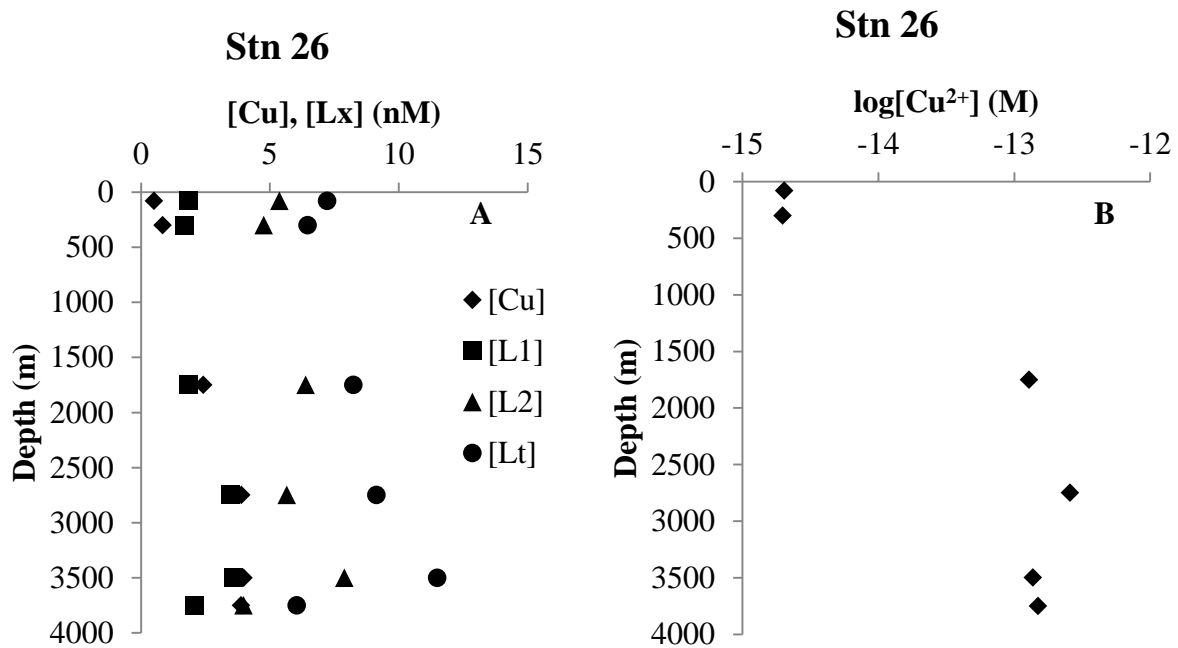


**Figure 2.3.** Profile of GP16 station 26 displaying (A) [Cu], [L<sub>1</sub>], [L<sub>2</sub>], and total ligand ([L<sub>t</sub>]) concentrations and (B) profile of free Cu ion concentrations.

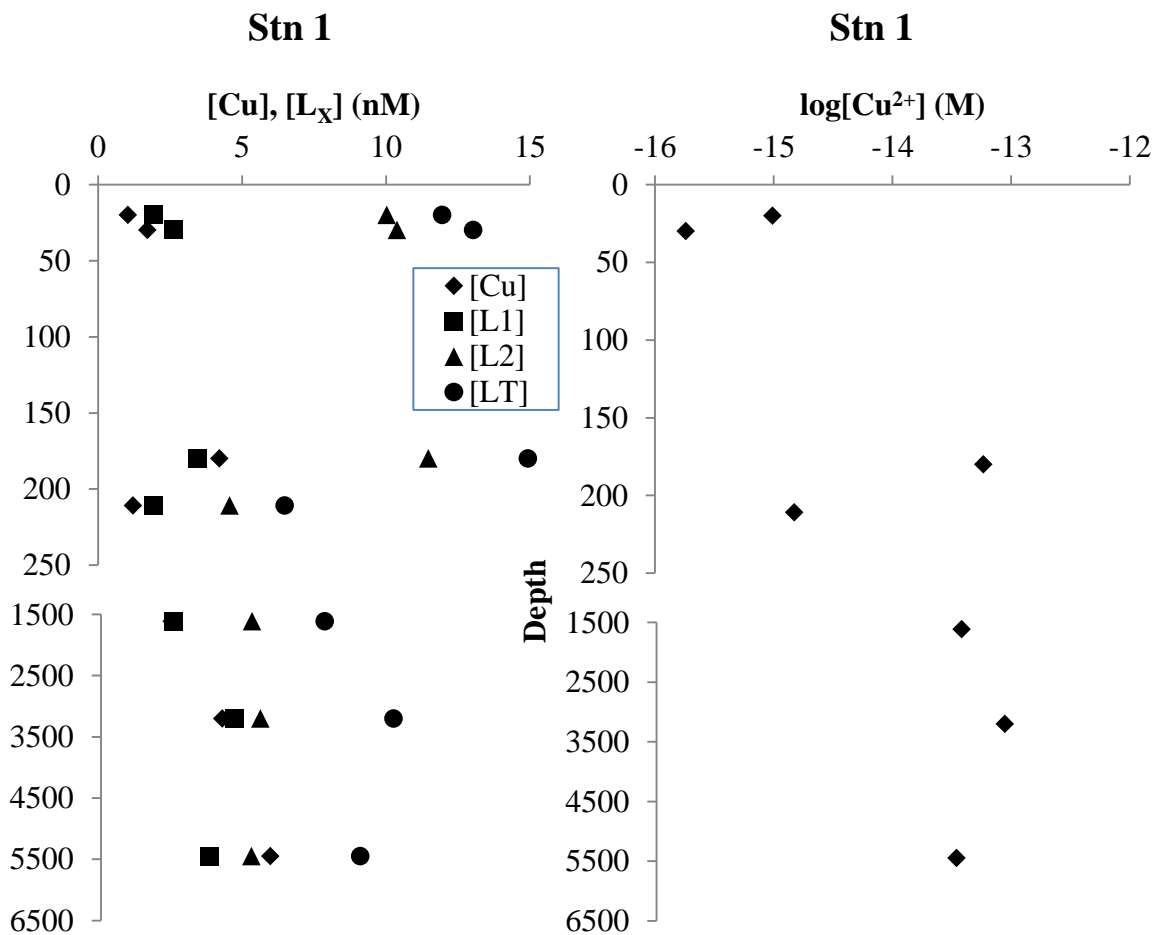


**Figure 2.4.** Profile of GP16 station 1 displaying (A) [Cu], [L<sub>1</sub>], [L<sub>2</sub>], and total ligand ([L<sub>t</sub>]) concentrations and (B) profile of free Cu ion concentrations.



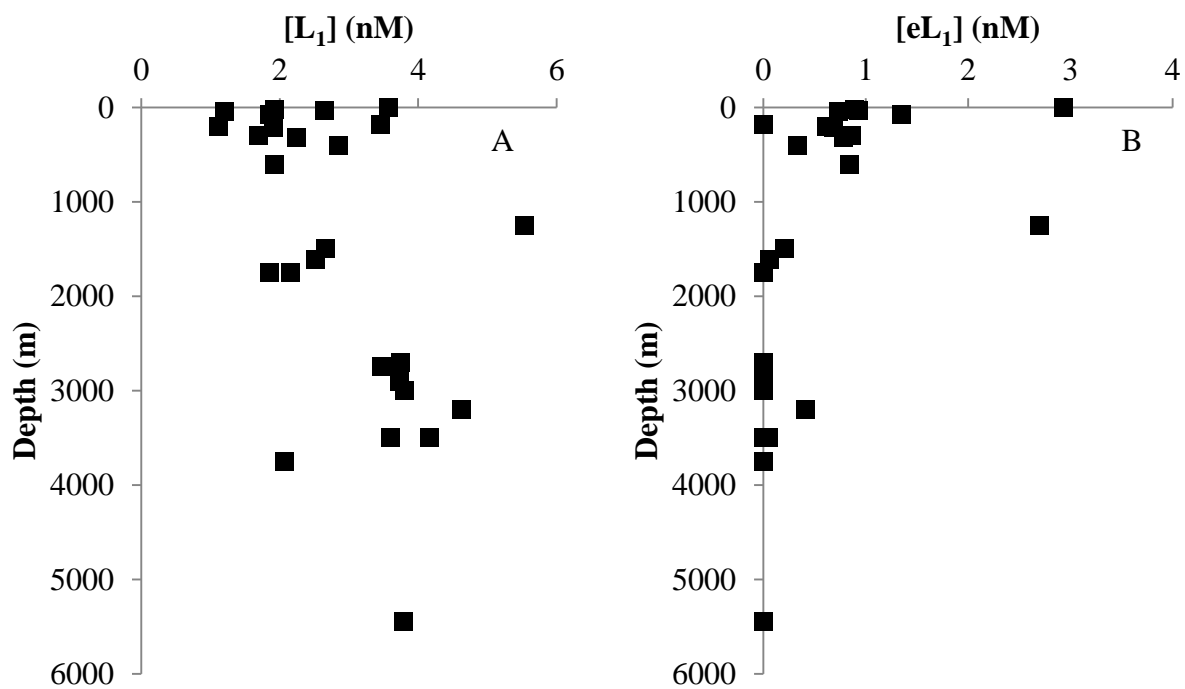


**Figure 2.5.** (A) Plot of all L<sub>1</sub> ligand concentrations in the dataset with depth. (B) Plot of excess L<sub>1</sub> ligands with depth.

## **2.7 ACKNOWLEDGEMENTS**

Funding for this project was provided through a National Science Foundation grant. We thank the captain and crew of the R/V Thompson as well as Claire Parker-Till and Cheryl Zurbrick for collecting the copper speciation samples during the two month GEOTRACES cruise. Saeed Roshan and Claire Parker-Till provided copper data for the samples processed in this section.

Chapter 2, in full, is currently being prepared for submission for publication of the material with the following co-authors: Ruacho, Angel; Bundy, Randelle; Barbeau, Katherine; The dissertation author was the primary author of this paper.

## 2.8 REFERENCES

- Abualhaja, Mahmoud M., Hannah Whitby, and Constant MG van den Berg. "Competition between copper and iron for humic ligands in estuarine waters." *Marine Chemistry* 172 (2015): 46-56.
- Billier, Dondra V., and Kenneth W. Bruland. "Analysis of Mn, Fe, Co, Ni, Cu, Zn, Cd, and Pb in seawater using the Nobias-chelate PA1 resin and magnetic sector inductively coupled plasma mass spectrometry (ICP-MS)." *Marine Chemistry* 130 (2012): 12-20.
- Brand, L. E.; Sunda, W. G.; Guillard, R. R. L., Reduction of marine-phytoplankton reproduction rates by copper and cadmium. *Journal of Experimental Marine Biology and Ecology* 1986, 96 (3), 225-250.
- Bruland, Kenneth W. "Oceanographic distributions of cadmium, zinc, nickel, and copper in the North Pacific." *Earth and Planetary Science Letters* 47, no. 2 (1980): 176-198.
- Bruland, Kenneth W., Eden L. Rue, John R. Donat, Stephen A. Skrabal, and James W. Moffett. "Intercomparison of voltammetric techniques to determine the chemical speciation of dissolved copper in a coastal seawater sample." *Analytica Chimica Acta* 405, no. 1-2 (2000): 99-113.
- Bruland, K. W., Rue, E. L., Smith, G. J., and DiTullio, G. R. (2005). Iron, macronutrients and diatom blooms in the Peru upwelling regime: brown and blue waters of Peru. *Mar. Chem.* 93, 81–103. doi:10.1016/j.marchem.2004.06.011
- Buck, K. N., and Bruland, K. W. (2005). Copper speciation in San Francisco Bay: A novel approach using multiple analytical windows. *Mar. Chem.* 96, 185–198. doi:10.1016/j.marchem.2005.01.001.
- Buck, K. N., Sedwick, P. N., Sohst, B., & Carlson, C. A. (2018). Organic complexation of iron in the eastern tropical South Pacific: results from US GEOTRACES Eastern Pacific Zonal Transect (GEOTRACES cruise GP16). *Marine Chemistry*, 201, 229-241.
- Bundy, R. M., Barbeau, K. A., and Buck, K. N. (2013). Sources of strong copper-binding ligands in Antarctic Peninsula surface waters. *Deep. Res. Part II Top. Stud. Oceanogr.* 90, 134–146. doi:10.1016/j.dsr2.2012.07.023.
- Campos, M. L. A. M., and van den Berg, C. M. G. (1994). Determination of copper complexation in sea water by cathodic stripping voltammetry and ligand competition with salicylaldoxime. *Anal. Chim. Acta* 284, 481–496. doi:10.1016/0003-2670(94)85055-0.

- Chadwick, D. B., Zirino, A., Rivera-Duarte, I., Katz, C. N., & Blake, A. C. (2004). Modeling the mass balance and fate of copper in San Diego Bay. *Limnology and Oceanography*, 49(2), 355-366.
- Cutter, Gregory, Karen Casciotti, Peter Croot, Walter Geibert, Lars-Eric Heimbürger, Maeve Lohan, H el ene Planquette, and Tina van de Flierdt. "Sampling and Sample-handling Protocols for GEOTRACES Cruises. Version 3, August 2017." (2017).
- Hudson, Robert JM, Eden L. Rue, and Kenneth W. Bruland. "Modeling complexometric titrations of natural water samples." *Environmental science & technology* 37, no. 8 (2003): 1553-1562.
- Hudson, 2014 R.J.M. Hudson, Software: KINETEQL Multiwindow Solver (KMS), Version 1.0 <https://sites.google.com/site/kineteql/> (2014)
- Jacquot, Jeremy E., Yoshiko Kondo, Angela N. Knapp, and James W. Moffett. "The speciation of copper across active gradients in nitrogen-cycle processes in the eastern tropical South Pacific." *Limnology and Oceanography* 58, no. 4 (2013): 1387-1394.
- Jacquot, Jeremy E., and James W. Moffett. "Copper distribution and speciation across the International GEOTRACES Section GA03." *Deep Sea Research Part II: Topical Studies in Oceanography* 116 (2015): 187-207.
- Kogut, Megan B., and Bettina M. Voelker. "Strong copper-binding behavior of terrestrial humic substances in seawater." *Environmental science & technology* 35, no. 6 (2001): 1149-1156.
- Moffett, J. W., Brand, L. E., Croot, P. L., & Barbeau, K. A. (1997). Cu speciation and cyanobacterial distribution in harbors subject to anthropogenic Cu inputs. *Limnology and Oceanography*, 42(5), 789-799.
- Moffett, J. W., R. G. Zika, and Larry E. Brand. "Distribution and potential sources and sinks of copper chelators in the Sargasso Sea." *Deep Sea Research Part A. Oceanographic Research Papers* 37, no. 1 (1990): 27-36.
- Omanovi c, Dario, C edric Garnier, and Ivanka Pi zeta. "ProMCC: an all-in-one tool for trace metal complexation studies." *Marine Chemistry* 173 (2015): 25-39.
- Parker, C. E., M. T. Brown, and K. W. Bruland. "Scandium in the open ocean: A comparison with other group 3 trivalent metals." *Geophysical Research Letters* 43, no. 6 (2016): 2758-2764.
- Peers, G., Quesnel, S. A., & Price, N. M. (2005). Copper requirements for iron acquisition and growth of coastal and oceanic diatoms. *Limnology and oceanography*, 50(4), 1149-1158.

- Peers, G., & Price, N. M. (2006). Copper-containing plastocyanin used for electron transport by an oceanic diatom. *Nature*, 441(7091), 341-344.
- Pistocchi, R., Mormile, M. A., Guerrini, F., Isani, G., & Boni, L. (2000). Increased production of extra-and intracellular metal-ligands in phytoplankton exposed to copper and cadmium. *Journal of Applied phycology*, 12(3-5), 469-477.
- Pižeta, I., Sander, S.G., Hudson, R.J., Omanović, D., Baars, O., Barbeau, K.A., Buck, K.N., Bundy, R.M., Carrasco, G., Croot, P.L. and Garnier, C., 2015. Interpretation of complexometric titration data: An intercomparison of methods for estimating models of trace metal complexation by natural organic ligands. *Marine Chemistry*, 173, pp.3-24.
- Roshan, Saeed, and Jingfeng Wu. "Dissolved and colloidal copper in the tropical South Pacific." *Geochimica et Cosmochimica Acta* 233 (2018): 81-94.
- Sander, Sylvia G., Keith A. Hunter, Hauke Harms, and Mona Wells. "Numerical approach to speciation and estimation of parameters used in modeling trace metal bioavailability." *Environmental science & technology* 45, no. 15 (2011): 6388-6395.
- Swarr, G. J., Kading, T., Lamborg, C. H., Hammerschmidt, C. R., & Bowman, K. L. (2016). Dissolved low-molecular weight thiol concentrations from the US GEOTRACES North Atlantic Ocean zonal transect. *Deep Sea Research Part I: Oceanographic Research Papers*, 116, 77-87.
- Thompson, C. M., M. J. Ellwood, and Sylvia G. Sander. "Dissolved copper speciation in the Tasman Sea, SW Pacific ocean." *Marine Chemistry* 164 (2014): 84-94.
- van den Berg, C.M.G., 1987. Organic complexation and its control on the dissolved concentrations of copper and zinc in the Scheldt Estuary. *Estuarine Coastal Shelf Sci.* 24 (6), 785–797.
- Voelker, Bettina M., and Megan B. Kogut. "Interpretation of metal speciation data in coastal waters: the effects of humic substances on copper binding as a test case." *Marine Chemistry* 74, no. 4 (2001): 303-318.
- Walker, C.B., de la Torre, J.R., Klotz, M.G., Urakawa, H., Pinel, N., Arp, D.J., Brochier-Armanet, C., Chain, P.S.G., Chan, P.P., Gollagbir, A., Hemp, J., Hügler, M., Karr, E.A., Könneke, M., Shin, M., Lawton, T.J., Lowe, T., Martens-Habbena, W., Sayavedra-Soto, L.A., Lang, D., Sievert, S.M., Rosenzweig, A.C., Manning, G., Stahl, D.A., 2010. *Nitrosopumilus maritimus* genome reveals unique mechanisms for nitrification and autotrophy in globally distributed marine Crenarchaea. *PNAS* 107 (19), 8818–8823.
- Wells, Mona, Kristen N. Buck, and Sylvia G. Sander. "New approach to analysis of voltammetric ligand titration data improves understanding of metal speciation in natural waters." *Limnology and Oceanography: Methods* 11, no. 9 (2013): 450-465.

- Whitby, Hannah, Anna M. Posacka, Maria T. Maldonado, and Constant MG van den Berg. "Copper-binding ligands in the NE Pacific." *Marine Chemistry* 204 (2018): 36-48.
- Whitby, H., & van den Berg, C. M. (2015). Evidence for copper-binding humic substances in seawater. *Marine Chemistry*, 173, 282-290.
- Wong, Kuo Hong, Hajime Obata, Taejin Kim, Asami Suzuki Mashio, Hideki Fukuda, and Hiroshi Ogawa. "Organic complexation of copper in estuarine waters: An assessment of the multi-detection window approach." *Marine Chemistry* 204 (2018): 144-151.
- Wong, Kuo Hong, Hajime Obata, Taejin Kim, Yohei Wakuta, and Shigenobu Takeda. "Distribution and speciation of copper and its relationship with FDOM in the East China Sea." *Marine Chemistry* 212 (2019): 96-107.
- Wu, J., Boyle, E.A., 1997. Low blank preconcentration technique for the determination of lead, copper, and cadmium in small-volume seawater samples by isotope dilution ICPMS. *Anal. Chem.* 69, 2464–2470. <http://dx.doi.org/10.1021/ac961204u>.

## **CHAPTER 3: Copper Speciation and Toxicity in San Diego Bay**

### 3.1 ABSTRACT

Seven sites within San Diego Bay were sampled during three different seasons and analyzed for dissolved copper (Cu) and Cu speciation using a competitive ligand exchange electrochemical technique with multiple analytical windows (MAW) for accurate determination of  $\text{Cu}^{2+}$  in order to evaluate copper toxicity within the Bay. A bioindicator, the marine cyanobacterium *Synechococcus sp.*, was used to study the relationship between elevated  $\text{Cu}^{2+}$  concentrations and *Synechococcus* counts *in situ* as further validation of copper toxicity. The majority of stations within the Bay were found to have  $\text{Cu}^{2+}$  concentrations below the toxicity threshold despite high dissolved Cu concentrations. The only site found with  $\text{Cu}^{2+}$  concentrations consistently exceeding the *Synechococcus* toxicity threshold ( $10^{-11}$  M) and associated with reduced *Synechococcus* cell counts was the Shelter Island Yacht Basin site. Shelter Island Yacht Basin is an enclosed marina with a high density of recreational vessels and subject to elevated inputs of anthropogenic Cu from antifouling boat paint. The utilization of MAW competitive ligand exchange electrochemical titrations to evaluate the ligand pool at impacted coastal sites provides information on the ligand pool's ability to buffer the site from reaching toxic Cu levels, as well as enabling an accurate determination of  $[\text{Cu}^{2+}]$ .

### 3.2 INTRODUCTION

Copper (Cu) is a trace metal found in nanomolar concentrations in the ocean with subnanomolar concentrations found in open ocean surface waters. Despite low oceanic dissolved concentrations Cu plays a vital role for facilitating various biological processes in marine and aquatic microorganisms such as the acquisition of iron (Fe) (Peers et al, 2005), photosynthesis (Peers and Price, 2006) as well as ammonia oxidation by archaea, which use multiple multi-copper oxidases (Walker et al, 2010). The majority of Cu in marine waters (>99%) is bound to



organic metal binding ligands (van den Berg, 1987). Although Cu is a vital micro-nutrient for organisms, when concentrations of the unbound  $\text{Cu}^{2+}$  ion reach levels in excess of about  $10^{-11}$  M (Brand et al, 1986), Cu becomes toxic to organisms such as cyanobacteria which exhibit a reduction in reproduction rates. The toxicity of Cu highlights the important role played by organic Cu binding ligands, as ligands are able to buffer the free Cu ion and keep  $\text{Cu}^{2+}$  from reaching toxic levels. Considering the low concentrations of Cu found in oceanic environments few open ocean regions have been shown to have  $\text{Cu}^{2+}$  concentrations in the toxic range. However, coastal areas in dense urban environments are subjected to anthropogenic sources of Cu producing some of the most impacted sites for Cu toxicity (Blake et al., 2004; Moffett et al., 1997; Oldham et al., 2014). Many of these impacted sites lie within enclosed protected harbors that limit water movement and are subjected to seasonal runoff.

Boat harbors have historically been sites of acute pollution, in particular for heavy metals due to the high concentration of watercraft as well as the mostly stagnant waters that make for ideal harbor locations. Runoff of heavy metals into harbors is one source of metal contamination. Another significant source, particularly for Cu, derives from antifouling boat paint. Antifouling boat paint is made up of a Cu base that is designed to slowly release over time to act as a biocide preventing algae and other encrusting organisms from attaching to the hull (Earley et al., 2013). The use of Cu based antifouling boat paint as well as regular cleaning of the hull are important for proper boat maintenance but are the main reason harbors are subjected to toxic concentrations of Cu (Earley et al., 2013).

San Diego Bay is home to many private as well as commercial and military docks with thousands of watercraft, all potentially a source of Cu. Copper levels within San Diego Bay exceed water quality criteria leading to regulatory controls like a Total Maximum Daily Loads

(TMDL) to limit the loading of Cu into the Bay, particularly at yacht basins and marinas (Port of San Diego, 2011). The Shelter Island Yacht Basin has been identified to exceed state and federal standards for Cu pollution, leading to a regulatory order for boaters, marinas, hull cleaners, and the Port of San Diego to reduce Cu pollution. The San Diego Regional Water Quality Control Board has implemented a TMDL regulatory program, based on total dissolved Cu concentration, to reduce Cu emissions by 76% from boats in Shelter Island Yacht Basin by 2022. The current TMDL is a numeric water quality objective based on generalized national water quality criteria designed to be protective of aquatic organisms in a wide range of natural environments. The TMDL ignores the physical and chemical characteristics of ambient water at a particular site that may result in an increase or decrease in the bioavailability and/or toxicity of copper. Considering that the unbound  $\text{Cu}^{2+}$  ion is the toxicant, the total amount of dissolved Cu present may not be the most salient regulatory factor, as the Cu ligands in the system will ultimately determine how much Cu is left unbound and if that amount is in a toxic range. In the case of dynamic coastal and urban water ways, water quality objectives based on site-specific criteria may offer a more robust and appropriate regulatory tool than blanket national criteria.

In addition to Cu associated with boating activity, San Diego Bay is also affected by Cu from brake pad dust, as brake pads have Cu that flakes off during braking action. The majority of this dust is washed into the Bay and other water ways during rain events which are limited primarily to the winter in Southern California. Southern California can be subjected to dry periods with no rain lasting the majority of the year. Any rain event after a prolonged dry period has the potential to inject a pulse of Cu from runoff into the Bay, potentially leading to acute Cu pollution. Storm events can also possibly exacerbate Cu toxicity by stirring up the sediments in

San Diego Bay, which have been shown to contain elevated levels of Cu (NOAA, 1991).

Purposeful dredging activities can have similar effects.

San Diego Bay is highlighted by its unique crescent shape with an opening to the ocean at the northern end. There are several creeks that feed freshwater and particulate matter into the Bay but this occurs infrequently during the rainy season and is virtually non-existent during the remainder of the year (Largier et al. 1997). For our study we evaluated total dissolved Cu and the ligand pool at various sites within San Diego Bay to identify locations experiencing Cu toxicity. Cell counts of the marine cyanobacterium *Synechococcus*, due to its well-documented sensitivity to Cu (Sunda and Guillard 1976; Brand et al. 1986), were determined at each site and used as a bioindicator for toxicity in conjunction with electrochemical determinations of  $\text{Cu}^{2+}$  concentrations. Sampling was carried out to capture a view of *Synechococcus*, total Cu and Cu ligands during times of peak boat activity (summer), at the end of the rainy season (spring) which can impact the Bay with runoff water, and finally during the fall which follows the end of the summer boat activity and normally a prolonged dry period in San Diego. In order to determine the concentration of the toxic  $\text{Cu}^{2+}$  ion in our samples, we applied a sophisticated electrochemical competitive ligand exchange analysis with titrations at multiple analytical windows (MAW) (i.e. titrations at a range of competition strengths with the added ligand) and direct modeling of titration data. This approach, which reflects recent advances in the interpretation of complexometric titration data (Hudson et al. 2003; Pizeta et al. 2015; Omanovic et al. 2015) has previously been applied in San Francisco Bay in support of the development of site-specific copper toxicity objectives there (Buck and Bruland, 2005; Sander et al. 2015). Our study represents the first time this approach has been applied in the Southern California region, where restricted, high traffic embayments like San Diego Bay represent a significantly more

dynamic range of total copper and copper ion concentrations than typically encountered in the San Francisco Bay region. The MAW method applied here is described in Chapter 2 as it utilizes the “optimized” MAW processing method to characterize the ligand pool. The use of  $\text{Cu}^{2+}$  and *Synechococcus* together may provide a more direct link between Cu levels and biological toxicity, an observation a previous San Diego study (Schiff et al. 2007) lacked as that study did not determine free Cu concentrations. Schiff et al. 2007 used a biological indicator (bivalve larvae) for toxicity in San Diego marinas and showed a relationship between total dissolved copper levels and toxic effects, but the actual occurrence of toxicity was shown to be much less frequent than the frequency of exceedance of state water quality standards as defined by total dissolved copper concentrations (Schiff et al. 2007). By linking  $\text{Cu}^{2+}$  concentrations with *Synechococcus*, observations of toxicity can be directly related to free Cu concentrations and not just total dissolved Cu (Moffett et al., 1997). Though there have been studies in San Diego Bay that determined free Cu concentrations (Zirino et al., 1998; Blake et al. 2004) through an ion selective probe a complicating factor for these studies is the presence of organic matter which buffers  $\text{Cu}^{2+}$  to varying degrees based on the concentration and binding strengths of the organic ligands present in the waters. Our method of determining free Cu concentrations is more chemically precise than electrochemical methods that directly measure labile copper, which is an operationally defined pool specific to the electrode and chemical conditions employed, and may include a variety of copper species other than  $\text{Cu}^{2+}$  which may or may not be toxic to aquatic organisms.

### **3.3 METHODS**

#### ***3.3.1 Sampling and location***

The study site is comprised of 7 stations within the harbor of San Diego Bay, beginning near the mouth of the Bay and ending in the inner Bay near the San Diego Bay National Wildlife Refuge (Fig. 3.1). Locations of note from the sampling include: site E which is near the 10<sup>th</sup> Ave Marine Terminal where various commercial and non-commercial ships can dock; site F just south of the Coronado Bridge with daily traffic around 75,000 cars; and the Shelter Island Yacht Basin (site C). The sampling occurred onboard a 17 ft. Boston Whaler with a 10 ft. fiberglass pole equipped with trace metal clean sampling bottles on the end. At each station the boat came to a stop and bottles were held away from the boat as much as possible with the 10 ft. pole and dipped about a meter into the water, filled and rinsed with water three times before collecting a sample for Cu speciation. The sample bottle was then stored in a cooler filled with ice until returned to the lab several hours later. Once in the lab each sample was filtered in a laminar flow hood on an acid cleaned Teflon filter rig with acid cleaned 0.45  $\mu$ M polycarbonate filters and then stored in a -20 C freezer until analysis.

Along with collecting speciation samples, samples for *Synechococcus* cell counts were collected in 50 mL Falcon tubes and kept in a cooler in the dark until preserved in the lab with 0.25% glutaraldehyde (Sigma-Aldrich, St Louis, MO, USA) before being stored in a -80 freezer until analysis. Measurements of pH, water temperature, and oxygen were made with a Yellow Springs Instrument (YSI) probe at each station. Three sampling events took place over a year with each of the 7 sites sampled during each sampling trip. The first sampling took place during summer 2015 during the peak of boat activity in the Bay and on an incoming tide (Fig 3.2). The second sampling occurred during early Spring in 2016 which is usually the end of the rainy season in the region, sampling began during the through of the low tide (Fig 3.2). The final

sampling occurred during Fall 2016 after the peak of summer activity and a prolonged period of no rains in the region, sampling began on an outgoing tide (Fig 3.2).

### **3.3.2 Reagents**

The boric acid (BA) buffer was prepared by dissolving boric acid (Alfa Aesar, 99.99%) in 0.4 N aqueous  $\text{NH}_4\text{OH}$  (Optima, Fisher Scientific). A 4 mM stock of salicylaldoxime (SA; > 98%) was prepared in methanol (Optima LC/MS, Fisher Scientific) and replaced every six months or as needed. Cu standards (100 nM to 10  $\mu\text{M}$ ) were diluted from an atomic adsorption standard (1000 ppm, Spex CertiPrep) into pH 2 MQ water (acidified with Optima grade HCl). All reagents were stored in trace metal clean Teflon bottles.

### **3.3.3 Acid washing**

Fluorinated polyethylene (FLPE; 1 L) bottles were used for the collection of copper speciation samples and were put through a shortened acid washing cleaning prior to use as FLPE bottles have previously been used and acid cleaned. The bottles were washed in a hydrochloric acid (3 M) (HCl) bath for a week before being rinsed with milli-Q (MQ;  $18 \text{ M}\Omega \text{ cm}^{-1}$ ) and partially filled with MQ water and bagged until use. The Teflon filter rigs were also treated in a similar fashion as they were kept in HCl for a week before being stored cleanly until use. The 0.45  $\mu\text{M}$  polycarbonate filters were cleaned by first placing them in acetic acid for a week before rinsing and placing them in 3 M HCl for another week and finally storing in pH 2 MQ.

### **3.3.4 Dissolved copper analysis**

An aliquot of about 100 mL was taken from the 1 L FLPE bottle in which the speciation sample was stored. Prior to an aliquot being collected the sample was thawed in a refrigerator for two days and shaken vigorously. Dissolved Cu was determined through standard addition with the use of cathodic stripping voltammetry after UV oxidation of the sample for 8 hrs, utilizing

the same electrochemical parameters for Cu speciation which are outlined in (Bundy et al. 2013; Buck and Bruland 2005). The boric acid buffer as well as 25  $\mu$ M SA was used to measure Cu on a BaSI (Bioanalytical Systems Incorporated) hanging mercury drop electrode. Short deposition times were used for standard additions ranging from 10 to 30 seconds. Standard additions were done for each sample collected, due to volume considerations no replicate standard additions were done for Cu determination.

### ***3.3.5 Dissolved carbon analysis***

Samples for dissolved organic carbon were collected from an aliquot of the FLPE bottle with the speciation sample after thawing. The aliquot was collected in a combusted 60 mL glass tube and acidified with two drops of concentrated HCl, the vials were then sealed with acid washed vial caps with septa. Samples were stored at room temperature in the dark until analyzed via high-temperature combustion on a Shimadzu 500 V-CSN/TNM-1 (Shimadzu Corp, Kyoto, Japan).

### ***3.3.6 Synechococcus and picoeukaryote concentration determination***

Samples were thawed after storage in a -80 freezer then processed as described in Collier and Palenik (2003). Cell abundance counts were normalized using pre-counted 0.94  $\mu$ m green fluorescent beads (Duke Scientific Corporation, Palo Alto, CA, USA) that were added to each sample. Events falling within specific regions were counted as *Synechococcus* or picoeukaryote cells.

### ***3.3.7 Copper speciation***

Speciation samples from San Diego Bay were analyzed with a competitive ligand exchange adsorptive cathodic stripping voltammetry technique (CLE-ACSV) utilizing multiple analytical windows (MAW). The theory of the CLE-ACSV method is detailed in Buck and

Bruland (2005). This method employs the competition for Cu between a well-characterized added ligand (SA) and the natural seawater ligands to determine the thermodynamic stabilities of the natural ligands (originally published in Campos and van den Berg, 1994). The analytical methods and electrochemical parameters are outlined in Bundy et al. (2013) and Buck and Bruland (2005). Frozen samples were thawed in a refrigerator and vigorously shaken prior to analysis. The samples were then aliquoted (10 mL) into pre-conditioned Teflon vials and buffered with 1.5 M boric acid-ammonia (BA) to pH 8.2. The vials were spiked with increasing concentrations of Cu ranging from 0-350 nM to saturate the natural ligands. The boric acid buffer and Cu were equilibrated with the natural ligands for two hours, after which the competing ligand, SA, was added. Five titrations were carried out in this manner with a concentration of SA of 1, 2.5, 5, 10, or 25  $\mu\text{M}$ . Titrations with SA concentration between 5 and 25  $\mu\text{M}$  were equilibrated with SA for at least 15 minutes, while titrations with SA concentrations of 1 and 2.5  $\mu\text{M}$  were equilibrated with SA for at least 30 minutes. Deposition times ranged from 10 s to 60 s depending on the Cu concentration. During the deposition step the Cu-SA complex accumulates onto the mercury drop before a reduction current is used to generate a measureable peak. Speciation samples were analyzed in 11-point titrations carried out on a controlled growth mercury electrode (Bioanalytical Systems Incorporated). Peaks generated from titrations were extracted using the ECDSOFT software package (Omanović et al., 2015). Titration data from the 2.5, 5, and 10  $\mu\text{M}$  were used to determine Cu ligand parameters utilizing the optimized MAW method described in Chapter 2. The titration data was first simultaneously processed with the KINETEQL solver and the sensitivity determined by KINETEQL was used to correct the titration peak data before final processing in ProMCC utilizing a two ligand fitting model (Hudson et al. 2003; Omanovic et al., 2015). Final processing from ProMCC produced Cu



speciation data for ligand concentrations ( $L_1$  and  $L_2$ ), binding strength ( $\log K$ ), and  $\text{Cu}^{2+}$  concentrations.

## **3.4 RESULTS**

### ***3.4.1 Hydrography***

Measurements of temperature, salinity, pH, and dissolved oxygen (DO) are presented in Table 3.1. Surface temperatures during sampling were highest during the summer sampling, exceeding 20 C. Salinity within the Bay is similar to ocean salinity, highlighting the lack of freshwater influence. The highest salinity was found in the back Bay during the Fall sampling. The pH within the Bay ranged from around 7.5 to just above 8 and the DO was between 7 and 9 mg /L during the summer and spring sampling. During the fall sampling DO values were not recorded due to difficulties with the YSI probe.

### ***3.4.2 Dissolved organic carbon***

Results for dissolved organic carbon (DOC) for all sampling events are presented in Fig. 3.3 and Table 3.2. Due to volume constraints no DOC data is available for Station B in the summer, Station F in the spring, and Station G in the fall. DOC within the Bay was found in slightly higher concentrations than the coastal ocean. Overall there was a slight increase in DOC towards the back Bay, with some of the highest DOC concentrations found at Station G, the station deepest in the Bay and furthest from the ocean-Bay interface. Station G is also closest to the saltmarsh and intertidal mudflat habitats of the San Diego Bay National Wildlife Refuge, which may impact DOC concentrations. The lowest DOC concentrations were found at Stations A and B, which experience the most exchange with the ocean.

### ***3.4.3 Synechococcus results***

*Synechococcus* cell counts were used as a bioindicator for Cu toxicity and are presented in Fig 3.4 and Table 3.2. *Synechococcus* counts observed in San Diego Bay were mostly comparable, on the lower end, with *Synechococcus* counts observed at the nearby Scripps Pier (Nagarkar et al., 2018). Station C, Shelter Island Yacht Basin, had the lowest concentrations during the first two samplings. During the fall sampling, Stations A and B had higher counts than previously observed, while Stations C-G had lower than expected *Synechococcus* counts.

#### **3.4.4 Dissolved copper**

Dissolved Cu was determined at each station during all sampling periods with cathodic stripping voltammetry, and results for dissolved Cu are presented in Fig 3.5. The lowest dissolved Cu concentrations, over all the sampling trips, were found at stations A and B. Station A in particular had the lowest concentration during the summer sampling. Sampling over the summer began as the high tide was approaching its peak, leaving Stations A and B to be heavily influenced by coastal ocean water. The highest dissolved Cu concentrations were consistently found at Station C, the Shelter Island Yacht Basin. Concentrations at Shelter Island ranged from 75 to 122 nM, similar to levels observed in previous studies (Zirino et al., 1998; Blake et al., 2004). The summer sampling at Station C had the highest recorded dissolved Cu, 122 nM, likely related to the peak of boat activity. The summer sampling also followed a weekend of very heavy thunderstorms, a rare event for the region in general especially during the summer, possibly injecting a pulse of runoff into the Bay. Subsequent sampling at Station C did not find the site to exceed 100 nM. The remaining stations over the three sampling periods had similar dissolved Cu concentrations ranging from 20-40 nM, with the two innermost stations (F and G) on the higher end.

### ***3.4.5 Copper speciation***

Copper ligands, binding strengths, and  $\text{Cu}^{2+}$  concentrations were determined using the optimized MAW processing method from Chapter 2. Results for Cu speciation parameters are presented in Table 3.2. The strongest ligands were found at Station A, which also had the lowest  $\text{Cu}^{2+}$  concentrations during all three sampling events. Some of the highest concentrations of total ligands were found at the Shelter Island Yacht Basin (Station C), with a large pool of the relatively weaker  $L_2$  ligands. The  $L_2$  ligands detected at Station C were also some of the weakest ligands detected between all the stations over all three sampling events. Through all three sampling events Station C consistently had the highest  $\text{Cu}^{2+}$  concentrations, Fig 3.6. The majority of stations in San Diego Bay, particularly Station G, had higher dissolved Cu concentrations than  $L_1$  concentrations. The  $L_2$  ligands at all stations, except Station C in the spring, were well in excess of dissolved Cu. The stronger  $L_1$  ligands detected in most of the inner Bay have similar binding strengths to the weaker  $L_2$  ligand that is detected in most ocean samples with multiple ligands (Chapter 2; Bundy et al., 2013; Whitby et al., 2018).

## **3.5 DISCUSSION**

### ***3.5.1 Previous San Diego Bay work***

Previous work in San Diego Bay evaluated the Bay during different seasons of the year for Cu toxicity by determining various labile and non-labile copper fractions through the use of an ion selective probe (Zirino et al. 1998) or through voltammetric means combined with an ion selective probe (Blake et al., 2004). Despite employing very different methodologies previous studies, like our study, show that the region of the Shelter Island Yacht Basin was persistently associated with elevated labile copper concentrations. The previous studies show that the inner Bay does not likely reach free Cu levels that are toxic for *Synechococcus*, and these findings are

similar to ours for the inner Bay. The Blake et al. (2004) study did find ion-specific electrode-based free Cu concentrations around the mouth of the Bay to be close to toxic levels ( $10^{-11}$  M), while in contrast our study found that region to be well outside the toxic range. The difference may be due to the time of year sampling occurred. In the Blake et al. (2004) study near-toxic levels at the mouth of the Bay were found during January, and none of our samplings took place during January or in the winter. Findings from our study are in line with previous studies highlighting that Shelter Island is persistently under Cu stress.

### ***3.5.2 Comparison with other harbors***

Studies in other harbors also impacted by anthropogenic Cu have been carried out, revealing important information about Cu speciation and its role in Cu toxicity. One such study evaluated several sites (harbors and ponds) in Cape Cod for Cu toxicity (Moffett et al., 1997). In their study Moffett et al. (1997) utilized  $\text{Cu}^{2+}$  (determined via CLE-ACSV) and *Synechococcus* as indicators of toxicity. Similar to our own work, they found *Synechococcus* cell counts to decrease as the free Cu ion increased, with high concentrations of the  $\text{Cu}^{2+}$  ion found in areas of heavy anthropogenic Cu inputs primarily from antifouling paint. A major finding from Moffett et al. (1997) was that the concentration of the strong  $L_1$  ligand in their study areas closely matched the concentration of dissolved Cu. When the strong  $L_1$  ligand was saturated by Cu, significant increases in  $\text{Cu}^{2+}$  were observed. Titrations were then carried out at different analytical windows, highlighting the effect that analytical window has on the  $\text{Cu}^{2+}$  concentration. The importance of utilizing a MAW approach when studying Cu impacted coastal waters is shown in Moffett et al. (1997) as the strong  $L_1$  ligand, the primary control on  $\text{Cu}^{2+}$ , was near the saturation point leaving the weaker ligands to provide a buffer and maintain free Cu low. Without the detection of weaker ligands free Cu concentrations may be overestimated when only a single strong ligand is

determined. In our study we also observed the effect of determining  $\text{Cu}^{2+}$  without employing a MAW approach in an environment impacted by anthropogenic Cu, Fig 3.7. Without probing the ligand pool with varying analytical windows we were limited in the ligands that could be detected, with those that were detected often exceeded by the dissolved Cu concentration. Despite the ligand detected being a strong  $L_1$  ligand, many sites within San Diego Bay would be incorrectly interpreted as being affected by Cu toxicity unless the weaker  $L_2$  ligands were detected and taken into account in calculating  $\text{Cu}^{2+}$ . The use of MAW for accurate determination of  $\text{Cu}^{2+}$  as well as the use of a secondary indicator for Cu toxicity, like *Synechococcus*, can aide in accurate identification of Cu toxicity.

In our work copper speciation results coupled with *Synechococcus*, as a bioindicator for Cu toxicity, point to persistent toxic conditions at the Shelter Island Yacht Basin (Station C). This is reflected in the free  $\text{Cu}^{2+}$  concentrations (Fig 3.6) and the low *Synechococcus* concentrations (Table 3.2) at Station C in all three sampling events. The toxic conditions at Station C reflect the strong effect that high boat density and prolonged water turnover time has for creating toxic Cu conditions. Unlike the Buck and Bruland (2005) study that evaluated locations within San Francisco Bay for Cu toxicity, we found that the  $L_2$  ligand pool was unable to buffer Cu at Station C and maintain it from reaching a toxic range for *Synechococcus*. The Buck and Bruland (2005) study did not identify any locations within San Francisco Bay as experiencing Cu toxicity. Both our study and the Buck and Bruland (2005) study evaluated the ligand pool through CLE-ACSV with MAW, though the original Buck and Bruland (2005) study did not employ a unified MAW analysis as we have done in this study. Titration data from Buck and Bruland (2005) was subsequently reprocessed as a single unified dataset (Sander et al.,

2015), and the reprocessing also did not reveal any sites with  $\text{Cu}^{2+}$  in the toxic range for *Synechococcus* in San Francisco Bay.

Possible reasons for the identification of a toxic site in San Diego Bay and not San Francisco Bay may be related to the higher concentrations of DOC found in San Francisco Bay (Buck and Bruland, 2005). DOC concentrations in San Francisco Bay range from 250 to 400  $\mu\text{M}$  while in San Diego Bay DOC concentrations ranged from 70 to 120  $\mu\text{M}$ . Given that organic matter has been suggested to provide additional binding sites (Blake et al., 2004) for metal ions, unlike in San Diego Bay, Cu in San Francisco Bay could have more available binding sites. The reason for higher organic matter in San Francisco Bay may be due to the higher freshwater influence, reflected in the lower salinity (Buck and Bruland, 2005). San Francisco Bay has more inputs of freshwater (salinity ranged from 0-26), and with multiple inputs of freshwater there is also more input of terrestrial organic matter into San Francisco Bay. Our study and a previous study (Zirino et al., 1998) show that San Diego Bay is negligently affected by freshwater inputs throughout the year.

Another factor possibly explaining the identification of a toxic site in San Diego Bay and not San Francisco Bay is the range of dissolved Cu in each respective Bay. San Diego Bay exhibited much higher concentrations of dissolved Cu compared to San Francisco Bay (Table 3.3). Dissolved Cu ranged from 3-122 nM in San Diego Bay while in San Francisco Bay the range was 20-50 nM (Buck and Bruland 2005). The range of Cu concentrations in San Francisco Bay is comparable to stations within inner San Diego Bay, however Station C in San Diego Bay exhibits elevated Cu concentrations not seen in the inner Bay in San Diego or in the San Francisco Bay samples. The elevated concentrations at Stations C set it apart from other samples in this study and the Buck and Bruland (2005) study, highlighting the localized effect of Cu

antifouling paint in an enclosed harbor. A simple parameter like DOC to dissolved Cu ratios might ultimately be useful to help predict Cu toxicity in coastal systems, with a ratio of 1 or below to indicate potential toxicity (Table 3.3), but more samples are needed as only 1 station between the two Bay studies exhibited Cu toxicity.

The remaining sites sampled in San Diego Bay in this study did not exhibit Cu toxicity as determined by both  $\text{Cu}^{2+}$  concentrations and *Synechococcus* cell counts. The sites had either an excess of  $\text{L}_1$  ligands relative to dissolved Cu or a large  $\text{L}_2$  ligand pool that helped keep  $\text{Cu}^{2+}$  below  $10^{-11}$  M during all samplings. The *Synechococcus* counts during the third sampling, however, were anomalously low for most of the inner Bay stations, including Station C. It is unknown what led to the drop in *Synechococcus*, as samples were all treated similarly and as noted above other than Station C  $\text{Cu}^{2+}$  concentrations were below the toxic range ( $10^{-11}$  M). Furthermore, cell counts for pico-eukaryotes during the third sampling did not uniformly exhibit anomalous low counts, demonstrating at least that the samples were in good condition (Table 3.2). There may have been another toxicant in the Bay leading to the drop in *Synechococcus* cell counts, but the identity of the toxicant remains unknown. Salinity measured during the fall sampling in the inner Bay was the highest salinity for each station over the three sampling events, which coincides with the low *Synechococcus* cell counts, but it remains unknown if salinity alone would lead to the low cell counts measured. It is thus possible that the low *Synechococcus* cell counts at Station C during the fall sampling is not entirely due to Cu toxicity, considering the similarly low *Synechococcus* counts in the rest of the Bay at that time.

### ***3.5.3 Copper speciation in San Diego Bay***

This study entailed some difficulties for Cu speciation determination via CLE-ACSV as San Diego Bay is a highly impacted environment for Cu, and thus during electrochemical

analysis the deposition time was kept short, ranging from 10 to 60 seconds. The short deposition time also helped reduced any surfactant effect that may take space on the mercury drop away from the Cu-SA complex. This is the strategy used by Moffett et al. (1997) to get around the surfactant effect. The interference of surfactants becomes more pronounced at longer deposition times. Fortunately the use of short deposition times works well in San Diego Bay as dissolved Cu is quite high, and longer deposition times would lead to peaks that push the instrument's ability for accurate measurement. Relatively low DOC concentrations in San Diego Bay also tend to reduce surfactant effects. The analytical windows chosen for this study, 2.5, 5, and 10  $\mu\text{M}$  SA, provide a wide range for targeting strong and weak ligands. The alpha value of the detected ligands with MAW was tested against the alpha values for each of the three windows to ensure alpha values within an order of magnitude from each other, an important consideration for ensuring that the analytical windows used are a good match for the ambient ligand pool. Overall we were able to get good determinations of the logKs for the detected ligands with minimal error, though logK errors at the Shelter Island Yacht Basin were the highest. Errors for ligand concentrations were quite variable especially for the L<sub>2</sub> ligand pool which is found in higher concentrations than the L<sub>1</sub> ligand pool, the error increased as the ligand concentrations increased. In an environment like San Diego Bay it is difficult to say what could contribute most to the high ligand concentration errors, possibly a combination of the high Cu concentrations and the need to utilize short deposition times introduced more error than usual into the measurements.

The identity of the Cu ligands within San Diego Bay remains unknown as this study did not set out to characterize the organic matter. Cu ligands, especially weaker L<sub>2</sub> ligands, are thought to be made up of humic substances which are terrestrially derived (Kogut and Voelker, 2001). Considering that San Diego Bay is not subjected to much freshwater input it is likely that



there is also little terrestrial input into San Diego Bay. In past studies *Synechococcus* has been shown to produce strong ligands ( $\log K \sim 13$ ) during Cu stress (Moffett et al. 1990; Moffett and Brand 1996). Ligands detected in San Diego Bay, particularly at Station C, may be products of *Synechococcus* attempting to alleviate Cu stress.

Cu speciation results in our study highlight the importance of the  $L_2$  ligand pool for buffering the majority of the Bay from Cu toxicity. All stations had  $L_1$  concentrations that were exceeded by dissolved Cu concentrations as shown by the deficit of excess  $L_1$  ligands, Figure 3.8. The majority of stations within the Bay exhibit deficits of the strong ligand especially within the Shelter Island Yacht Basin. The secondary ligand pool played an integral role in buffering inner Bay locations when Cu saturated the  $L_1$  ligand. Station C and, surprisingly, Station G, the station furthest away from the mouth of the Bay, had dissolved Cu concentrations that exceeded  $L_1$  concentrations during all three sampling events. Station C had the greatest difference (43-93 nM) between dissolved Cu and  $L_1$  concentrations, furthermore Station C had consistently one of the weakest  $L_2$  ligand pools relative to the other stations in the Bay. The weaker ligands at Station C are likely why the location was calculated to have free Cu in the toxic range despite a secondary ligand pool capable of bonding additional Cu. This could be due to the enclosed space of Station C coupled with long water residence times that leave the weak ligand pool more susceptible to photochemical degradation. In San Diego Bay the secondary ligand pool is a crucial buffer against Cu toxicity, but locations like Station C with the highest inputs of Cu and an enclosed region limiting water movement may not be able to buffer against Cu toxicity even with a large  $L_2$  pool. It is notable, however, that the secondary ligand pool was likely responsible for maintaining the inner Bay from reaching toxic Cu levels as the deficit of the strong ligand was smaller at these stations and the  $L_2$  ligand was stronger than at Station C. More studies in

other enclosed marinas within San Diego Bay are needed to see if results similar to Station C are also found there. The coupling of CLE-ACSV analysis with a bioindicator, *Synechococcus*, for Cu toxicity proved useful as the bioindicator was able to corroborate Cu toxicity based on  $\text{Cu}^{2+}$  at Station C on at least two occasions. Though the anomalous *Synechococcus* cell counts during the fall sampling are unexplained with available data, it does indicate that there may be other toxicants for *Synechococcus* to be aware of when using *Synechococcus* as a bioindicator of Cu toxicity in coastal environments. Previous studies have shown the sediments in San Diego Bay to exceed sediment quality guidelines for metals like Cu, zinc and mercury as well as other pollutants like polycyclic aromatic hydrocarbons, polychlorinated biphenyls and chlordane (Fairey et al., 2009). The Bay has various possible contaminants that may have had a negative impact on *Synechococcus*, Nonetheless clear drops in *Synechococcus* counts are seen during the summer and spring sampling at Station C, while the pico-eukaryote counts don't seem to be affected by Cu at Station C, lending evidence that  $\text{Cu}^{2+}$  is responsible for the drop in *Synechococcus*.

This study has reinforced previous studies (Blake et al., 2004; Moffett et al., 1997) in demonstrating that Cu toxicity may be constrained to locations of high boat density where the highest concentration of passive leaching from Cu-based antifouling paint is occurring. Despite elevated concentrations of Cu in inner San Diego Bay the secondary ligand pool proved capable of buffering the waters from reaching toxic levels of  $\text{Cu}^{2+}$ , similar to the findings of Buck and Bruland (2005) in San Francisco Bay. Unlike other harbors that have been studied, San Diego Bay has unique features that play a role in determining free Cu concentrations. The most unusual aspect of San Diego Bay is the lack of freshwater inputs, as reflected in the salinity. The lack of freshwater sources into the Bay means less sediment is transported into the Bay that may

otherwise provide more organic matter to act as additional binding sites for the excess Cu in the Bay. Unlike the harbors studied in Cape Cod that had a residence time of two days (Moffett et al. 1997), regions in San Diego Bay, especially in the back Bay, can have a residence time of up to 37 days (Chadwick et al., 2004). The long residence time in the Bay can allow for the accumulation of more Cu from leaching paints while ligands are left exposed to possible degradation by the sun which can in turn release more Cu (Skrabal et al., 2018) into surrounding waters in a sort of positive feedback.

### **3.5 CONCLUSION**

The majority of stations characterized in this study in San Diego Bay were not found with  $\text{Cu}^{2+}$  concentrations in the toxic range with the exception of Station C, the Shelter Island Yacht Basin. Observations from this study suggest that Cu toxicity is limited to boat marinas where Cu based antifouling paint has the most effect. Despite the high concentrations of dissolved Cu found in the inner Bay those stations were not found to have  $\text{Cu}^{2+}$  concentrations in the toxic range. Based on this work we predict that activities that introduce or release Cu from Cu paint will likely continue to dominate as the source of Cu pollution in San Diego Bay, thus Cu toxicity will be concentrated in boat harbors with a high density of boats and restricted circulation. Currently the Port of San Diego is working to reduce Cu pollution in the Bay and the state of California is legislating to reduce the use of Cu-based paint. As alternative non-biocide paints are implemented under new regulations anthropogenic Cu in the Bay will be reduced, which may alleviate Cu toxicity. The use of MAW CLE-ACSV to evaluate Cu speciation in San Diego Bay has proven to be a robust method for determining accurate concentrations of  $\text{Cu}^{2+}$ , which is the causative agent of Cu toxicity.

### 3.6 FIGURES and TABLES

**Table 3.1.** Hydrography data collected with a YSI probe at each station, DO values with n.d. indicate no data available.

Station	Season	Temperature (C)	Salinity	pH	DO (mg/L)
A	Summer	20.00	33.30	7.67	8.75
	Spring	16.00	33.49	7.48	7.85
	Fall	17.10	33.52	7.76	n.d.
B	Summer	21.10	33.24	7.94	8.23
	Spring	17.10	33.49	7.53	8.02
	Fall	16.70	33.53	7.82	n.d.
C	Summer	23.00	33.14	7.93	8.26
	Spring	17.70	33.49	7.66	8.25
	Fall	18.80	33.75	7.75	n.d.
D	Summer	22.90	33.47	7.97	7.62
	Spring	18.10	33.45	7.70	8.40
	Fall	19.80	34.07	7.74	n.d.
E	Summer	22.60	33.47	8.00	7.64
	Spring	18.30	33.45	7.80	7.70
	Fall	19.90	34.06	7.74	n.d.
F	Summer	24.10	33.45	8.04	7.26
	Spring	18.90	33.44	7.78	7.77
	Fall	21.10	34.49	7.76	n.d.
G	Summer	25.60	34.18	7.96	7.39
	Spring	19.00	33.34	7.85	7.15
	Fall	21.40	34.98	7.80	n.d.

**Table 3.2.** Results for dissolved Cu, Cu speciation, *Synechococcus*, picoeukaryotes, and DOC.

Station	Season	[Cu] (nM)	[L <sub>1</sub> ] (nM)	+/-	logK <sub>1</sub>	+/-	[L <sub>2</sub> ] (nM)	+/-	logK <sub>2</sub>	+/-	logCu <sup>2+</sup>	<i>Synechococcus</i> (cells/mL)	Pico-Eukaryote (cells/mL)	DOC (μM)
A	Summer	2.99	6.86	1.97	14.80	0.48	88.04	61.63	12.41	0.34	-14.98	62269	26606	89.80
	Spring	12.28	15.18	2.81	12.85	0.23	87.16	82.80	10.72	0.78	-12.37	72751	69686	71.96
	Fall	6.30	3.36	2.06	13.13	1.05	18.70	9.12	12.04	0.30	-12.64	138049	23629	81.77
B	Summer	17.04	21.39	2.57	12.73	0.19	68.45	49.62	10.63	0.45	-12.14	79583	83966	n.d.
	Spring	22.49	16.56	3.15	12.78	0.51	41.46	16.07	11.21	0.28	-11.85	78277	100006	82.69
	Fall	8.41	7.69	1.64	13.58	0.61	92.70	83.40	10.63	0.61	-12.48	179294	19211	81.77
C	Summer	122.97	29.36	6.02	13.31	6.95	138.20	50.10	10.83	0.22	-10.51	22526	55446	87.72
	Spring	75.57	31.94	8.06	12.40	6.60	54.50	24.25	10.75	0.40	-9.05	19517	85983	78.33
	Fall	86.49	14.49	4.53	13.56	7.29	167.50	71.20	9.98	0.23	-10.12	4220	86411	99.21
D	Summer	27.55	23.57	6.19	12.64	0.47	66.04	32.19	11.22	0.31	-12.04	112937	110686	93.71
	Spring	26.34	26.60	5.18	12.47	0.34	82.20	64.70	10.61	0.48	-11.83	75814	116509	111.08
	Fall	26.76	18.51	5.88	12.67	0.63	84.92	38.22	11.12	0.28	-11.94	3123	47434	107.10
E	Summer	27.19	30.28	5.91	12.86	0.39	81.74	51.09	11.06	0.39	-12.35	82823	73240	88.11
	Spring	26.26	13.53	4.57	12.83	6.64	68.94	27.58	11.09	0.25	-11.70	88866	114840	106.50
	Fall	24.26	17.79	1.96	12.77	0.22	127.60	37.30	10.76	0.16	-11.90	2654	51057	96.14
F	Summer	39.73	39.99	18.99	12.32	0.55	75.08	61.00	11.38	0.51	-12.04	163040	92794	102.42
	Spring	30.80	13.82	1.66	12.78	0.32	52.40	9.43	11.18	0.10	-11.44	96346	122491	n.d.
	Fall	27.08	9.38	2.13	12.76	0.61	114.70	19.50	11.00	0.09	-11.69	3506	90949	99.49
G	Summer	35.07	32.21	5.64	13.26	0.40	87.45	31.70	11.72	0.21	-12.65	81274	81617	120.91
	Spring	36.56	20.85	17.20	12.06	1.69	101.90	54.70	11.13	0.36	-11.69	38820	146086	111.60
	Fall	28.88	10.81	2.00	12.33	0.31	49.74	3.98	11.72	0.06	-11.83	5597	184703	n.d.

**Table 3.3.** Dissolved copper, DOC data and DOC:Cu ratios for all samples in San Diego Bay (this study) and San Francisco Bay (Buck and Bruland, 2005). Values in bold represent measurements from Shelter Island Yacht Basin (Station C).

San Diego Bay			San Francisco Bay		
[Cu] (nM)	DOC ( $\mu$ M)	DOC:Cu	DOC ( $\mu$ M)	[Cuamb] (nM)	DOC:Cu
2.99	89.80	30.03	380	33.7	11.28
12.28	71.96	5.86	253	27	9.37
6.30	81.77	12.98	398	26.4	15.08
17.04	n.d.	n.d.	222	25	8.88
22.49	82.69	3.68	343	22.9	14.98
8.41	81.77	9.72	210	27.1	7.75
<b>122.97</b>	<b>87.72</b>	<b>0.71</b>	294	18.9	15.56
<b>75.57</b>	<b>78.33</b>	<b>1.04</b>	264	17.9	14.75
<b>86.49</b>	<b>99.21</b>	<b>1.15</b>	305	25	12.2
27.55	93.71	3.40	279	20.3	13.74
26.34	111.08	4.22	308	27.7	11.12
26.76	107.10	4.00	307	49.6	6.19
27.19	88.11	3.24			
26.26	106.50	4.06			
24.26	96.14	3.96			
39.73	102.42	2.58			
30.80	n.d.	n.d.			
27.08	99.49	3.67			
35.07	120.91	3.45			
36.56	111.60	3.05			
28.88	n.d.	n.d.			



**Figure 3.1.** Map of stations sampled within San Diego Bay., with the Shelter Island Yacht Basin highlighted by the red marker. Map generated using Google Earth.

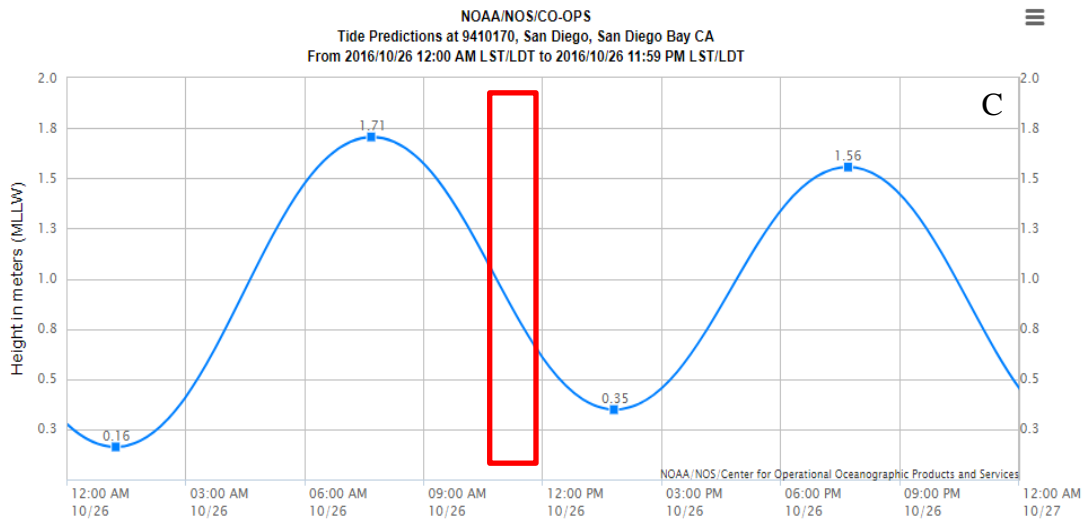
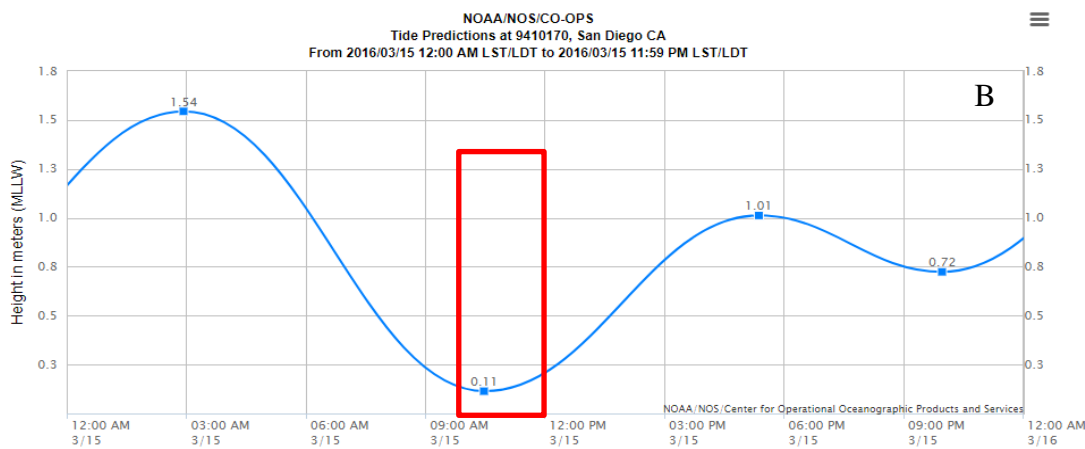
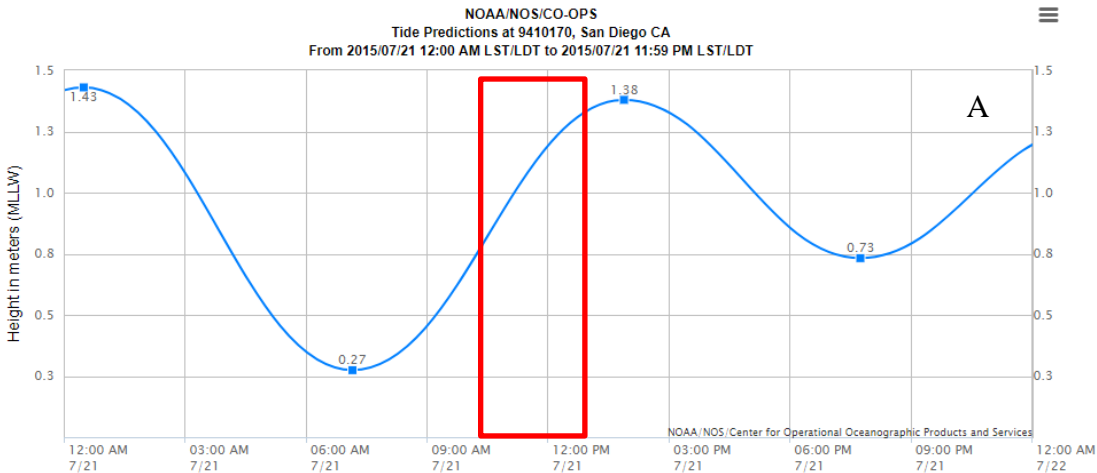


**Figure 3.2.** Graph of tides during each sampling event ((A) summer (B) spring, (C) fall) with a red box to indicate the time and duration of sampling. Graph and data generated by NOAA.



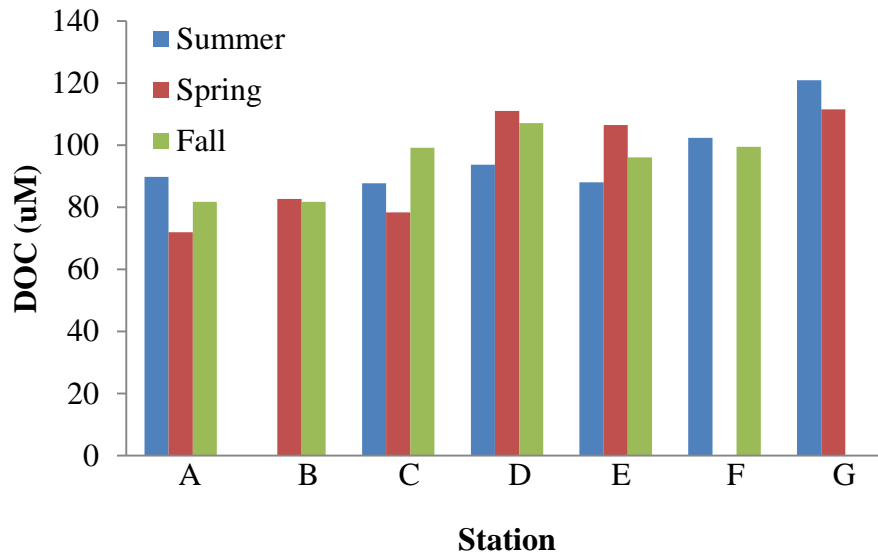


**Figure 3.3.** Results of DOC analysis for stations during the three sampling events. No DOC data available for Station B in the summer, Station F in the spring, and Station G in the fall.

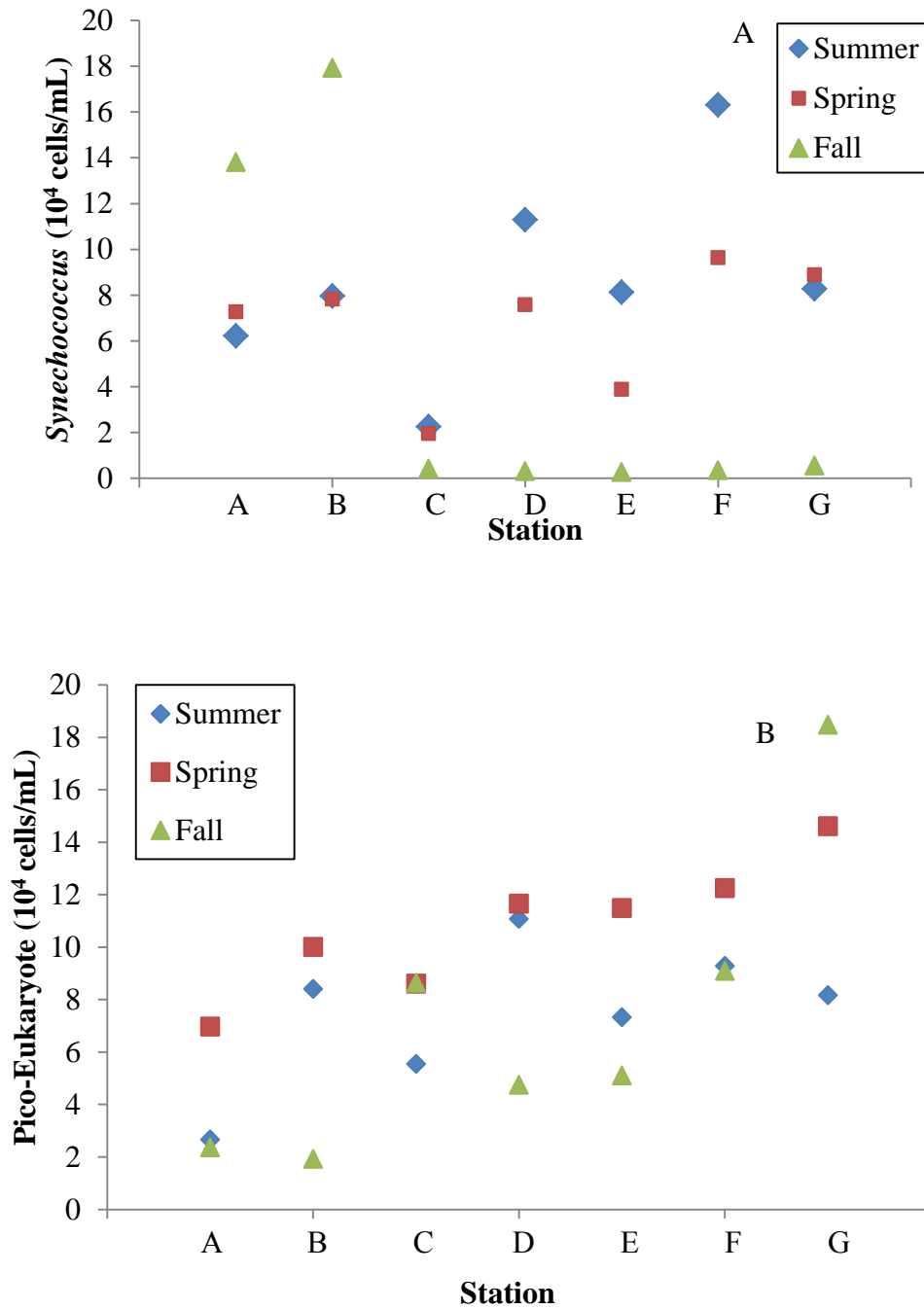


**Figure 3.4.** (A) *Synechococcus* counts for all sampling in San Diego Bay. (B) Picoeukaryote cell counts for each sampling in San Diego Bay.

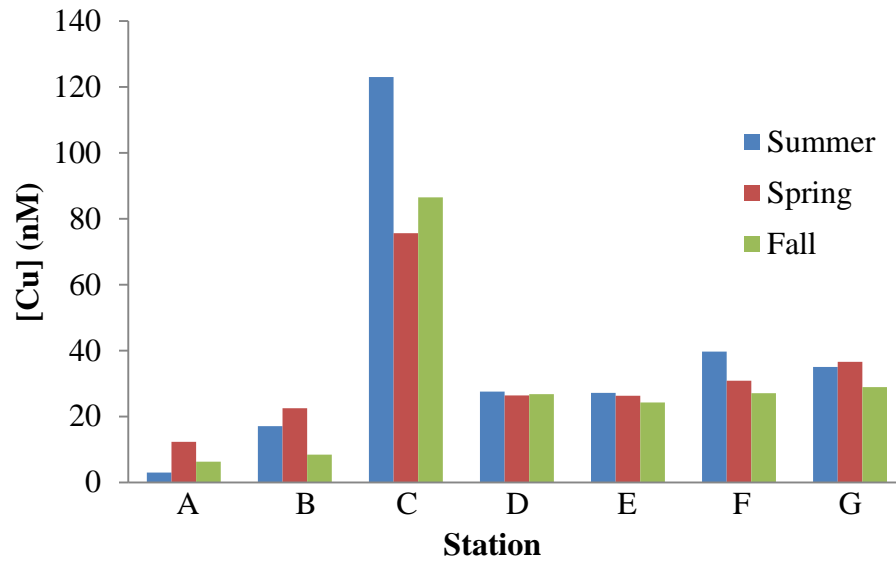


**Figure 3.5.** Dissolved copper determined for each station during the three sampling periods.

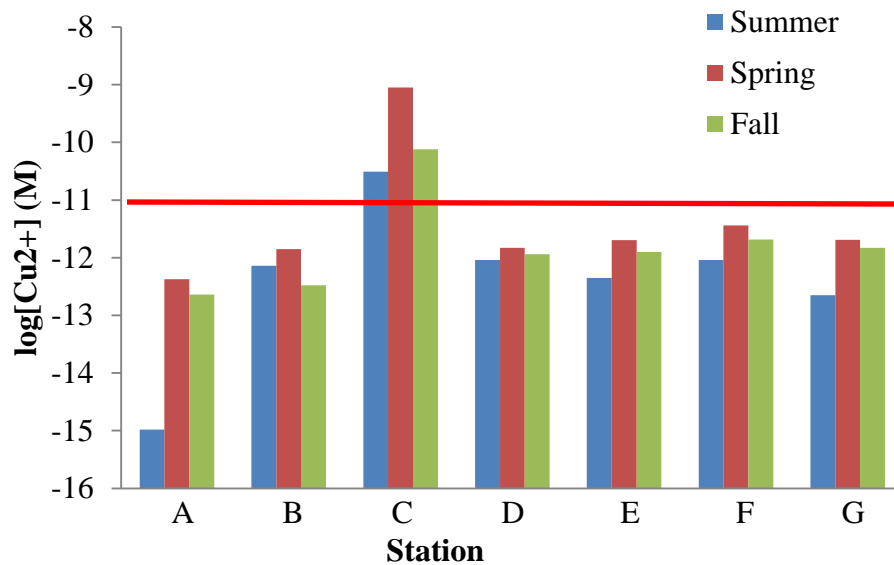


**Figure 3.6.** Free copper concentrations determined from MAW analysis through ProMCC. The red line represents the toxicity threshold for *Synechococcus*, anything above the red line exceeds the toxicity levels for *Synechococcus*.

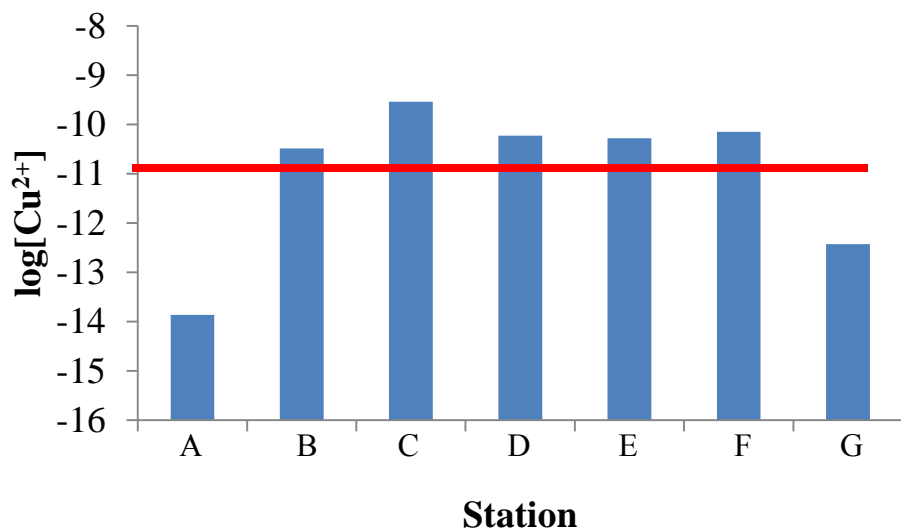


**Figure 3.7.** Free Cu concentrations determined from the 5 $\mu$ M SA analytical window results for the summer samples. The red line represents the toxicity threshold for *Synechococcus*, anything above the line represents Cu toxicity.

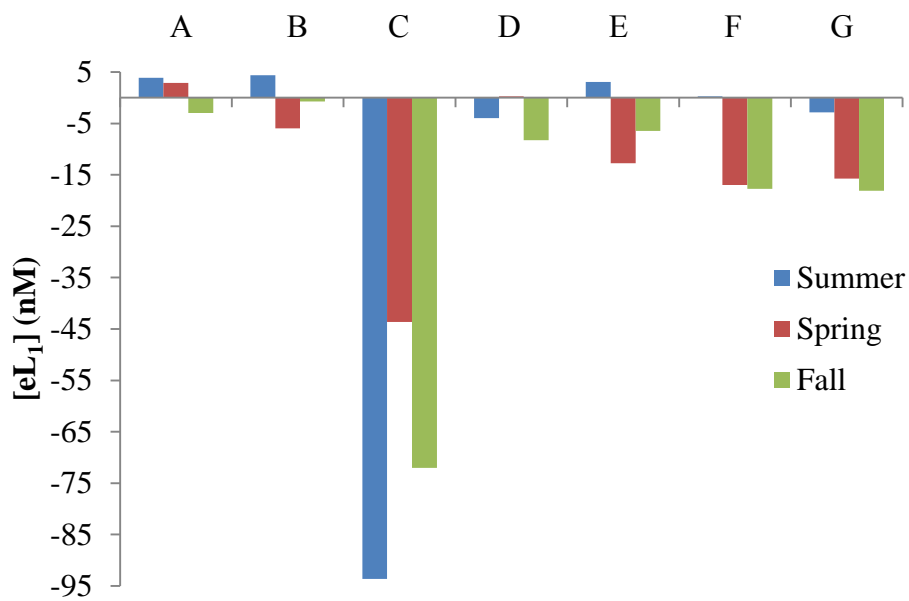


**Figure 3.8.** Plot of excess  $L_1$  ligand across San Diego Bay over all sampling events.

### 3.7 ACKNOWLEDGEMENTS

We thank Phil Zerofski for providing assistance in the sampling campaign by operating and transporting the boat used for carrying out the field work. We also thank the Palenik lab for their contribution to the field work and data generation for *Synechococcus* and picoeukaryotes. We thank the Aluwihare lab for providing DOC data.

Chapter 3, in full, is currently being prepared for submission for publication of the material with the following co-authors: Ruacho, Angel; Barbeau, Katherine; Nagakar, Maitreyi; Palenik, Brian. The dissertation author was the primary author of this paper.

### 3.8 REFERENCES

- Blake, A. C., Chadwick, D. B., Zirino, A., & Rivera-Duarte, I. (2004). Spatial and temporal variations in copper speciation in San Diego Bay. *Estuaries*, 27(3), 437-447.
- Brand, L. E.; Sunda, W. G.; Guillard, R. R. L., Reduction of marine-phytoplankton reproduction rates by copper and cadmium. *Journal of Experimental Marine Biology and Ecology* 1986, 96 (3), 225-250.
- Buck, K. N., and Bruland, K. W. (2005). Copper speciation in San Francisco Bay: A novel approach using multiple analytical windows. *Mar. Chem.* 96, 185–198.  
Doi:10.1016/j.marchem.2005.01.001.
- Bundy, R. M., Barbeau, K. A., and Buck, K. N. (2013). Sources of strong copper-binding ligands in Antarctic Peninsula surface waters. *Deep. Res. Part II Top. Stud. Oceanogr.* 90, 134–146. Doi:10.1016/j.dsr2.2012.07.023.
- Chadwick, D. B., Zirino, A., Rivera-Duarte, I., Katz, C. N., & Blake, A. C. (2004). Modeling the mass balance and fate of copper in San Diego Bay. *Limnology and Oceanography*, 49(2), 355-366.
- Collier, J. L., & Palenik, B. (2003). Phycoerythrin-containing picoplankton in the Southern California Bight. *Deep Sea Research Part II: Topical Studies in Oceanography*, 50(14-16), 2405-2422.
- Fairey, Russell, Cassandra Roberts, Michele Jacobi, Stewart Lamerdin, Ross Clark, James Downing, Edward Long et al. "Assessment of sediment toxicity and chemical concentrations in the San Diego Bay region, California, USA." *Environmental Toxicology and Chemistry: An International Journal* 17, no. 8 (1998): 1570-1581.
- Hudson, Robert JM, Eden L. Rue, and Kenneth W. Bruland. "Modeling complexometric titrations of natural water samples." *Environmental science & technology* 37, no. 8 (2003): 1553-1562.
- Kogut, Megan B., and Bettina M. Voelker. "Strong copper-binding behavior of terrestrial humic substances in seawater." *Environmental science & technology* 35, no. 6 (2001): 1149-1156.
- Largier, J. L., J. Hollibaugh, and S. Smith. 1997. Seasonally hypersaline estuaries in Mediterranean-climate regions. *Estuarine, Coastal and Shelf Science* 45:789-79
- Moffett, J. W., R. G. Zika, and Larry E. Brand. "Distribution and potential sources and sinks of copper chelators in the Sargasso Sea." *Deep Sea Research Part A. Oceanographic Research Papers* 37, no. 1 (1990): 27-36.



- Moffett, J. W., and L. E. BRAND. 1996. The production of strong, extra-cellular Cu chelators by marine cyanobacteria in response to Cu stress. *Limnol. Oceanogr.* 41: 288-293.
- Moffett, James W., Larry E. Brand, Peter L. Croot, and Katherine A. Barbeau. "Cu speciation and cyanobacterial distribution in harbors subject to anthropogenic Cu inputs." *Limnology and Oceanography* 42, no. 5 (1997): 789-799.
- Nagarkar, Maitreyi, Peter D. Countway, Yeong Du Yoo, Emy Daniels, Nicole J. Poulton, and Brian Palenik. "Temporal dynamics of eukaryotic microbial diversity at a coastal Pacific site." *The ISME journal* 12, no. 9 (2018): 2278.
- NOAA, 1991. Contaminant trends in the Southern California bight: inventory and assessment. NOAA Technical Memorandum, NOS ORCA 62, National Oceanic and Atmospheric Administration, National Ocean Service, Rockville, MD
- Oldham, V. E., M. M. Swenson, and K. N. Buck. "Spatial variability of total dissolved copper and copper speciation in the inshore waters of Bermuda." *Marine pollution bulletin* 79, no. 1-2 (2014): 314-320.
- Omanović, Dario, Cédric Garnier, and Ivanka Pižeta. "ProMCC: an all-in-one tool for trace metal complexation studies." *Marine Chemistry* 173 (2015): 25-39.
- Peers, G., Quesnel, S. A., & Price, N. M. (2005). Copper requirements for iron acquisition and growth of coastal and oceanic diatoms. *Limnology and oceanography*, 50(4), 1149-1158.
- Peers, G., & Price, N. M. (2006). Copper-containing plastocyanin used for electron transport by an oceanic diatom. *Nature*, 441(7091), 341-344.
- Port of San Diego. 2011. USEPA project, NP00946501-4: safer alternatives to copper antifouling paints for marine vessels. San Diego: US Environmental Protection Agency.
- Schiff, K., J. Brown, D. Diehl and D. Greenstein. 2007. Extent and magnitude of copper contamination in marinas of the San Diego region, California, USA. *Marine Pollution Bulletin* 54: 322-328.
- Skrabal, Stephen A., Alyssa M. McBurney, Linda A. Webb, G. Brooks Avery Jr, Robert J. Kieber, and Ralph N. Mead. "Photodissolution of copper from resuspended coastal marine sediments." *Limnology and Oceanography* 63, no. 2 (2018): 773-785.
- van den Berg, C.M.G., 1987. Organic complexation and its control on the dissolved concentrations of copper and zinc in the Scheldt Estuary. *Estuarine Coastal Shelf Sci.* 24 (6), 785-797.
- Walker, C.B., de la Torre, J.R., Klotz, M.G., Urakawa, H., Pinel, N., Arp, D.J., Brochier-Armanet, C., Chain, P.S.G., Chan, P.P., Gollagbir, A., Hemp, J., Hügler, M., Karr, E.A., Könneke, M., Shin, M., Lawton, T.J., Lowe, T., Martens-Habbena, W., Sayavedra-Soto,

- L.A., Lang, D., Sievert, S.M., Rosenzweig, A.C., Manning, G., Stahl, D.A., 2010. Nitrosopumilus maritimus genome reveals unique mechanisms for nitrification and autotrophy in globally distributed marine Crenarchaea. PNAS 107 (19), 8818–8823.
- Whitby, Hannah, Anna M. Posacka, Maria T. Maldonado, and Constant MG van den Berg. "Copper-binding ligands in the NE Pacific." Marine Chemistry 204 (2018): 36-48.
- Woods Hole Oceanographic Institution (WHOI), 1952. Marine fouling and its prevention. United States Naval Institute, Annapolis, MD, 388pp. (Contribution no. 580)
- Zirino, Alberto, Stuart L. Belli, and David A. Van der Weele. "Copper concentration and CuII activity in San Diego Bay." Electroanalysis: An International Journal Devoted to Fundamental and Practical Aspects of Electroanalysis 10, no. 6 (1998): 423-427.